Effect of salinity in the first phase of salt stress on leaf cell-wall components of maize with special reference to cell-wall extensibility

Md. Nesar Uddin

Institute of Plant Nutrition

Justus Liebig University Giessen

Professor Dr. Sven Schubert

Effect of salinity in the first phase of salt stress on leaf cell-wall components of maize with special reference to cell-wall extensibility

A thesis submitted for the requirement of the doctoral degree in agriculture from Faculty of Agricultural Sciences, Nutritional Sciences and Environmental Management Justus Liebig University Giessen

Submitted by

Md. Nesar Uddin

from Bogra, Bangladesh

Gießen, 2012

Date of defense: 09-11-2012

Examination Commission

Chairman: Prof. Dr. Sylvia Schnell

Supervisor: Prof. Dr. Sven Schubert

Co-supervisor: Prof. Dr. Dr. hc Wolfgang Friedt

Examiner: Dr. Rolf Alexander Düring

Examiner: Dr. Lutz Eckstein

To my beloved father, father in law and mother in law

whom I lost during my stay in Germany

May Allah keep their soul in peace

&

To my mother whose inspiration always lights me

&

Last but not the least to my wife for her endless support

throughout my stay in Germany

TABLE OF CONTENTS

List of abbreviations

Abbreviation		
% (v/v)	:	Percent volume to volume
% (w/w)	:	Percent weight to weight
°C	:	Degree Celsius
µg	:	Microgram
µL	:	Microliter
µm	:	Micrometer
µM	:	Micromole L^{-1}
Ara	:	Arabinose
CF	:	Correction factor
d	:	Day
DFA	:	Diferulic acid
dS m^{-1}	:	Decisiemens meter^{-1}
EC	:	Electrical conductivity
F1	:	First filial generation or hybrid
FA	:	Ferulic acid
Fig.	:	Figure
g	:	Gram
g	:	Gravitational force
Gal	:	Galactose
GAX	:	Glucuronoarabinoxylan
Glu	:	Glucose
h	:	Hour
HPAEC	:	High performance anion exchange chromatography
HPLC	:	High performance liquid chromatography

Abbreviation

L	:	Liter
m	:	Meter
M	:	Mole L^{-1}
Man	:	Mannose
min	:	Minute
mL	:	Milliliter
mM	:	Millimole L^{-1}
mm	:	Millimeter
NaExIl	:	Na^+ excluding inbred line
nm	:	Nanometer
P	:	Probability of error
PAD	:	Pulsed amperometric detection
PEG	:	Polyethylene glycol
PET	:	Polyester
PGA	:	Polygalacturonic acids
RF	:	Response factor
Rha	:	Rhamnose
RP	:	Reverse phase
SR	:	Salt-resistant
SWS	:	Osmotically resistant inbred line
TFA	:	Trifluoroacetic acid
Xyl	:	Xylose

1 Introduction

Soil salinity is characterized by a high concentration of soluble salts that account for an electrical conductivity (EC) of 4 dS m^{-1} ($\approx$ 40 mM NaCl) or more (USDA-ARS 2008). Above this EC, yield of most crops declines significantly (Munns and Tester 2008). As compared to a drought environment, in which plant growth is impaired due to an inadequate water supply, the saline environment may offer abundant but hardly extractable water for the plants. Reduction of plant growth in a saline environment is a complex phenomenon. The possible physiological, biochemical and molecular mechanisms behind the growth reduction of crops has not yet been adequately understood, and for this reason development of salt-resistant crops has been slow (Läuchli and Grattan 2007). Because of the complex nature of growth inhibition under salinity, it is important to know whether plants in a saline environment suffer from water stress or ion stress or from both. The well-known dogma in this context is known as "biphasic model" of growth responses to salinity (Munns 1993). This well accepted theory was a major breakthrough for plant scientists who work with the salt-resistance mechanisms of plant.

1.1 The biphasic model of growth responses to salinity
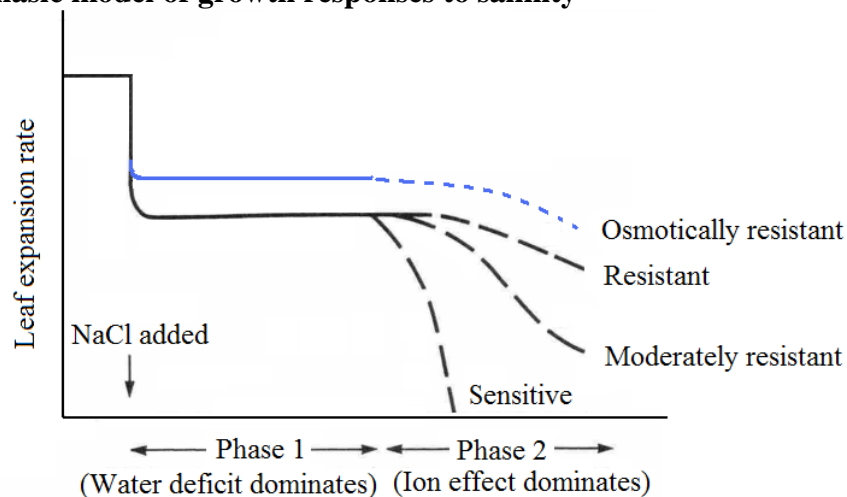
Figure 1-1: The two-phase model of plant growth under salt stress (modified after Munns 1993). Three black dashed-lines show the growth inhibition of sensitive, moderately resistant and resistant varieties of a specific genotype. On the other hand, the solid blue line shows the improvement of growth in the first phase of salt stress.

Some time ago, Munns (1993) proposed a widely accepted biphasic model for the growth inhibition of plants under salt stress (Fig. 1-1). According to this biphasic model, growth inhibition occurs in two phases. The first phase of salt stress, also known as osmotic phase, is characterized by the rapid response in growth reduction due to a decrease in soil water potential by decreasing the external osmotic potential. The reduction of shoot growth in this phase is due to a water-stress effect regulated by inhibitory signals from the roots (e.g. abscisic acid). Therefore, the growth reduction in the first phase is an effect of salt outside the plant rather than within it. The growth inhibition in the second phase of salt stress is due to the rapid increase in salt concentrations in apoplast or cytoplasm when vacuoles cannot sequester incoming salt ions. Thus the second phase is also known as the ionic phase. In the original model, Munns (1993) proposed that salt-sensitive and salt-resistant genotypes show identical growth inhibition in the first phase of salt stress, while their growth responses are different in the second phase. However, osmotically resistant genotypes (Fig. 1-1) were reported later that may partially compensate growth reduction in the first phase of salt stress (Neumann 1997; Schubert *et al.* 2009). The two-phase model once proposed for wheat and has been partially validated for maize (*Zea mays* L.) genotypes (Fortmeier and Schubert 1995). In maize, ion toxicity may also contribute to inhibit growth in the first phase of salt stress though the contribution is negligible (Sümer *et al.* 2004).

1.2 Schematic history of the development of salt-resistant maize hybrids

A moderately salt-resistant maize hybrid (F1) Pioneer 3906 was developed by crossing of two inbred lines, Pioneer 165 (efficient Na^+ exclusion at the root surface) and Pioneer 605 (efficient Na^+ exclusion from the shoot) (Fig. 1-2). Recurrent selections followed by selfings over seven generations led to establish a homogeneous Na^+-excluding inbred line (NaExIl) that excludes Na^+ at the root surface and also restricts translocation of Na^+ to the shoot (Schubert *et al.* 2009).
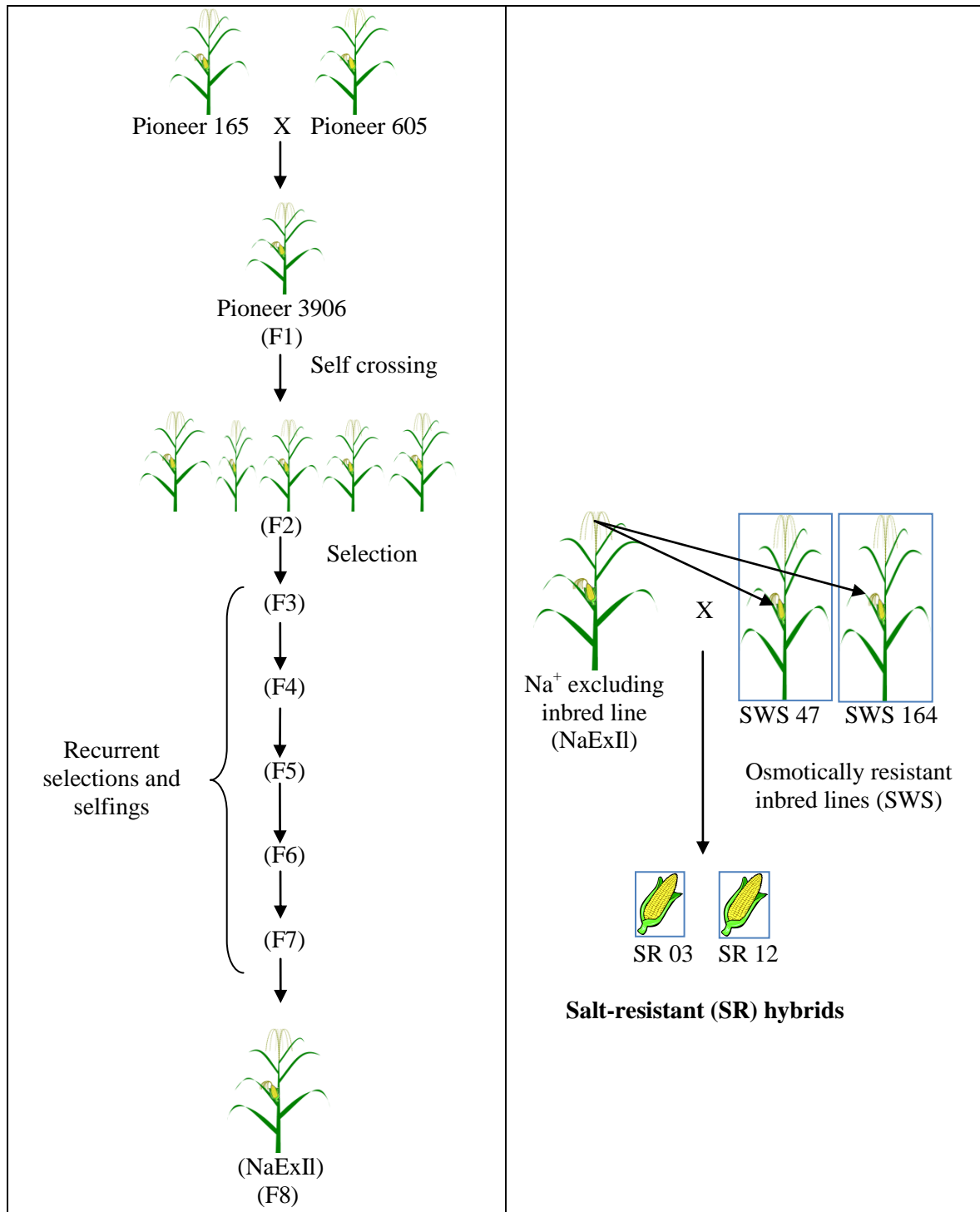
Figure 1-2: Schematic presentation of the development of maize SR hybrids (Schubert *et al.* 2009). A moderately salt-resistant maize-hybrid (F1) Pioneer 3906 was developed by crossing of two inbred lines, (i) Pioneer 165 (efficient Na$^+$ exclusion at the root surface) and (ii) Pioneer 605 (efficient Na$^+$ exclusion from the shoot). Recurrent selections followed by selfings were performed over seven generations to develop a homogeneous Na$^+$-excluding inbred line (NaExIl). Afterwards, several SR hybrids were developed by crossing NaExIl with osmotically resistant inbred lines (SWS).

Several salt-resistant (SR) maize hybrids with improved salt resistance (e.g. SR 12, SR 03) were developed by crossing a number of osmotically resistant maize inbred lines (SWS) with a Na^+-excluding maize inbred line (NaExIl) in the Institute of Plant Nutrition, Justus Liebig University, Giessen, Germany (Schubert *et al.* 2009). The breeding scheme for developing SR hybrids is demonstrated in Fig. 1-2. The newly established SR hybrids showed relative improvement in growth (in terms of shoot fresh mass and leaf area) during the first phase of salt stress compared to its parental hybrid Pioneer 3906 (Schubert *et al.* 2009). Also, the newly developed SR hybrids showed better exclusion of Na^+ at the root surface along with less root-to-shoot translocation of Na^+ compared to the parental hybrid Pioneer 3906.

1.3 Expansion of plant cells is a highly coordinated process

Expansion of plant cells occurs in three steps: (i) Plant cells uptake water across the plasma membrane due to the gradient in water potential ($\Delta\psi_w$), (ii) Turgor pressure ($\Delta\psi_p$) builds up inside the cells because of the rigidity of the cell wall and (iii) Biochemical wall-loosening occurs, allowing the cell to expand in response to turgor pressure (Taiz and Zeiger 2000).

A model for the expansion of plant cells has been developed by Lockhart (1965) and is popularly known as "Lockhart equation":

$$GR = m (\psi_p - Y)$$

where, GR is growth rate,

m is extensibility of the cell wall,

ψ_p is turgor pressure and

Y is yield threshold (i.e. the minimum pressure required for growth)

This equation clearly shows that the rate of cell expansion depends on turgor pressure and the mechanical properties of the cell-wall (extensibility). Thus it is evident that the principal players behind extension growth of plant cells are located in the symplast (turgor pressure) as well as in the apoplast (cell-wall extensibility).

1.4 What hinders growth of plants during the first phase of salt stress ?

Growth inhibition in the first phase of salt stress is one of the core questions in the field of stress physiology and the mechanisms are not yet precisely known (Munns and Tester 2008). As a salt-sensitive crop, maize shows a strong inhibition in shoot growth in the first phase of salt stress (Pitann *et al.* 2009; Hatzig *et al.* 2010). Munns (1993) suggested that both salt-sensitive and salt-resistant genotypes show similar growth reductions in the first phase of salt stress, though recent evidence (Neumann 1997; Schubert *et al.* 2009) suggests that significant genotypic variation exists even in this first phase of salt stress.

It was generally believed that salt stress may reduce the turgor pressure (symplastic player in Lockhart´s equation) of plants and thereby reduce growth. However, there is evidence that maize can maintain turgor during water-limiting and saline conditions (Neumann *et al*. 1994; Van Volkenburgh and Boyer 1985). The newly developed salt-resistant maize hybrids SR 03 and SR 12 (Schubert and Zörb 2005; Schubert *et al.* 2009) are also able to maintain shoot turgor under salt stress (De Costa *et al.* 2007). Moreover, assimilate supply to the growing tissue under salt stress was not limiting (De Costa *et al.* 2007) suggesting photosynthesis in the first phase of salt stress does not account for the growth inhibition in maize. Additionally, water uptake by maize plants from the saline solution did not limit growth (Ingold 2009). Thus, a decrease in cell-wall extensibility (apoplastic player in Lockhart´s equation) is likely to be the mechanism for leaf growth reduction under salt stress (Cramer 1994). The term extensibility generally refers to the ability of the wall to

expand or extend irreversibly during growth (Cosgrove 1997a). A decrease in cell-wall extensibility is triggered by a root-born signal such as abscisic acid and/or pH (Montero *et al.* 1997; Jia and Davies 2007). Growth inhibition in expanding maize leaves due to water stress imposed by PEG was accompanied by a significant decrease of leaf and cell-wall extensibility (Lu and Neumann 1998).

According to Cosgrove (1997a), three factors may reduce the cell-wall extensibility. These comprise (i) a decrease in wall-loosening processes, (ii) a change in cell-wall composition, and (iii) an increase in cross-linking of cell-wall polymers resulting in a more tightened wall structure or one that is less susceptible to wall loosening.

1.5 Factors governing cell-wall extensibility

1.5.1 Cell-wall loosening processes

According to the acid growth theory, H^+ secreted by plasma membrane H^+-ATPase into the cell-wall space serve as cell-wall loosening factor through activation of hydrolytic enzymes in the apoplast (Hager 2003, Fig. 1-3 a). The cell-wall loosening process takes place by means of hydrolysis of covalent bonds, transglycosylation or disruption of non-covalent bonds. Wall-loosening proteins expansins are activated under acidic condition of the apoplast (Cosgrove 1993, 2005). Expansins weaken the non-covalent binding between wall polysaccharides (e.g. H-bond), thereby allowing turgor-driven wall expansion (Fig. 1-3 b). Besides expansins, other wall-loosening enzymes such as xyloglucan hydrolase (XGH) and xyloglucan endotransglycosylase (XET) are also activated at acidic pH (Fry *et al.* 1992), and they are involved in breaking and ligation of glycosidic bonds (Cosgrove 2005). In a nut shell, the acidification of the apoplast may affect cell-wall proteins such as expansins and xyloglucan endotransglycosylases (XET) and cell-wall polysaccharide linkages, thereby loosening the load-bearing cellulose-hemicellulose-pectin networks

which in turn augment cell expansion (Rayle and Cleland 1970; Hager *et al.* 1971; Cosgrove 2005).
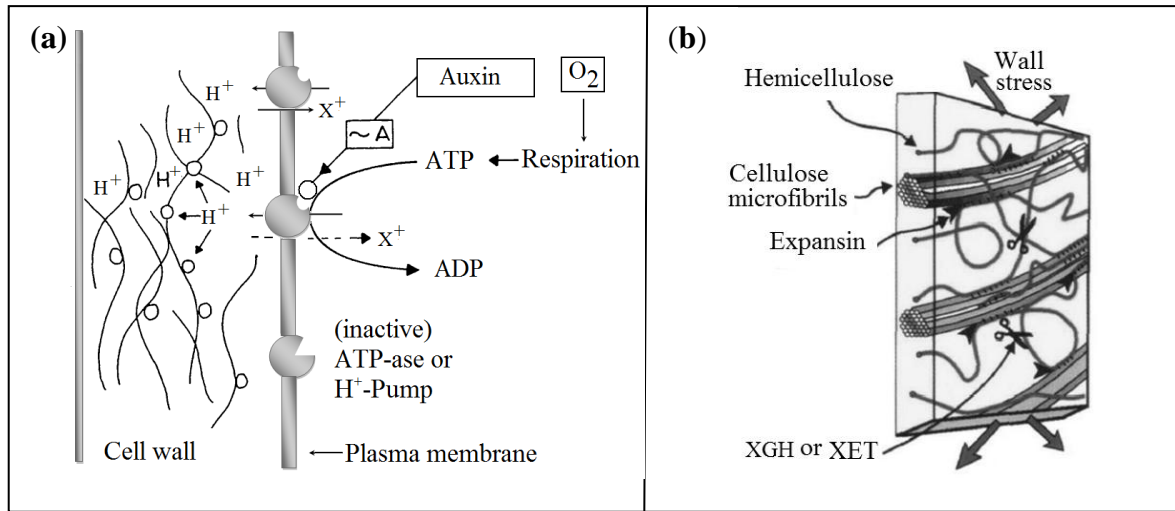
Figure 1-3: Illustration of (a) the acid-growth theory (modified after Hager *et al.* 1971) and (b) mechanisms for stress relaxation and growth of cell walls (modified after Cosgrove 1997b). An activated form of auxin (~A) activates a plasma membrane H^+-ATPase which pumps H^+ to the apoplast from the cytosol. This acidification of apoplast activates of enzymes (Fig. b) that loosen the cell-wall matrix and thus trigger cell elongation (XGH = xyloglucan hydrolases, XET = xyloglucan endotransglycosylase).

The plasma membrane H^+-ATPase-mediated cell-wall acidification was studied in three different maize genotypes namely salt-senisitive Pioneer 3906, and salt-resistant genotypes SR 12 and SR 03 (Pitann *et al.* 2009; Hatzig *et al.* 2010). Surprisingly, only SR 03 can maintain plasma membrane H^+-ATPase-mediated acidification of the apoplast, while SR 12 and Pioneer 3906 cannot maintain wall acidification during salt stress. Also, the growing shoot of salt-resistant SR 03 maintains growth-mediating β-expansin proteins in the shoot under salt stress (Geilfus *et al.* 2010). Thus, better growth of SR 03 under salt stress may be due to the maintenance of low wall pH and high activity of β-expansin proteins that are involved in the wall-loosening process in order to increase cell-wall extensibility. Surprisingly, the genotype SR 12 showed some resistance in the first phase of salt stress, which could not be explained in terms of wall acidification. This suggests that besides apoplastic pH (Pitann *et al.* 2009) additional factors control cell-wall extensibility

and thereby cell-wall growth under salt stress. Thus, a change in cell-wall chemical composition and cross-linking of cell-wall polymers might play an important role in reducing cell-wall extensibility.

1.5.2 Chemical composition and architecture of primary cell walls of grasses and their sites of synthesis

A cell wall is a layer of structural material found in the apoplast and it serves two common primary functions, (i) regulating cell volume and (ii) stabilizing cell shape. A primary wall is one whose polysaccharide structure was deposited for the period of growth at cell surface (Fry 1988). Primary wall has special characteristics that are reasonably the topic of intensive study. The cell wall of grasses (Fig. 1-4) is quite different in composition compared to dicot and non-commelinoid monocot species and is called type II cell wall (Carpita 1996).
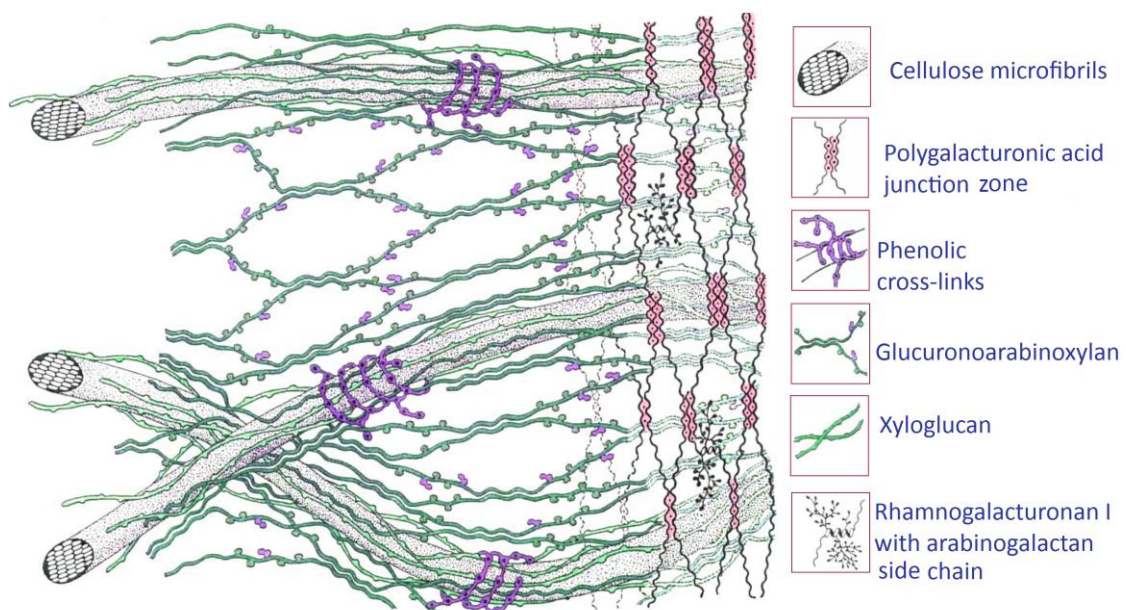
Figure 1-4: The type II cell-wall (modified after Carpita and Gibeaut 1993, reproduced with permission from John Wiley and Sons) of the Poaceae represents cellulose microfibrils that are coated with hemicelluloses such as glucuronoarabinoxylans (GAX) and GAX themselves are cross-linked with polyphenolic acids. Pectins form an interlocking hydrated matrix gel, in which all other structures are embedded (Brett and Waldron 1996) and which possibly interacts with structural proteins.

The type II monocot cell-wall is characterized by cellulose microfibrils cross-linked by glucuronoarabinoxylan (GAX) and a network of polyphenolic substances (Carpita and Gibeaut 1993; Carpita 1996). Grass cell-wall also contains developmentally regulated polymers, the mixed-linkage (1→3), (1→4)-β-D-glucans (Carpita 1996).

1.5.2.1 Cellulose

Cellulose microfibrils are made of about three dozen linear chains of (1→4)-β-linked D-glucose condensed to form a long paracrystalline structure around each cell (Delmer and Amor 1995). In primary cell walls, cellulose microfibrils are embedded in a highly hydrated matrix (Fig. 1-5), and it gives both strength and flexibility to the wall.
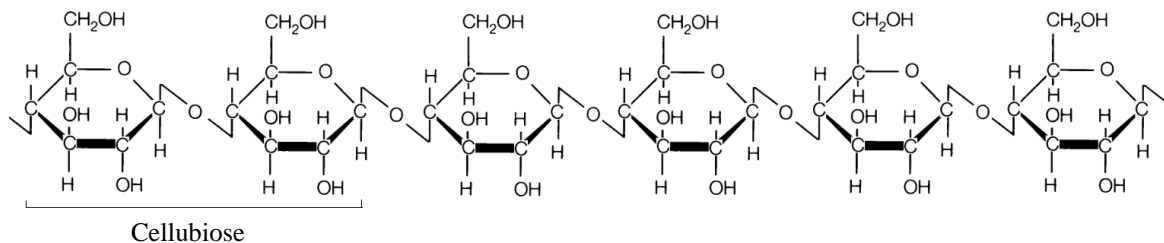
Cellubiose

Figure 1-5: The cellulose molecule consists of a repeating cellubiose unit.

1.5.2.2 Hemicelluloses

Glucuronoarabinoxylan (GAX) is a major hemicellulosic unit in grass cell-wall that is composed of a xylan backbone (xylose monomeric unit) with arabinose and less frequently glucuronic acid side chains (Fig. 1-6 a). Glucuronoarabinoxylan is the principal polymer in grass cell-wall that interlocks the microfibrils in dividing cells (Carpita and Gibeaut 1993). Another unique feature of grass cell-wall is that it contains noncellulosic glucans (Fig. 1-6 b) at specific developmental stages, particularly in the seed brans. These unbranched "mixed-linked" glucans (β-D-glucans) contain both (β1→3) and (β1→4)-linkages. Small amounts of other two hemicelluloses, xyloglucan and glucomannan, are also found in grasses (Carpita 1996).
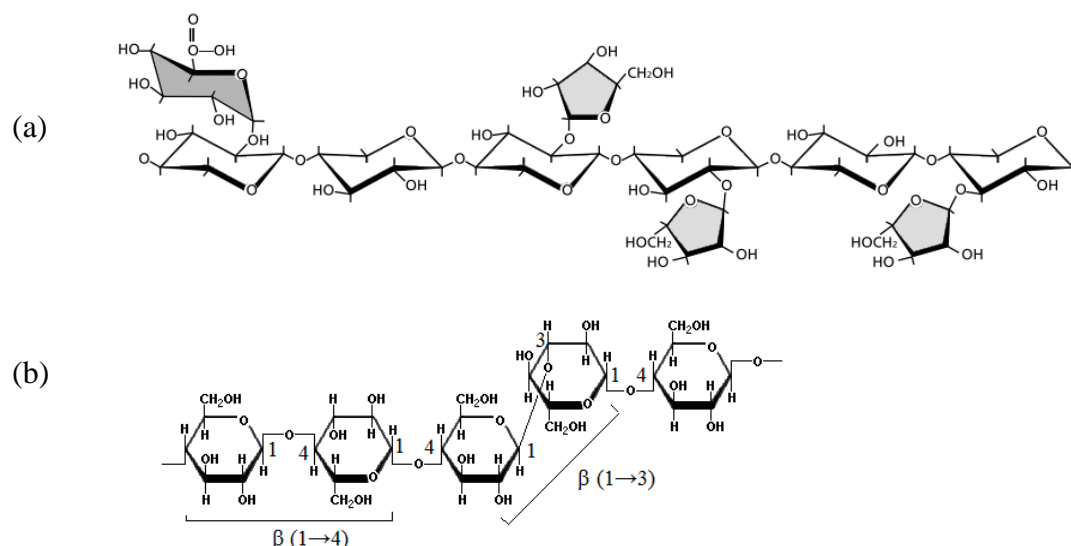
Figure 1-6: Structure of (a) glucuronoarabinoxylan (GAX) and (b) (1→3), (1→4)-β-D-glucan of grass cell-wall.

1.5.2.3 Pectin and pectic sugars

Two major constituents of grass pectins are homogalacturonan (PGA) and rhamnogalacturonan I (RG I) (Fig. 1-7). Homogalacturonan is a homopolymer of (1→4)-α-D-galacturonic acid, and the galacturonic acid residues are often methyl esterified. Rhamnogalacturonan I (RG I) contains a backbone of repeating heteropolymer (1→2)-α-L-rhamnosyl-(1→4)-α-D-galacturonic acid, and often RG I also contains arabinans, galactans, and highly branched arabinogalactans of various configurations and sizes as side chains (Fig. 1-7). All these side chains are attached to the O-4 of the rhamnosyl moieties of RG I (Carpita 1989; Shibuya and Nakane 1984).

1.5.2.4 Phenolics

The type II primary wall of monocots is characterized by the presence of substantial amount of phenolic substances (Fig. 1-8) that cross-link the glucuronoarabinoxylans (Carpita and Gibeaut 1993; Carpita 1996). The glucuronoarabinoxylans are cross-linked in walls by both esterified and etherified hydroxycinnamates and by other phenolic substances (Iiyama *et al.* 1993; Scalbert *et al.* 1985).
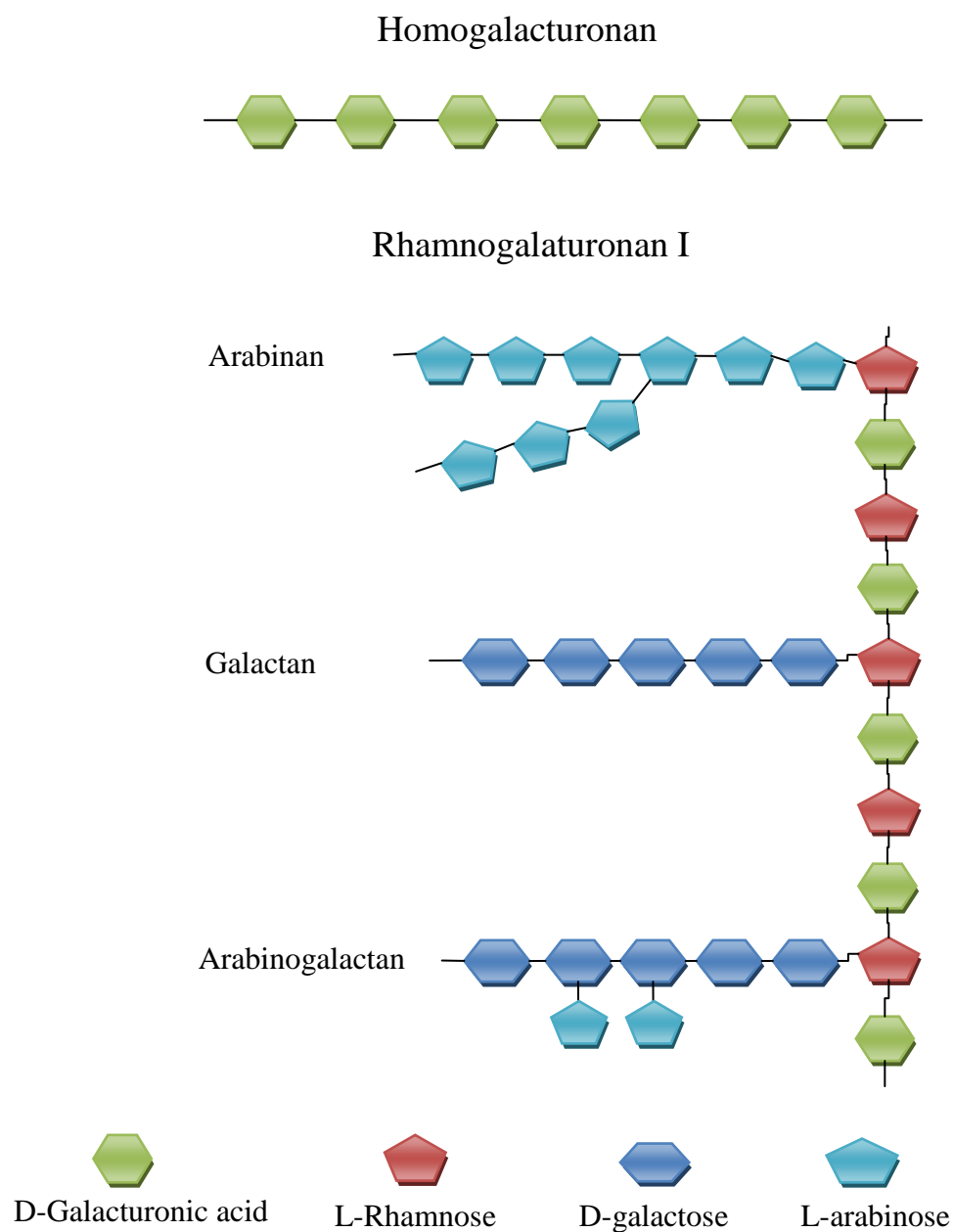
Figure 1-7: Schematic representation of homogalacturonan and rhamnogalacturonan I (RG I) of grass pectin (based on Carpita and Gibeaut 1993).

(a)

(b)
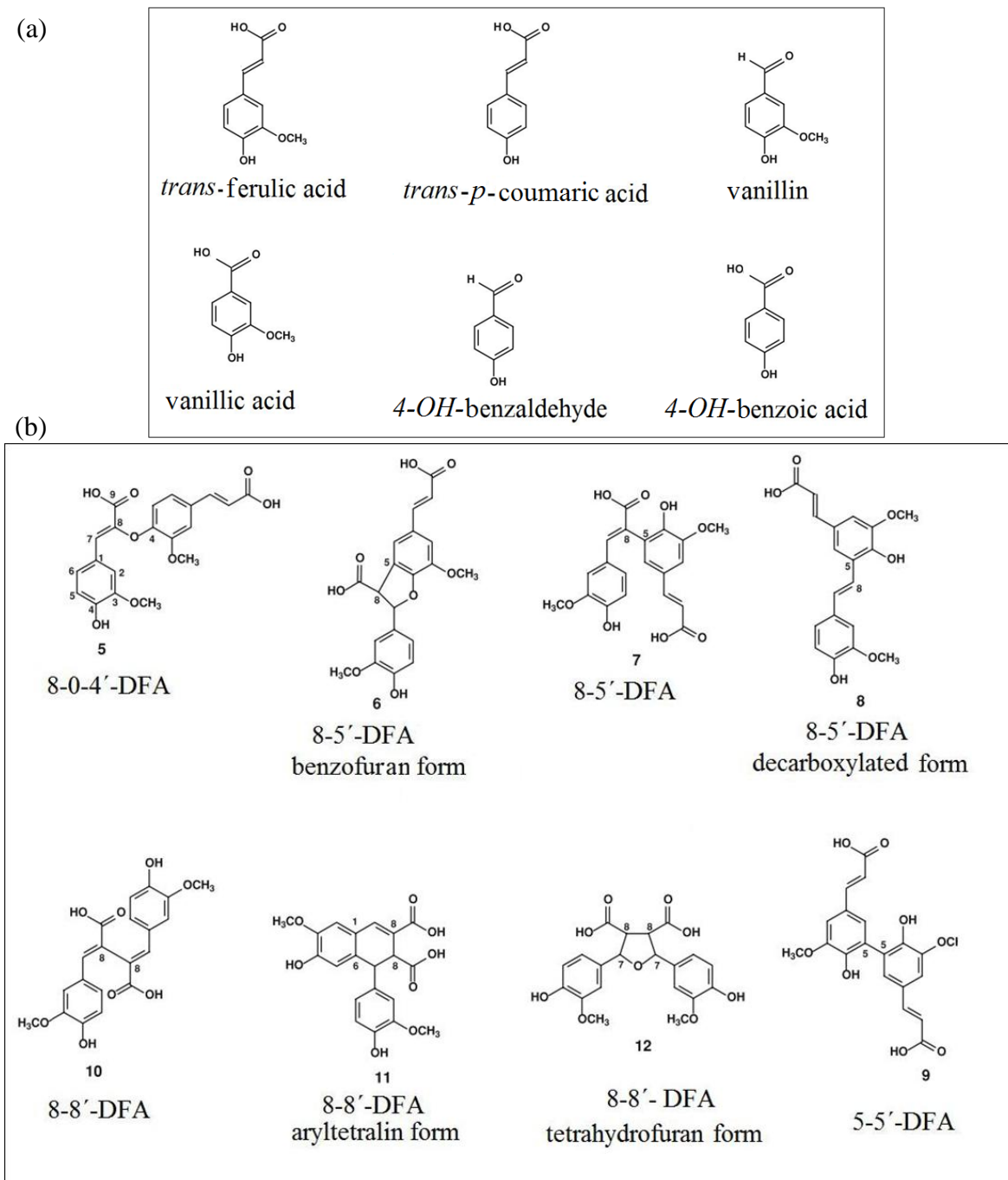
Figure 1-8: Various (a) monomeric phenols and (b) diferulic acids (DFA) present in grass cell-walls (Bunzel 2010).

1.5.2.5 Synthesis site of cell-wall components

Syntheses of various wall components take place in different organelles and membranes of the cell (Carpita and McCann 2000; Fig. 1-9). Synthesis of cellulose occurs at the surface of plasma membrane, while the syntheses of almost all other non-cellulosic polysaccharides
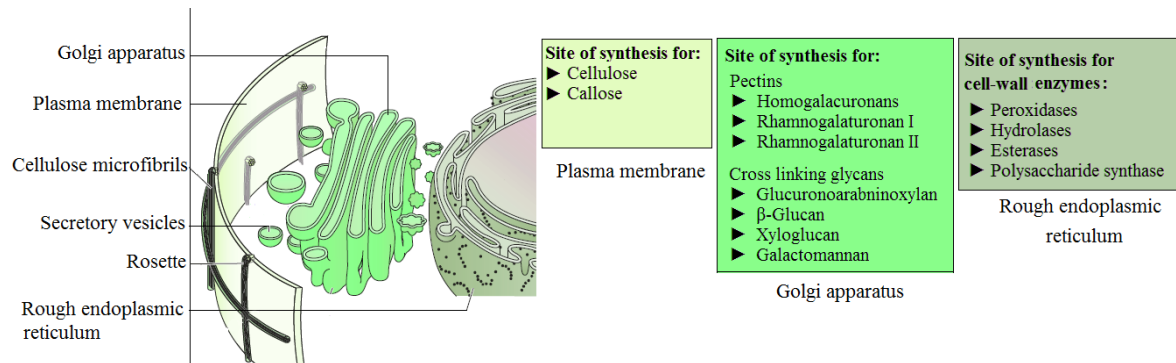
Figure 1-9: Biosynthesis of the major cell-wall components and wall modifying enzymes at the plasma membrane, Golgi apparatus and rough endoplasmic reticulum (modified after Carpita and McCann 2000, reproduced with permission from the American Society of Plant Biologists).

such as pectins (homogalacturonan, rhamnogalacturonan I, rhamnogalacturonan II) and cross-linking glycans (glucuronoarabinoxylan, β-glucan, xyloglucan, galactomannan) take place in the Golgi apparatus. Polysaccharide synthase along with some major wall-modifying enzymes e.g. esterases, peroxidases and hydrolases are synthesized at the rough endoplasmic reticulum. Synthesis of cell-wall proteins such as arabinogalactan proteins (AGPs), hydroxyproline-rich glycoproteins (HRGPs), proline-rich polypeptides (PRPs) and glycine-rich proteins (GRPs) also take place at the rough endoplasmic reticulum.

1.5.2.6 Are cell-wall compositions altered during salt stress to limit cell-wall extensibility?

Cell-wall loosening (acidification of apoplast) only partially answers the large growth inhibition in maize genotypes grown in the first phase of salt stress (Pitann *et al.* 2009;

Hatzig *et al.* 2010). Thus, it is supposed that an altered cell-wall composition in the first phase of salt stress may directly be involved in growth inhibition. Changes in cell-wall chemical properties as influenced by salt or drought stress have been documented for roots of some monocots (Piro *et al.* 2003; Leucci *et al.* 2008). Although the root represents the first organ in sensing salt stress, shoots are more sensitive to salt stress than roots (Munns and Sharp 1993). Salt stress-induced changes in enzyme activities in maize leaf cell-walls have been reported (Cramer *et al.* 2001; Geilfus *et al.* 2010). Still, there is a lack of information about the changes in cell-wall polymer composition that are relevant for extension growth during the first phase of salt stress in the growing shoots of maize genotypes differing in salt resistance.

1.5.3 Cross-linking of cell-wall polymers

Along with the chemical composition of cell walls, an understanding of wall cross-links is essential for any attempt to explain the control of wall extensibility and plant growth. Covalent cross-linking between/among wall polymers (Fig. 1-10) is an important biochemical mechanism for tightening wall components at the end of cell expansion (Iiyama *et al.* 1994). Wall polymers can be cross-linked via various diferulates (DFA) and triferulates (Bunzel 2010). The formation of cross-link between hemicellulosic polysaccharides via DFA-bridges and the increase in the amount of feruloylated polysaccharides in cell walls have been considered to cause a decrease in cell-wall extensibility (Fry 1979). In Poaceae, the increase in the wall-bound DFA and ferulic acid (FA) maintains a close correlation with a decrease in the cell-wall extensibility (Kamisaka *et al.* 1990; Parvez *et al.* 1997; Tan *et al.* 1991), and conversely the reduction in FA and DFA maintains the extensibility (Kawamura *et al.* 2000; Wakabayashi *et al.* 1997a, b).

There is evidence in maize that endogenous apoplastic H_2O_2 and peroxidase are responsible for the formation of diferulates by oxidatively coupling feruloyl groups

(Encina and Fry 2005). In fact, a transient increase in apoplastic peroxidase leads to termination of segmental elongation (De Souza and MacAdam 1998, 2001). The availability of apoplastic H_2O_2 and peroxidases limit formation of diferulates cross-links in the maize cell-wall (Grabber *et al.* 1995; Lindsay and Fry 2008; Burr and Fry 2009). The simultaneous increase of peroxidase activity and phenolic compounds in maize corroborates a role of this enzyme in oxidation of phenolics (Devi and Prasad 1996).

Legends:
❶ Direct ester linkage
❷ Direct ether linkage
❸ Hydroxycinnamic acid ester
❹ Hydroxycinnamic acid ether
❺ Ferulic acid bridge
❻ Dehydrodiferulic acid diester bridge
❼ Dehydrodiferulic acid diester bridge
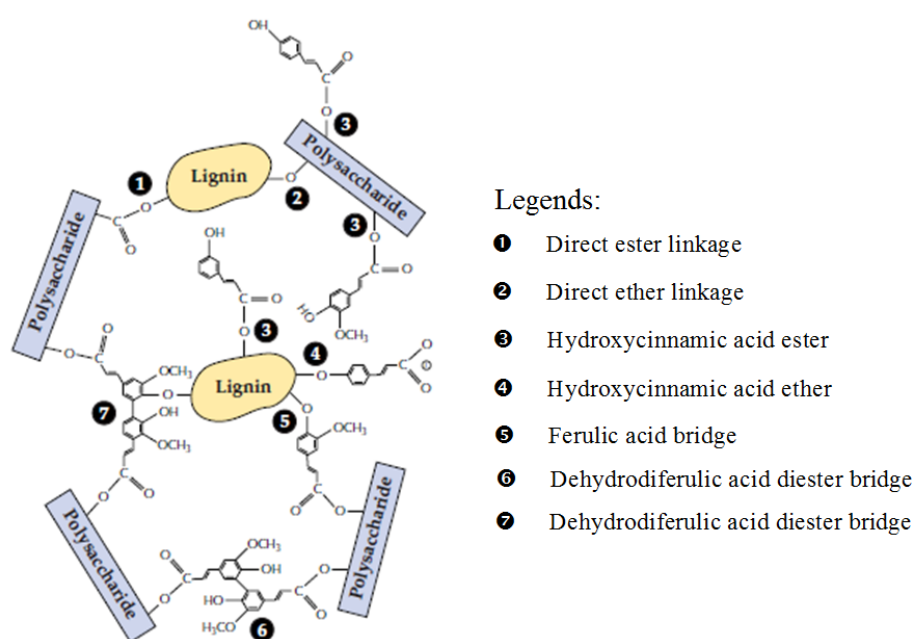
Figure 1-10: Schematic diagram showing possible covalent cross-links between/among wall polymers (Carpita and McCann 2000, reproduced with permission from the American Society of Plant Biologists).

A significant reduction of leaf and cell-wall extensibility was observed in expanding maize leaves with a concomitant reduction in leaf growth as a result of water stress imposed by PEG (Lu and Neumann 1998). Still, there is a lack of information about the changes in cell-wall polymers composition and cross-linking molecules that are relevant to extension growth of maize shoot during the first phase of salt stress. Moreover, the knowledge of a salt-induced change in cell-wall components, if any, in sensitive and newly developed resistant SR hybrids (Schubert *et al.* 2009) may help to find other genotypes with improved salt resistance in the first phase of salt stress.

Determination of the chemical composition of cell-wall polysaccharides is generally performed by some chemical analytical methods. However, before determining the chemical composition, the cell walls must first be isolated and cleaned from the intracellular contents. For that reason, a convenient and simple method for cell-wall isolation in necessary. A set of various laboratory protocols are required to determine cell-wall matrix polymers such as cellulose, hemicellulosic sugars, pectin, methylation of pectin, lignin and various monomeric phenols and diferulates.

In such a context, an experiment (**Experiment 1**) was conducted with the following objectives:

(i) To optimize a method of cell-wall isolation from maize shoot.

(ii) To standardize laboratory protocols for determining cellulose, hemicellulosic sugars, uronic acid, non-methylated uronic acid, degrees of methylation (methyl-esterification) of uronic acid, lignin, monomeric phenols and various diferulates.

Another experiment **(Experiment 2)** was carried out to test the influence of salt stress on leaf cell-wall components. The following three hypotheses were tested in this experiment:

(i) Leaf-growth inhibition in the first phase of salt stress is concomitant with changes in leaf cell-wall polysaccharides, which result in tightening of cell wall in growing leaves of two maize genotypes (Pioneer 3906 and SR 12) differing in salt resistance.

(ii) Leaf-growth reduction is accompanied by changes in leaf cell-wall monomeric phenols and various diferulates during the first phase of salt stress in two maize genotypes showing different salt resistance.

(iii) Salt stress-induced changes in cell-wall components are different in a salt-sensitive (Pioneer 3906) and a salt-resistant (SR 12) genotype.

2 Material and methods

2.1 Material and methods of Experiment 1

2.1.1 Plant cultivation

An experiment was conducted in plastic containers in a climate chamber. Maize (*Zea mays* L.) cv. Amadeo was grown in 70 L containers (each with 70 plants). The caryopses were soaked in an aerated 1 mM $CaSO_4$ solution for 24 h and allowed to germinate at $25^{o}C$ in the dark between two layers of filter paper moistened with 1.0 mM $CaSO_4$. On day 4, plants were exposed to the light. On day 6, 70 seedlings were transferred to each container with 70 L of a 1/4 concentrated nutrient solution. The composition of the full-strength nutrient solution is presented in Table 2-1 (Pitann *et al.* 2009).

Table 2-1: Composition of the full-strength nutrient solution

Macronutrients		Micronutrients	
Substrate	**Concentration**	**Substrate**	**Concentration**
$Ca(NO_3)_2$	2.5 mM	H_3BO_4	1.0 μM
K_2SO_4	1.0 mM	$MnSO_4$	2.0 μM
KH_2PO_4	0.2 mM	$ZnSO_4$	0.5 μM
$MgSO_4$	0.5 mM	$CuSO_4$	0.3 μM
$CaCl_2$	2.0 mM	$(NH_4)_6 Mo_7O_{24}$	0.01 μM
		Fe-EDTA	200 μM

Gradually the concentration of nutrient solution was increased to $^1/_2$, $^3/_4$ and full strength, respectively, in the following three consecutive days. On day 10, salt stress started with the addition of 25 mM NaCl directly to the root medium. Then on the following three days, the doses of NaCl were gradually increased to 50, 75 and 100 mM, respectively. Control treatment was maintained with 1 mM NaCl till harvest. On day 21, plants were cut at the

base of the shoot and the fresh mass of shoots and roots was recorded accordingly. Plants from each treatment were divided into three groups and each group was treated as a replicate (thus they were not in fact the biological replicates). Shoots of each group were chopped into smaller pieces and were shocked in liquid N_2 for short time to stop any enzyme activities. After then all shoot materials were stored at -80^oC till use.

2.1.2 Cell-wall isolation

2.1.2.1 Disruption of cells

The isolation of cell wall from the plant material was carried out according to the method of Goldberg (1985) with some modifications (Fig. 2-1). A number of trial runs were performed to find out the optimum quantity of plant materials and volume of different solutions during cell-wall isolation. In brief, 20 g plant material were added to a blender (type: Waring Blender, Waring, New Hartford, Connecticut, USA) together with 80 mL of 0.4 M ice-cold sucrose solution and then crushed. In total, 12 min crushing was performed with 12 breaks each with 1 min time and in-between cooling with ice slurry at less than 4^oC.

2.1.2.2 Recovering cell walls after elimination of contaminants

The crushed plant materials were centrifuged and sequentially extracted with 0.6 and 1.0 M sucrose solutions, respectively (Fig. 2-1). In order to eliminate any membrane components, the pellet was thoroughly washed with chilled 0.1% Triton X100. The suspension was then rinsed intensively with distilled water through nylon sieves with a mesh size of 405 and 250 μm, respectively, stacked on each other. Thorough rinsing of cell-wall pellets with distilled water was done to eliminate Triton X100 with cytoplasmic contaminants. Thus the cell wall isolated from 405 μm sieve was termed "> 405 μm cell-wall fraction" and that collected from 250 μm sieve was termed "250-405 μm cell-wall fraction". The extracted cell-wall pellets were freeze-dried and stored at $-80°C$ till further use.

Breaking of maize shoot-tissue in a Sorvall omnimixer; 20000 rpm for 12 min

Broken cells

Centrifugations with 0.4, 0.6 and 1 M sucrose; 700 g for 15 min

Supernatant discarded

Pellet

Centrifugation with 0.1% Triton; 1000 g for 10 min

Supernatant discarded

Pellet

Washing of pellets with H_2O through nylon sieves

405 μm
250 μm

Washed cell-walls fractions in two sieves

Freeze drying

Freeze dried cell-walls of > 405 μm fraction

Freeze-dried cell walls of 250-405 μm fraction

Figure 2-1: Diagrammatic presentation of cell-wall isolation from shoot tissue of maize cv. Amadeo.

2.1.3 Cellulose determination
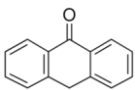
2.1.3.1 Principle

The cellulose determination was done by the method of Updegraff (1969) and Fry (1988) with minor modification. The method is based on elimination of lignin, hemicellulose and xylosans from the cell wall with the help of a reagent composed of acetic acid and nitric acid. Then the remaining cellulose is dissolved in 67% (v/v) H_2SO_4 and determined with the anthrone reagent. In the anthrone assay, glucose from the cellulose is dehydrated using concentrated H_2SO_4 to form furfural, which in turn condenses with anthrone to 10-keto-9,10 dihydroanthracene, which is a bluish green complex that can be measured calorimetrically at 620 nm using a spectrophotometer.
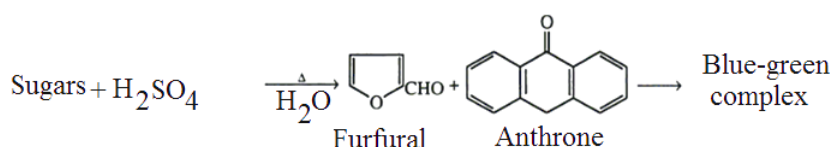
2.1.3.2 Chemicals required and preparation of reagents

Table 2-2: List of chemicals

Chemicals	Chemical formula	Source
Acetic acid	$(CH_3)_2CO$	Roth
Nitric acid	HNO_3	Sigma-Aldrich
Sulfuric acid	H_2SO_4	Merck
Anthrone		Merck

The anthrone reagent was prepared dissolving 200 mg of anthrone in 100 mL of concentrated H_2SO_4. The solution was prepared fresh daily and chilled for 2 h in a refrigerator prior to use.

To prepare the stock standard, 60 mg cellulose were dried for 6 h at 105°C and then cooled in a silica gel based desiccators. Exactly, 50 mg of dried cellulose were transferred into a 500 mL volumetric flask. Then content was dissolved in a 10 mL 67% (v/v) H_2SO_4 with gentle heat and volumed to 500 mL with distilled water to contain 100 µg cellulose mL^{-1}.

2.1.3.3 Optimized method for cellulose determination

In brief, 10 mg freeze-dried cell wall were suspended in acetic-nitric reagent (Acetic acid : Water : Nitric acid = 8 : 2 : 1) in test tubes. The tubes were then placed in a boiling water bath for 0.5 h to hydrolyze non-cellulosic polysaccharides. The cell-wall suspensions were then centrifuged for 5 min at 2500 *g*. The supernatants were discarded and the pellets washed two times with 10 mL each of water and acetone. The supernatants were discarded and the pellets were dried with a mild flow of pressed air. Dry pellets were hydrolyzed in 2 mL 67% (v/v) H_2SO_4 by placing the tubes on water bath for 1 h at 25^oC with continuous shaking. After then, 20 µL of 5 times diluted hydrolysates were transferred to Eppendorf tubes having 480 µL water inside. Then 1 mL chilled anthrone reagent was added to each Eppendorf tube and vigorously mixed with the vortex. All tubes were incubated in a boiling water bath for 5 min while the tubes were closed with cap. The tubes were then allowed to cool in an ice bath for 2-3 min. After keeping the Eppendorf tubes at room temperature for 5-10 min, the absorbance was read at 620 nm against a reagent blank (0.5 mL of bidistillated water + 1 mL anthrone). Stock standard for cellulose was prepared according to Updegraff (1969). Then the standards equivalent to 10, 15, 20, 30 and 40 µg mL^{-1} cellulose were subjected to the color reactions in the same way as cell-wall hydrolysates.

2.1.4 HPAEC-PAD analysis of cell-wall neutral sugars

2.1.4.1 Principle

High performance anion exchange chromatography with pulsed amperometric detection (HPAE-PAD or HPAEC-PAD) was used to separate and quantify neutral sugars in the cell wall. The amperometric detector measures a change in current due to oxidation, reduction, or complex formation of an analyte at the surface of an electrode (Henshall 1999). Carbohydrates are good candidates for electrochemical detection because they are easily oxidized on gold or platinum electrodes at a high pH (12-14). Oxyanions are formed from the neutral sugars at a high pH and these anions facilitate separation by their different ion exchange properties. Relative affinity of the analyte ion in competition with the eluent ion for the same exchange sites is the basis of ion exchange separation (Fig. 2-2 a). The longer retention time is expected when the affinity of the ion is higher and vice versa.

(a) (b)
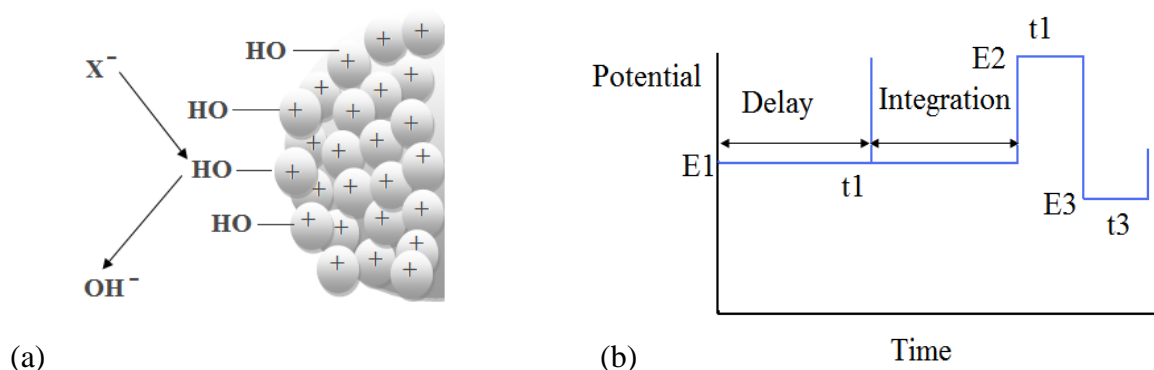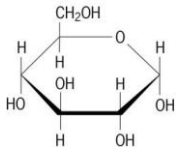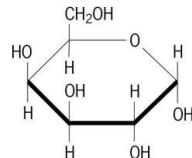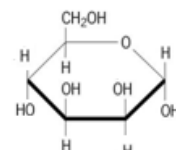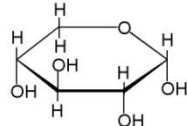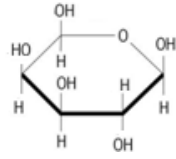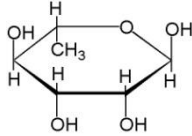
Figure 2-2: Diagrammatic presentation of (a) ion exchange separations based on the relative affinities of the analyte ions (X^-) in competition with the eluent ion (OH^-) for the same exchange sites (b) triple potential sequence used in PAD. A repeating sequence of a high positive potential followed by a high negative potential is used to clean electrode surface for consistent best quality measurement (modified after Henshall 1999).

The basic principle of PAD is illustrated in Fig. 2-2 b. PAD uses a repeating cycle of high positive (E2) and high negative potentials (E3) following each measurement to clean electrode surface that ensures very high quality response. A specific potential (E1)

appropriate for the particular analyte is used to get the detector signal by integrating the current for a fixed length of time and storing the resulting charge in a sample-and-hold amplifier until the next measurement (Henshall 1999).

2.1.4.2 Chemicals required

Table 2-3: List of chemicals

Chemicals	Formula	Source
Sulfuric acid	H_2SO_4	Merck
50% (w/v) sodium hydroxide	NaOH	Sigma-Aldrich
D-(+)-Glucose		Sigma-Aldrich
D-(+)-Galactose		Sigma-Aldrich
D-(+)-Mannose		Fluka
D-(+)-Xylose		Sigma-Aldrich
L-(+)-Arabinose		Sigma-Aldrich
L-Rhamnose		Fluka

2.1.4.3 Optimized method for cell-wall neutral sugar analysis

2.1.4.3.1 Cell-wall hydrolysis

Acid hydrolysis was performed according to the method described by Willför *et al.* (2009). In brief, 10 mg of freeze-dried cell wall were weighed in a hydrolysis tube. Then, 200 µL of 72% (w/w) sulfuric acid were added and the sample was pre-hydrolyzed at 30 ^{o}C in a water bath for 1 h. The samples were then transferred into 25 mL volumetric flask together with 5.6 mL of ultra-pure water. Flasks were sealed with aluminum foil and autoclaved for 60 min at 120°C. After hydrolysis, the samples were cooled and filtered through a 0.45 µm PET membrane filter (membraPure GmbH, Germany).

2.1.4.3.2 Optimized HPAEC-PAD for neutral sugars analysis

Neutral sugars from the cell wall were determined following high-performance anion-exchange chromatography (HPAEC-PAD) analysis as suggested by Willför *et al.* (2009) after some modifications. The HPAEC-PAD analysis of non-cellulosic neutral sugars was performed using a CarboPac PA-10 column (analytical column 2 mm $\times$ 250 mm and guard column 2 mm $\times$ 50 mm) coupled with a pulsed amperometric detector (Dionex ED 50 gold electrode). After injection of the 20 µL sample the monosaccharides were isocratically separated using 2 mM NaOH at a flow rate of 0.25 mL min^{-1}. Chromeleon software was used to process the data.

2.1.5 Analysis of total uronic acid
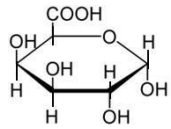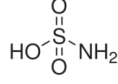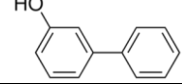
2.1.5.1 Principle

Generally total uronic acid is determined using colorimetric methods after first hydrolyzing the cell-wall polysaccharides in concentrated sulfuric acid (Ahmed and Labavitch 1977; Selvendran *et al.* 1979). Nonetheless, all these methods have some pitfalls in determining total uronic acid concentration from cell walls. Colorimetric determination of uronic acids

may be influenced by neutral-sugars of the cell wall and their degradation products from acid hydrolysis. Filisetti-Cozzi and Carpita (1991) proposed a procedure that solves the problem. With this new method, uronic acids can be determined in presence of ten times their weight of neutral sugars in the cell-wall hydrolysate. Thus, this technique is currently the colorimetric method of choice. The sulfamate suppresses brown coloration from the cell-wall neutral sugars, while tetraborate augments the sensitivity of the reaction with uronic acids. A pink color develops after addition of *m*-hydroxydiphenyl solution, which can be measured at 525 nm against the reagent control.

2.1.5.2 Chemicals required and preparation of reagents

Table 2-4: List of chemicals

Chemicals	Formula	Source
Sulfuric acid	H_2SO_4	Merck
Sodium hydroxide	NaOH	Sigma-Aldrich
Sodium tetraborate	$Na_2B_4O_7$	Merck
D-galacturonic acid		Fluka
Sulfamic acid		Fluka
m-hydroxydiphenyl		Aldrich

Exactly 150 mg of *m*-hydroxydiphenyl were weighed into a 100 mL volumetric flask. Then the content was dissolved in < 100 mL of 0.5% (w/v) NaOH and the final volume was adjusted to 100 mL with the same. The final reagent mixture was stored in a dark bottle at 4°C, and in this state the solution may stable for around 1 month (Melton and Smith 2001).

Sulfamic acid (molecular weight, 97.09) amounting to 38.84 g was weighed in a 100 mL volumetric flask and after addition of 50 mL of water the content was stirred vigorously. Saturated KOH (30 g of KOH were dissolved into 20 mL of water) was added drop-wise until the sulfamic acid had been dissolved. The sulfamic acid solution was allowed to cool and then the pH was carefully adjusted to 1.6 with saturated KOH. The final volume of 100 mL was adjusted with some drops of water to give a final concentration of 4 M. The reagent was then stored at room temperature.

2.1.5.3 Optimized method for uronic acid determination from maize shoot cell-wall

Cell walls were first hydrolyzed using the method of Ahmed and Labavitch (1977) and the uronic acid concentrations determined using the method of Filisetti-Cozzi and Carpita (1991) with little modifications suggested by Melton and Smith (2001). In brief, 5 mg of cell walls were transferred to a borosilicate glass tube and 1 mL concentrated sulfuric acid added to it. A reagent control tube was set up with only 1 mL concentrated sulfuric acid. The rack with tubes was placed on ice slurry on a magnetic stirrer. The contents were stirred for 5 min by placing small spin bars in each of the tubes. Stirring continued for another 3 times 5 min with the successive addition of 1.0 mL concentrated sulfuric acid, 0.5 mL + 0.5 mL water. Then the content of each tube was diluted into 10 mL from which 1800 µL hydrolysate were transferred into an Eppendorf tube and centrifuged for 5 min at 36000 g at 4°C to get clear hydrolysate. There were three and two 15 mL borosilicate glass tubes for each hydrolysate and reagent control, respectively. Aliquots of 400 µL clear suspension from each hydrolysate and reagent control were placed into the respective tubes. Then 40 µL of 4 M sulfamic acid/potassium sulfamate solution (pH 1.6) were added. After vortexing the content, 2.4 mL of 75 mM sodium tetraborate in sulfuric acid were added followed by vigorous shaking with vortex. Then, the tubes were placed in a 100°C water bath for 20 min and then cooled by plunging tubes into an ice bath for 10 min.

Exactly 80 µL *m*-hydroxydiphenyl solution were added to two tubes of each sample and the two reagent control tubes. The third tube of each sample received 80 µL of 0.5% NaOH instead of *m*-hydroxydiphenyl (this was the sample control). The content of the tubes was vortexed three times and allowed to stand for 10 min to develop a pink color complex. Absorbance was taken at 525 nm against the reagent control. Standard curve was made using D-galacturonic acid as a standard with the concentrations of 2.5, 5.0, 10.0, 15.0, 20.0 and 30.0 µg/400 µL.
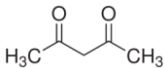
2.1.6 Determining the degree of methylation of uronic acid and the concentration of methylated uronic acid

2.1.6.1 Principle

Methyl-esters of uronic acid are saponified to yield methanol and the free acids with a modified procedure of Wood and Siddiqui (1971). Methanol is oxidized to formaldehyde by acidic permanganate. Formaldehyde is then condensed with pentane-2,4-dione (acetylacetone) and ammonia to give the yellow product, 3,5-diacetyl-1,4-dihydro-2,6-methylpyridine. Oxidation in the presence of sulfuric acid followed by reduction of excess permanganate with sodium arsenite allows sensitive determination of methanol. Paired assays of uronic acid give the proportion of methylated uronic acid.

2.1.6.2 Chemicals required and preparation of reagents

Table 2-5: List of chemicals

Chemicals	Formula	Source
Sulfuric acid	H_2SO_4	Merck
Sodium hydroxide	NaOH	Sigma-Aldrich
Potassium permanganate	$KMnO_4$	Fluka
Sodium arsenite	$NaAsO_2$	Sigma-Aldrich
Pentane-2,4-dione (acetyl acetone)		Fluka

NH$_4$OH (0.2 moles, 13.5 mL of 14.8 M stock solution of NH$_4$OH) was added to 50 mL of water and the content was gently stirred in a 100 mL beaker placed in an ice bath. Then 0.25 mole glacial acetic acid (14.4 mL of 17.4 M stock) was added. After the solution had cooled to ambient temperature, the content was brought to 100 mL with distilled water and this was the 2.0 M CH$_3$COONH$_4$/0.5 M CH$_3$COOH solution. Pentane-2,4-dione (202 mg) was poured into a 100 mL volumetric flask and then brought up to the mark with the freshly made 2.0 M CH$_3$COONH$_4$/0.5 M CH$_3$COOH.

2.1.6.3 Optimized method for determining degree of methylation of maize cell-wall

Exactly 5 mg of cell-wall material and 1.125 mL of distilled water were filled into 2.0 mL Eppendorf centrifuge vials. Afterwards, 375 µL of 1.5 M NaOH were added to each of the vials with occasional vortexing for 30 min. The vials were chilled on ice slurry and then 375 µL of 4.5 M H$_2$SO$_4$ were added and the vials were placed on ice slurry for 10 min. The samples were then centrifuged for 10 min at 0°C at 36000 *g*. Afterwards, 1.0 mL of the clear saponified acidic supernatant was pipetted directly to the bottom of a 10 mL glass tube placed on ice slurry.

After addition of 200 µL of 2% (w/v) KMnO$_4$ to the saponified acidic supernatant, the vials were kept chilled on ice for 15 min. Extra care was taken not to run any trace of the KMnO$_4$ down the sides of the tube. Then exactly 200 µL of Na-arsenite reagent (0.5 M in 0.06 M H$_2$SO$_4$) were added and after vortexing the sample was allowed to stand at ambient temperature for 60 min. Finally, 2.0 mL of a freshly prepared pentane-2,4-dione reagent (0.02 M pentane-2,4-dione in 2.0 M CH$_3$COONH$_4$/0.5 M CH$_3$COOH) were added to each vial and vortexed quickly. The tubes were capped with marbles and heated at 60°C for 15 min and then allowed to cool down to room temperature for full color development. The absorbance of yellow chromagen was measured at 412 nm. By this way, methanol release

(mmol) from a specific amount of cell wall was calculated. The degree of methylation of uronic acids was then calculated based on the uronic acid concentrations of cell wall. Using the data of degree of methylation of uronic acids in cell wall, the concentrations of methylated uronic acids were quantified. The concentrations of non-methylated uronic acids were calculated by subtracting the values for concentrations of methylated uronic-acids from the values of concentrations of total uronic acids.

2.1.7 Determination of lignin

2.1.7.1 Principle

A spectrophotometric method was used for determining the lignin concentration by dissolving cell walls in acetyl-bromide reagent ($CH_3COBr : CH_3COOH = 1 : 3$, v/v) and measuring the absorbance at 280 nm (Johnson *et al.* 1961). The method results in the formation of acetyl derivatives of unsubstituted OH groups of lignin macromolecule and Br replacement of α-carbon OH groups making the lignin molecule soluble in acetic acid (Fig. 2-3).
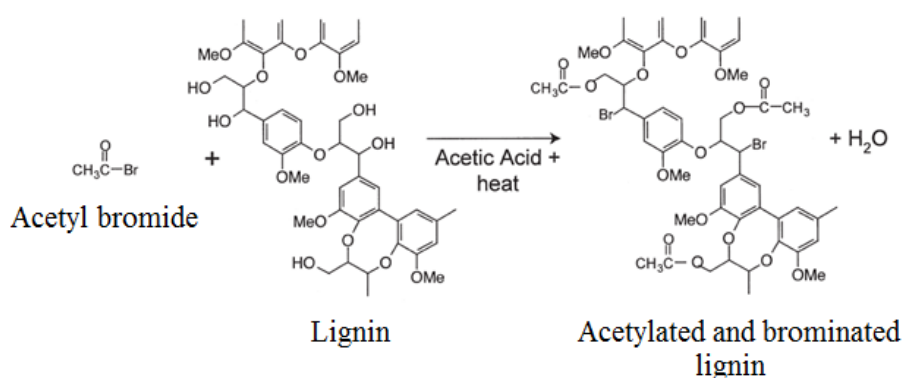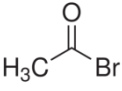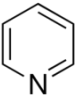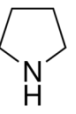
Figure 2-3: Reaction mechanisms of for acetyl derivatization of lignin by acetyl bromide reagent in order to solubilize lignin in acidic solution (Hatfield and Fukushima 2005).

However, proteins and substituted cinnamic acids (e.g. ferulic acid, *p*-coumaric acid) in grass cell-walls may interfere with the lignin determination. Nearly 90-95% of these

cinnamic acid constituents can be removed by a pretreatment of cell-wall with pyridine : pyrrolidine (1 : 1, v/v). Finally, washing of cell-wall materials with methanol and subsequently with hot water can efficiently remove proteins. This allows more precise determination of lignin by the modified acetyl bromide method (Morrison and Stewart 1995).

2.1.7.2 Chemicals required

Table 2-6: List of chemicals

Chemicals	Formula	Source
Acetyl bromide	H₃C—C(=O)—Br	Sigma-Aldrich
Sodium hydroxide	NaOH	Fluka
Hydroxylamine	NH_2OH	Aldrich
Glacial acetic acid	CH_3COOH	Merck
Pyridine	(pyridine ring)	Sigma-Aldrich
Pyrrolidine	(pyrrolidine ring)	Fluka
Methanol	CH_3OH	Roth

2.1.7.3 Optimized method for lignin determination

2.1.7.3.1 Removal of non-lignin phenolics and protein

Exactly 20 mg freeze-dried cell-wall materials were taken into a glass vial and 1 mL of pyrrolidine : pyridine (1 : 1, v/v) was poured to it. Then all vials were closed with the teflon-lined cap and were placed in a water bath at 80°C for 18 h (Mansson and Samuelsson 1981). Then the reaction mixture was transferred to a 15 mL centrifuge tube with the help of 5 mL methanol. After centrifuging at 350 *g* for 20 min, the solution was

pipetted out and the residue was washed with methanol and recentrifuged for further 5 times each with 4 mL methanol. After discarding the methanol, 4 mL of water were added to cell-wall residues. All tubes were then placed in a water bath at 70°C for 3 h by keeping a glass marble on top of each tube. All tubes were then recentrifuged as before and the supernatants were discarded. The pellet was washed with cold water and finally with the methanol followed by centrifugation. Then the resultant pellets were transferred into the screw capped tubes and were placed in an oven to dry the pellets at 50°C overnight.

2.1.7.3.2 Modified optimized acetyl bromide method to determine lignin in cell wall

Individual samples were removed from the oven and 2.5 mL of freshly prepared acetyl bromide reagent (acetyl bromide : glacial acetic acid = 1 : 3, v/v) were added. The tubes were capped immediately with a PTFE-coated silicone cap and heated in water bath at 50°C for 4 h with occasional shaking. Then the sample was quantitatively transferred to a 50 mL volumetric flask with a reagent mixture containing 10 mL of 2 M NaOH and 12 mL of acetic acid. Exactly 1750 μL of 0.5 M hydroxylamine were added to each flask, and samples were diluted to 50 mL with glacial acetic acid. The absorption of the final solution was measured at 280 nm. Finally the lignin concentration was determined using the following formulas (Morrison 1972):

(i) Absorbance value = $\dfrac{\text{Absorbance of sample} - \text{Absorbance of blank}}{\text{Concentration of sample (g L}^{-1})}$

(ii) Lignin concentration (mg g^{-1} cell wall) = (33.6 × Absorbance value) − 11.1

2.1.8 Determination of cell-wall esterified phenolics using RP-HPLC

2.1.8.1 Principle
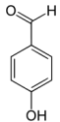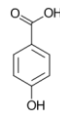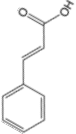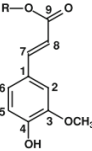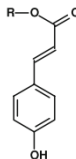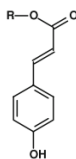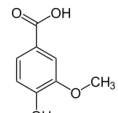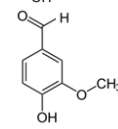
Wall-bound phenolics are released by sequential alkaline hydrolysis of isolated cell-wall material under progressively more vigorous conditions (Hartley and Morrison 1991). The sequential treatments to extract the cell wall-bound esterified phenolics is as follows: 0.1 M NaOH for 1 h, 0.1 M NaOH for 24 h, 1 M NaOH for 24 h and finally 2 M NaOH for another 24 h. The general reaction mechanism of releasing cell-wall esterified phenolics under alkaline condition is presented below.
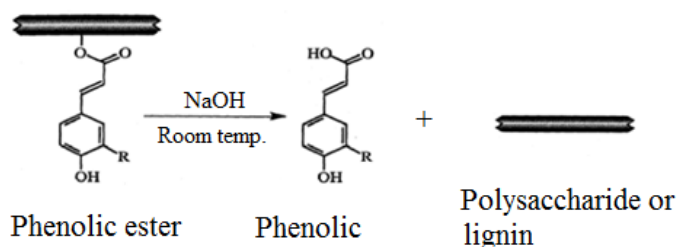
Reverse phase high performance liquid chromatography (RP-HPLC) with ultra violet (UV) detection can be used successfully in the separation and determination of diferulic acids, monomeric cell wall phenolic acids and aldehydes (Waldron *et al.* 1996).

2.1.8.2 Chemicals required

Table 2-7: List of chemicals

Chemicals	Formula	Source
HPLC grade water	H_2O	Roth
50% (w/v) sodium hydroxide	NaOH	Sigma-Aldrich
Methanol, ROTISOLV® Ultra LC-MS	CH_3OH	Roth
Acetonitrile, ROTISOLV® Ultra LC-MS	CH_3CN	Roth
p-OH-benzaldehyde		Sigma-Aldrich
p-OH-benzoic acid		Sigma-Aldrich
trans-cinnamic acid		Sigma-Aldrich
trans-ferulic acid		Sigma-Aldrich
trans-p-coumaric acid		Sigma-Aldrich
Trifluoroacetic acid		Sigma-Aldrich
trans-p-coumaric acid		Sigma-Aldrich
Vanillic acid		Fluka
Vanillin		Fluka

2.1.8.3 Optimized method for the determination of cell-wall esterified phenolics

The procedure described by Waldron *et al.* (1996) was followed with some modifications to fit the extraction procedure to the micro level. Exactly 30 mg cell-wall materials were taken in an Eppendorf tube and then 600 µL of 0.1 M anaerobic (degassed with N_2) NaOH were added. After addition of 6 µg *trans*-cinnamic acid as an internal standard, the liquid was covered with N_2 gas and then the lid closed tightly. Afterwards all tubes were placed in a water bath for 1 h at 25^oC with continuous shaking in darkness.

The Eppendorf tubes containing alkaline hydrolysates were centrifuged at 36000 *g* for 10 min and afterwards the supernatant was carefully collected in a new tube with a micropipette. The solution was acidified with HCl to a pH < 2 and the phenols in acidified supernatant were extracted with three volumes of acetic ethyl-ester. After extraction, acetic ethyl-esters were removed in a vacuum evaporator and the remaining solid was dissolved in 300 µL of 50% (v/v) aqueous methanol for subsequent analysis in HPLC.

The cell-wall materials remaining in the Eppendorf tube after first extraction were further extracted sequentially with 0.1 M NaOH for 24 h, 1 M NaOH for 24 h, and 2 M NaOH for 24 h. The same procedure described before was followed to get the sample ready for HPLC-analysis. Thus from each cell-wall sample, four HPLC vials were ready for the final analyses.

The standards of various monomeric phenols were dissolved in 50% (v/v) aqueous methanol; *trans*-cinnamic acid was added to the mixtures as an internal standard. An aliquot of 25 µL was injected by the autosampler (Dionex A550) and analyzed on a RP-HPLC column (LiChrospher ®100 RP-18 end capped 5 µm column (250 mm × 4.6 mm), Techlab, Erkerode, Germany). The gradient profile developed by Waldron *et al.* (1996) for the separation of cell-wall esterified phenolic monomers and dimers was used with

modification: initially 90% Solvent A (10% (v/v) aqueous acetonitrile plus TFA to 1 mM), 5% Solvent B (80% (v/v) aqueous methanol plus TFA to 1 mM) and 5% Solvent C (80% (v/v) aqueous acetonitrile plus TFA to 1 mM); linear gradient over 25 min to 26% A, 37% B and 37% C; linear gradient over 5 min to 0% A, 50% B and 50% C. Linear gradient over 15 min to 90% A, 5% B and 5% C; this composition of eluent was kept for further 10 min. Peak area was recorded at 210, 265, 280 and 325 nm.

Quantitation was based on integration of peak areas at 280 nm. Monophenols were quantified based on their standard substances. Phenolic dimers were identified through analysis at 210, 265, 280 and 325 nm. Four different diferulic acids (8-5´-DFA, 5-5´-DFA, 8-0-4´-DFA and 8-5´-DFA (benzofuran form) were quantified with the following formulae (Waldron *et al.* 1996):

(i) *trans*-FA equivalent of DFA $= \dfrac{\text{Peak area of DFA at 280 nm} \times \text{amount of } trans\text{-FA } (\mu g\ g^{-1})\ \text{on that particular run}}{\text{Area of } trans\text{-FA}}$

(ii) DFA ($\mu g\ g^{-1}$ cell wall) $= \dfrac{trans\text{-FA equivalent of DFA} \times \text{RF of } trans\text{-FA according to Waldron } et\ al.\ (1996)}{\text{RF of that DFA according to Waldron } et\ al.\ (1996)}$

(a) 8-5´-DFA ($\mu g\ g^{-1}$ cell wall) $= \dfrac{trans\text{-FA equivalent of 8-5´-DFA} \times 0.36}{0.18}$

(b) 5-5´-DFA ($\mu g\ g^{-1}$ cell wall) $= \dfrac{trans\text{-FA equivalent of 5-5´-DFA} \times 0.36}{0.21}$

(c) 8-0-4´-DFA ($\mu g\ g^{-1}$ cell wall) $= \dfrac{trans\text{-FA equivalent of 8-0-4´-DFA} \times 0.36}{0.14}$

(d) 8-5´-DFA (benzofuran form) ($\mu g\ g^{-1}$ cell wall) $= \dfrac{trans\text{-FA equivalent of 8-5´-DFA (benzofuran form)} \times 0.36}{0.12}$

Here, FA = *trans*-ferulic acid; DFA = diferulic acid; RF = response factor

2.1.9 Synthesis of diferulates using horse radish peroxidase (HRP) and ferulic acid

An attempt was made to prepare some diferulates in the laboratory (Ward *et al*. 2001). Oxidation of *trans*-ferulic acid was done with peroxidase from horseradish (SERVA Electrophoresis; EC 1.11.1.7; 1000 U mg^{-1}) in 100 mM citric acid + KOH buffer, pH 3.5, in a total reaction volume of 1 mL in the Eppendorf vial. H_2O_2-dependent inactivation of horseradish peroxidase was prevented by stepwise addition of H_2O_2 in aliquots of 100 nmol min^{-1} for a period of 30 min. Three concentrations of *trans*-FA (0.1, 0.3 and 1.2 mM) were tested with 1 μM enzyme. Two controls were set, first one with *trans*-ferulic acid and H_2O_2 in the assay medium but without enzyme; second one with *trans*-ferulic acid in the assay medium but without enzyme and H_2O_2. One min after addition of last aliquot of H_2O_2 the reaction mixture was extracted with three volumes of acetic ethyl-ester. The extract was dried in a vacuum evaporator and the remaining solid was dissolved in 50% (v/v) aqueous methanol for subsequent analysis with RP-HPLC.

2.1.10 Statistical analysis

In Experiment 1, plants were grown in three groups in one pot per treatment. Results are given as arithmetic means of these three groups with standard errors of means (SE). As there was a lack of true biological replication no test was performed for determining significant differences between treatments.

2.2 Material and methods of Experiment 2

2.2.1 Plant cultivation

Maize (*Zea mays* L. hybrids Pioneer 3906 and SR 12) were grown in hydroponics in a climate chamber with two treatments (control with 1 mM NaCl and salt treatment with 100 mM NaCl) and four replications in each. Plants of each genotype were cultivated in 10 L plastic containers, each container with eight plants. The caryopses were soaked in an aerated 1 mM $CaSO_4$ solution for 24 h. Germination took place in the dark at 25°C in sandwich culture. The caryopses were placed between two layers of filter paper moistened with 0.5 mM $CaSO_4$ solution. On day 4, plants were exposed to the light. On day 7, eight seedlings were transferred to each container with 10 L of a one-fourth concentrated nutrient solution. The composition of the full-strength nutrient solution was as described by Pitann *et al.* (2009): 2.0 mM $Ca(NO_3)_2$, 0.2 mM KH_2PO_4, 1.0 mM K_2SO_4, 0.5 mM $MgSO_4$, 2.0 mM $CaCl_2$, 1 mM NaCl, 1.0 μM H_3BO_4, 2.0 μM $MnSO_4$, 0.5 μM $ZnSO_4$, 0.3 μM $CuSO_4$, 0.01 μM $(NH4)_6Mo_7O_{24}$, 200 μM Fe–EDTA. On day 9 and 11, the concentration of nutrient solution was increased to half and full strength, respectively. The salt treatment started on day 14 with 25 mM NaCl. It was increased daily with 25 mM NaCl increments till a concentration of 100 mM NaCl was reached on day 17 and maintained till harvest on day 23. The nutrient solution was changed on day 17, 19 and 21. The control treatment was maintained with 1 mM NaCl from day 14 till harvest. The plants were grown with 200 W m^{-2} (Philips Master HP1-T Plus) light intensity at 26°C for 16 h and 18°C for 8 h. The relative humidity was 70%.

2.2.2 Harvesting technique

Plants were harvested on day 23 after 6 d application of 100 mM NaCl to ensure that the plants were in the first phase of salt stress at harvest. Shoot fresh mass was recorded on the

day of harvest. The shoot was divided into upper shoot (cut below the blade of 4th leaf) and the lower shoot (below the 4th leaf) (Fig. 2-4). However, the 4th leaf, which had already expanded, was excluded from the analysis to focus more on the expanding tissues. Then the basal 10 cm of the upper shoot (5th and above leaf blades) were separated as the youngest shoot and the rest part of the upper shoot without the basal 10 cm segment was designated as the young shoot. After chopping with scissors, shoot material was immersed in liquid nitrogen for a short time to stop any enzymatic activity. Afterwards the samples were stored at -80°C till further use.
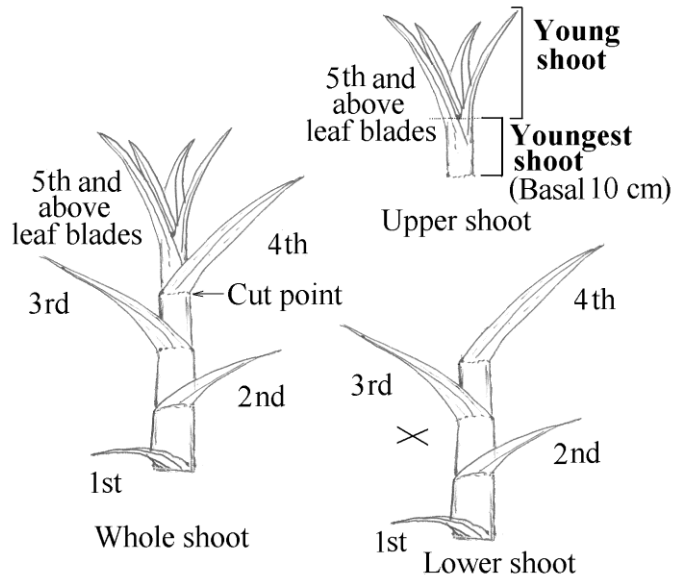
Figure 2-4: Schematic presentation of shoot separation. The whole shoot was divided into upper shoot (above 4th leaf) and the lower shoot. The 4th leaf, which was already expanded, was excluded from the analysis to focus more on the expanding tissues. Thus the basal 10 cm of the upper shoot were separated as the youngest shoot and the remaining part of the upper shoot was designated as young shoot.

2.2.3 Extraction of cell wall

Extraction of cell wall was done following the optimized standard method described in the Experiment 1 in section 2.1.2. Cell wall of the 250-405 μm fraction was analyzed for the chemical composition.

2.2.4 Analyses of cellulose, neutral sugars, total uronic acid and degree of methylation of uronic acid

Cellulose, neutral sugars, total uronic acid and degree of methylation of uronic acid were analyzed following the optimized standard method described in the experiment in section 2.1.3, 2.1.4, 2.1.5 and 2.1.6, respectively.

2.2.5 Analysis of cell-wall phenolics

2.2.5.1 Extraction of phenolics from cell wall

The method used in the Experiment 1 (section 2.1.8.3) was modified to a single-step extraction (Jung and Shalita-Jones 1990). In brief, 10 mg cell-wall materials were taken in an Eppendorf tube and then 600 μL of 2 M anaerobic (degassed with N_2) NaOH were added. After addition of *trans*-cinnamic acid as an internal standard, the liquid was covered with N_2 gas and then the lid closed tightly. Afterwards all tubes were placed in a water bath for 24 h at 39°C (Jung and Shalita-Jones 1990) with continuous shaking in darkness. The tubes were centrifuged at 36000 *g* for 10 min and afterwards the supernatant was carefully collected in a new tube with a micropipette. The solution was acidified with HCl to a pH < 2 and the phenols in acidified supernatant were extracted with three volumes of acetic ethyl-ester. After extraction, acetic ethyl-ester was removed in a vacuum evaporator and the remaining solid was dissolved in 300 μL of 50% (v/v) aqueous methanol for subsequent analysis in HPLC.

2.2.5.2 Analysis of phenols by HPLC

This method was also slightly modified from that described in the Experiment 1 (section 2.1.8).The standards of various monomeric phenols (vanillin and vanillic acid were from Fluka; *trans*-ferulic acid, *trans-p*-coumaric acid, *trans*-cinnamic acid, *p-OH*-benzoic acid and *p-OH*-benzaldehyde were from Sigma-Aldrich) and differnt diferulates (a kind gift

from Prof. Dr. Mirko Bunzel, Department of Food Science and Nutrition, University of Minnesota, USA) were dissolved in 50% (v/v) aqueous methanol; *trans*-cinnamic acid was added to the mixtures as an internal standard. An aliquot of 17 μL was injected by the autosampler (Dionex A550) and analyzed on a RP-HPLC column (LiChrospher ®100 RP-18 end capped 5 μm column (250 mm × 4.6 mm), Techlab, Erkerode, Germany). The gradient profile developed by Waldron *et al.* (1996) for the separation of cell-wall esterified phenolic monomers and dimers was used with modification: initially 90% Solvent A (10% (v/v) aqueous acetonitrile plus TFA to 1 mM), 5% Solvent B (80% (v/v) aqueous methanol plus TFA to 1 mM) and 5% Solvent C (80% (v/v) aqueous acetonitrile plus TFA to 1 mM); linear gradient over 25 min to 26% A, 37% B and 37% C. Linear gradient over 5 min to 0% A, 50% B and 50% C; this composition of eluent was kept for further 5 min. Linear gradient over 15 min to 90% A, 5% B and 5% C; this composition of eluent was kept for further10 min. Phenolic monomers and dimers were identified through analysis at 210, 265, 280 and 325 nm. Quantitation was based on peak areas at 280 nm. For the quantification of monomeric phenols except *cis*-ferulic acid, a two-point calibration curve was used with the standard substances. An attempt to produce *cis*-ferulic acid by exposing *trans*-ferulic acid solution (in a diluted ammonia) to UV radiation was unsuccessful possibly due to the destruction of the structure of *trans*-ferulic acid at low wave UV (280 nm) radiation. Thus a different procedure was followed to determine *cis* isomer of ferulic acid using the following two formulae:

$$\text{(i) } \textit{trans}\text{-FA equivalent of } \textit{cis}\text{-FA (µg g}^{-1}\text{ cell wall)} = \frac{\text{Peak area of } \textit{cis}\text{-FA at 280 nm} \times \text{amount of } \textit{trans}\text{-FA (µg g}^{-1}\text{) on that particular run}}{\text{Area of } \textit{trans}\text{-FA}}$$

$$\text{(ii) } \textit{cis}\text{-FA (µg g}^{-1}\text{ cell wall)} = \frac{\textit{trans}\text{-FA equivalent of } \textit{cis}\text{-FA} \times \text{RF of } \textit{trans}\text{-FA according to Waldron } \textit{et al.}\text{ (1996)}}{\text{RF of } \textit{cis}\text{-FA according to Waldron } \textit{et al.}\text{ (1996)}}$$

$$= \frac{\textit{trans}\text{-FA equivalent of } \textit{cis}\text{-FA} \times 0.36}{0.32}$$

Here, FA = *trans*-ferulic acid; RF = response factor

40

Seven different diferulic acids namely 8-8´-DFA (aryltetralin form), 8-8´-DFA, 8-5´-DFA, 5-5´-DFA, 8-0-4´-DFA, 8-5´-DFA (benzofuran form) and 8-5´-DFA (decarboxylated form) from the maize cell-wall were detected and quantified (Fig. B-13 and B-14). Except 8-8´-DFA (decarboxylated form), other six diferulates were quantified in the same way as for *cis*-ferulic acid using following formulae (Waldron *et al*. 1996):

$$\text{(i) 8-8´-DFA (aryltetralin form) (µg g}^{-1}\text{ cell wall)} = \frac{\textit{trans}\text{-FA equivalent of 8-8´-DFA (aryltetralin form)} \times 0.36}{0.04}$$

$$\text{(ii) 8-8´-DFA (µg g}^{-1}\text{ cell wall)} = \frac{\textit{trans}\text{-FA equivalent of 8-8´-DFA} \times 0.36}{0.17}$$

$$\text{(ii) 8-5´-DFA (µg g}^{-1}\text{ cell wall)} = \frac{\textit{trans}\text{-FA equivalent of 8-5´-DFA} \times 0.36}{0.18}$$

$$\text{(iv) 5-5´-DFA (µg g}^{-1}\text{ cell wall)} = \frac{\textit{trans}\text{-FA equivalent of 5-5´-DFA} \times 0.36}{0.21}$$

$$\text{(v) 8-0-4´-DFA (µg g}^{-1}\text{ cell wall)} = \frac{\textit{trans}\text{-FA equivalent of 8-0-4´-DFA} \times 0.36}{0.14}$$

$$\text{(vi) 8-5´-DFA (benzofuran form) (µg g}^{-1}\text{ cell wall)} = \frac{\textit{trans}\text{-FA equivalent of 8-5´-DFA (benzofuran form)} \times 0.36}{0.12}$$

Here, FA = *trans*-ferulic acid; DFA = diferulic acid; RF = response factor

As the response factor (RF) of decarboxylated 8-5´-DFA was not reported by Waldron et al. (1996) the correction factor (CF) of this compound (Dobberstein and Bunzel 2010) was used to calculate a modified response factor for quantification. The formulae for quantitation are given below:

$$\text{(i) RF of decarboxylated 8-5´-DFA} = \frac{\text{CF of 8-0-4´-DFA (Dobberstein and Bunzel 2010)} \times \text{RF of 8-0-4´-DFA (Waldron \textit{et al}. 1996)}}{\text{CF of decarboxylated 8-5´-DFA (Dobberstein and Bunzel 2010)}}$$

$$= \frac{0.845 \times 0.14}{1.341} = 0.088$$

$$\text{(ii) 8-5´-DFA (decarboxylated form) (µg g}^{-1}\text{ cell wall)} = \frac{\textit{trans}\text{-FA equivalent of 8-5´-DFA (decarboxylated form)} \times 0.36}{0.088}$$

2.2.6 Analysis of cell-wall lignin

Analysis of lignin was performed following the method described in Experiment 1 (section 2.1.7) with a little modification. Use of perchloric acid was avoided as perchloric acid may degrade xylan that gives absorption at 280 nm (Hatfield *et al.* 1999). The modified method is described here. Exactly 20 mg freeze-dried cell wall were taken in a glass vial and 1 mL of pyrrolidine : pyridine (1 : 1, v/v) was poured to it. Then all vials were closed with the teflon-lined cap and were placed in a water bath at 80°C for 18 h. The reaction mixture was transferred to a 15 mL centrifuge tube with the help of 5 mL methanol. After centrifuging at 350 *g* for 20 min, the solution was pipetted off and the residue was washed with methanol and recentrifuged for further five times each with 4 mL methanol. After discarding the methanol, 4 mL of water were added to cell-wall residues. All tubes were then placed in a water bath at 70°C for 3 h by putting a glass marble on top of each tube. All tubes were then recentrifuged as before and the supernatants were discarded. The pellet was washed with cold water and finally with methanol followed by centrifugation. Then the resultant pellets were transferred into the screw-capped tubes and were placed in an oven to dry the pellets at 50°C overnight.

Individual samples were removed from the oven, 2.5 mL of freshly prepared acetyl bromide reagent (acetyl bromide : glacial acetic acid = 1 : 3, v/v) were added. The tubes were capped immediately with PTFE-coated silicone cap and heated in water bath at 50°C for 4 h with occasional shaking. Then the sample was quantitatively transferred to a 50 mL volumetric flask with a reagent mixture containing 10 mL of 2 M NaOH and 12 mL of acetic acid. Exactly 1750 µL of 0.5 M hydroxylamine were added to each flask, and samples were diluted to 50 mL with glacial acetic acid. The absorption of the final solution

was measured at 280 nm. Finally the lignin concentration was determined using the following two formulae (Morrison 1972):

(i) Absorbance value = $\dfrac{\text{Absorbance of sample} - \text{Absorbance of blank}}{\text{Concentration of sample (g L}^{-1})}$

(ii) Lignin concentration (mg g^{-1} cell wall) = (33.6 × Absorbance value) – 11.1

2.2.7 Statistical analysis

Values are given as arithmetic means of four replicates with standard error of means (SE). To determine significant differences between treatments or parameters, Student´s t-test was performed at a level of P ≤ 5% (*), P ≤ 1% (**), and P ≤ 0.1% (***) using Microsoft Office Excel (Windows version 2007).

3 Results

3.1 Results of Experiment 1

3.1.1 Shoot fresh mass production
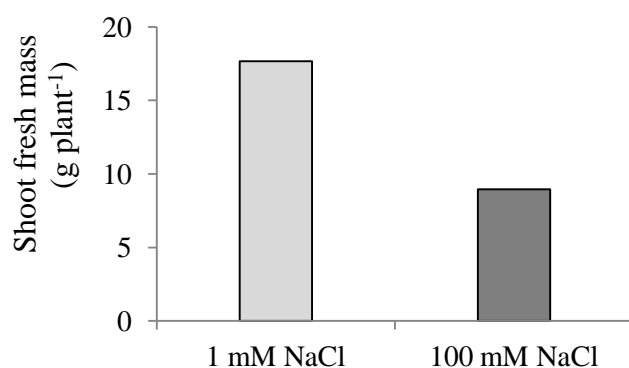
Figure 3-1: Effect of salt stress on shoot fresh mass production of 21 d old maize cv. Amadeo.

Salt stress (100 mM NaCl) caused a 51% reduction in shoot fresh mass of maize cv. Amadeo compared to the control (1 mM NaCl) treatment (Fig. 3-1).

3.1.2 Isolation of cell walls

> 405 µm cell-wall fraction   250-405 µm cell-wall fraction

Figure 3-2: Freeze-dried cell wall of maize cv. Amadeo. Cell wall collected from 405 µm mesh sieve was termed "> 405 µm cell-wall fraction" and that collected from 250 µm mesh sieve was termed "250-405 µm cell-wall fraction".

Cell walls were isolated from the 21 d old shoots of maize cv. Amadeo following the procedures described in the section 2.1.2 It was found that that 12 min crushing of maize

shoots in the blender could effectively break tissues thus allowing them to be bathed with the hypertonic sucrose solution. After final washing with 0.1% (v/v) aqueous Triton X100, the crushed cell walls were cleaned with distilled water through two sieves (mesh size of 405 and 250 µm, respectively) stacked on each other. Thus the cell wall isolated from 405 µm sieve was termed "> 405 µm cell-wall fraction" and that collected from 250 µm was termed "250-405 µm cell wall fraction" (Fig. 3-2).
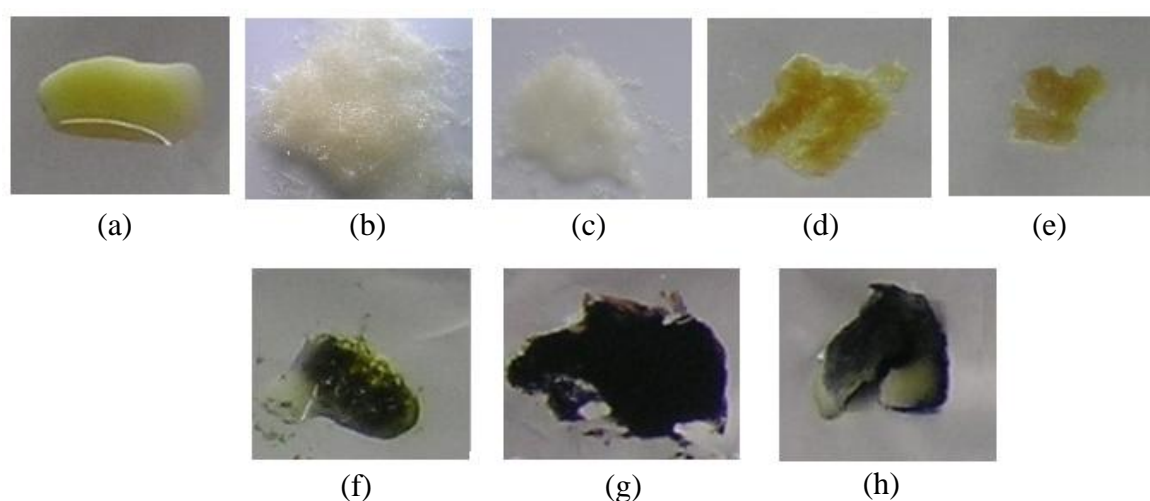
Figure 3-3: A color test for the presence of starch in isolated cell-walls. Image (a) shows light green-colored iodine reagent, while (b) and (c) show the > 405 µm and 250-405 µm cell-wall fractions, respectively. Images (d) and (e) show the > 405 µm and 250-405 µm cell-wall fractions, respectively, after the reaction with iodine reagent. Both the cell wall fractions show no change in color with iodine reagent. On the contrary, image (f) shows dark coloration of macerated whole leaf with the iodine reagent. Image (e) and (f) demonstrate the typical iodine reaction (dark coloration) with pure starch and starch-rich potato tuber, respectively.

Iodine test was done to test whether the isolated cell-wall fractions contained starch or not. There was no change in color of both the cell-wall fractions after the addition of iodine reagent (Fig. 3-3). Light microscopy was performed for both the cell-wall fractions and it was found that both the fractions contained clean cell-wall (Fig. 3-4). No chloroplast was found in the isolated cell-walls. These two cell-wall fractions were quite different in tissue

composition (Fig. 3-4 b). The 250-405 μm fraction was dominated by the mesophyll and epidermal tissues, whereas > 405 μm fraction was dominated by vascular and fiber tissues.

(a)   (b)   (c)

(d)   (e)
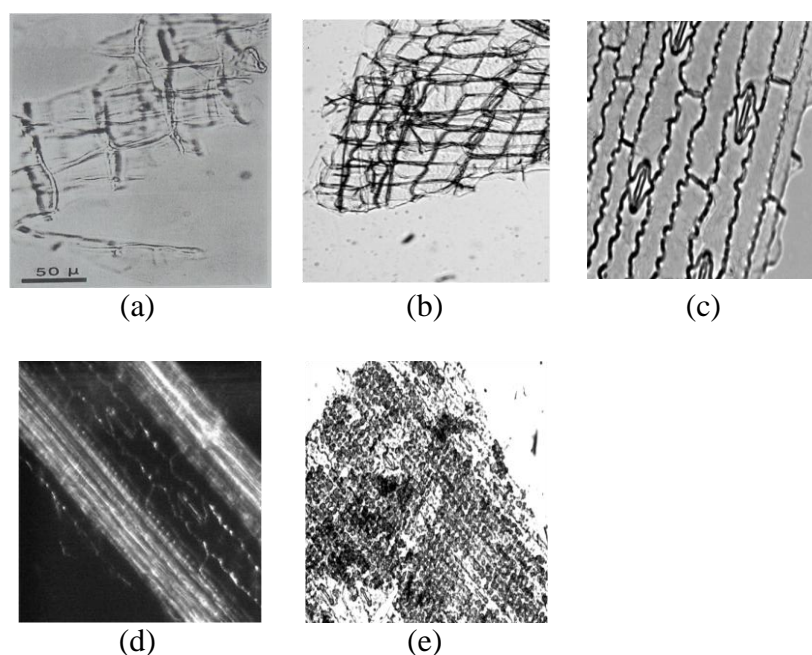
Figure 3-4**:** Light microscopic observation of isolated cell wall from the 21 d old shoot of maize cv. Amadeo. Image (a) represents extracted hypocotyl cell walls (Goldberg 1985). Image (b) and (c) represent cell walls of the 250-405 μm fraction that consists of mesophyll and epidermal tissues, respectively. On the contrary, image (d) highlights the extracted tissue of the > 405 μm fraction which is dominated by fibers and vascular tissues. Image (e) shows the un-extracted maize leaf-tissues.

3.1.3 Cellulose concentration

$y = 0.0157x + 0.0178$
$R^2 = 0.9995$
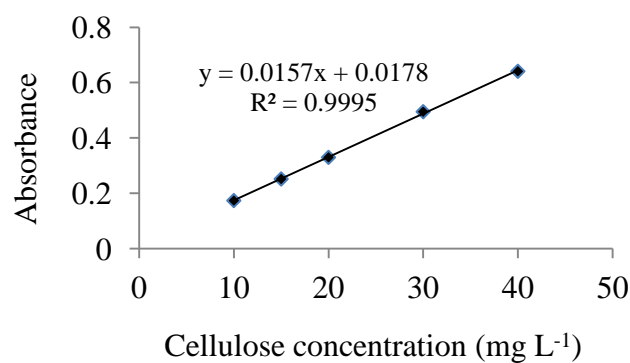
Figure 3-**5:** Calibration curve for determining cellulose concentration.

An absorbance of 0.373 was recorded from 20 µg mL^{-1} cellulose standard, and it was in the expected range of 0.34-0.37 reported by Updegraff (1969). The coefficient of determination (R^2) of the standard curve for the determination of cellulose was 99.9% (Fig. 3-5). Thus 99.9% variation of the dependent variable (absorbance) is explained by the independent variable (concentration).

The regression equation of the standard curve (Fig. 3-5) was as follows:

y = 0.0157x + 0.0178

or, x = (0.0178 − y) ÷ 0157

where,

x = Concentration of cellulose in mg L^{-1}

y = Corrected absorbance value
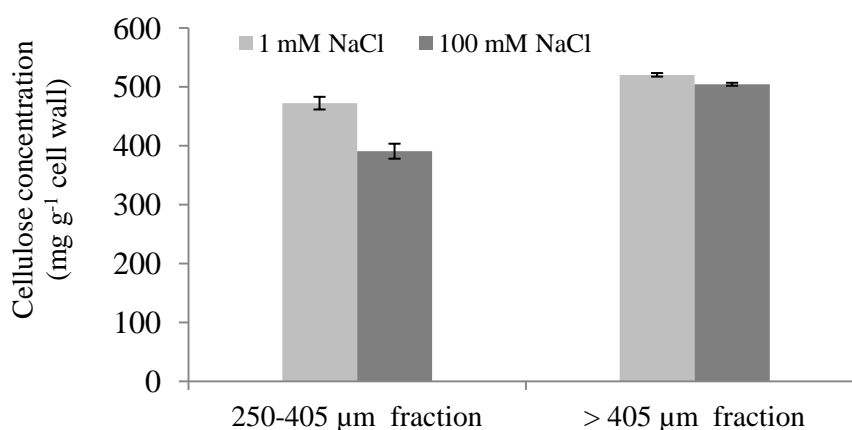
Figure 3-6: Cellulose concentrations in two different fractions of cell wall (250-405 µm and > 405 µm fractions). Error bars represent ± SE of three replicates.

Cellulose from the cell wall of both control and salt-treated plants was analyzed (Fig. 3-6). Cellulose declined by 18% in the 250-405 µm cell-wall fraction due to the salt treatment. On the other hand, salt stress caused only 3% reduction of cellulose in the > 405 µm cell-wall fraction.

3.1.4 Concentrations of neutral sugars

3.1.4.1 Optimum eluent (NaOH) concentration for separation of neutral sugars
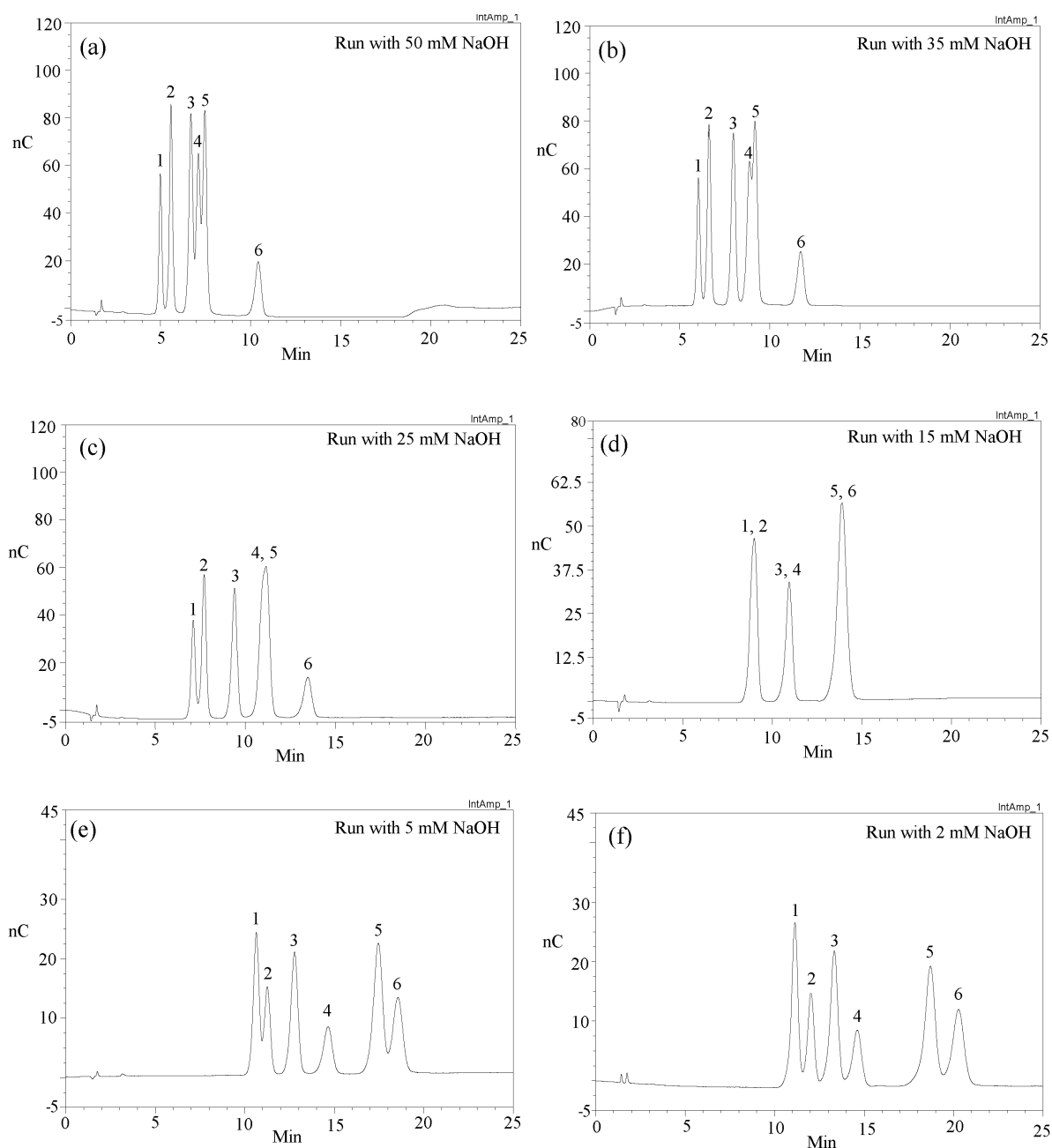
Figure 3-7: HPAEC-PAD elution profiles during method development for the separation of neutral sugar-standards using CarboPac PA-10 column (analytical column 2 mm × 250 mm and guard column 2 mm × 50 mm) coupled with a pulsed amperometric detector (Dionex ED 50 gold electrode). Explanation for peak identification: 1, L-arabinose; 2, L-rhamnose; 3, D-galactose; 4, D-glucose; 5, D-xylose; 6, D-mannose. As an eluent, a range of different concentrations of NaOH was tested to find out the optimum separation profile of cell-wall neutral sugars.

To find out the optimum separation of cell-wall neutral sugars (glucose, xylose, arabinose, galactose, mannose and rhamnose), different concentrations of NaOH ranging from 1 to 60 mM were run as eluent (Fig. 3-7). At a concentration of 15 mM NaOH, there were only three peaks (Fig. 3-7 d) for six different sugars. Any further higher concentration of NaOH above 15 mM also could not produce better separation of these six sugars. However, 5 mM and lower concentrations of NaOH yielded satisfactory separation of sugars. 2 mM NaOH was optimum for the satisfactory separation of all six neutral sugars in the cell-wall hydrolysates. For the detection of minor sugars, mannose and rhamnose, a higher concentration of cell-wall hydrolysate may be required. However, this high concentration of cell wall produced overloaded-peak for major cell-wall neutral sugars such as glucose and xylose. Thus a relatively diluted cell-wall hydrolysate (50 mg L^{-1}) may be required for their separation and determination (Fig. 3-8).

(a)   (b)
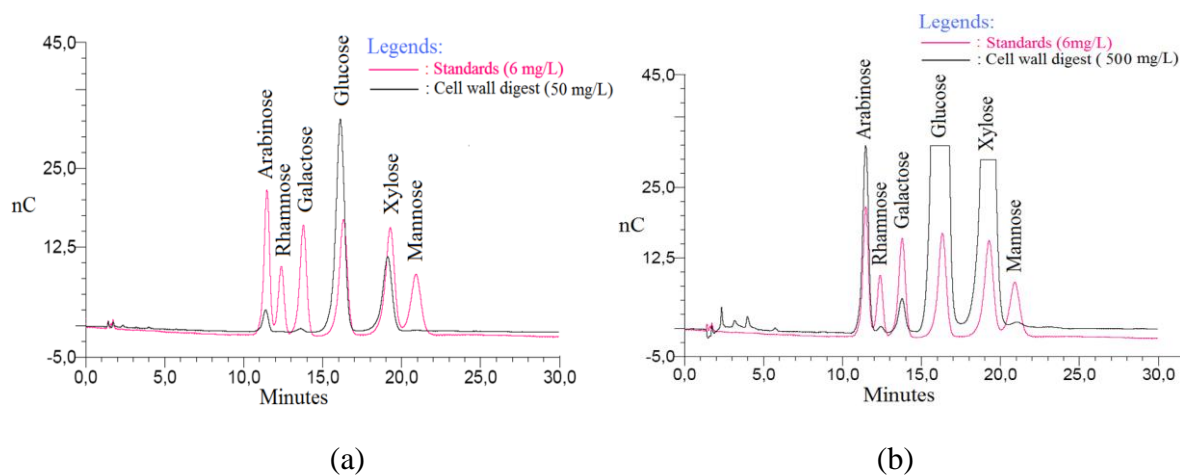
Figure 3-8: Separation of neutral sugars from the cell-wall hydrolysates in HPAEC-PAD system. Except rhamnose and mannose, other sugars can be separated and detected at 50 mg L^{-1} cell-wall digest. However, these two sugars can be detected at higher concentration (e.g. 500 mg L^{-1} cell-wall digest).

3.1.4.2 Reproducibility of HPAEC-PAD and cell-wall hydrolysate for determining the neutral sugars
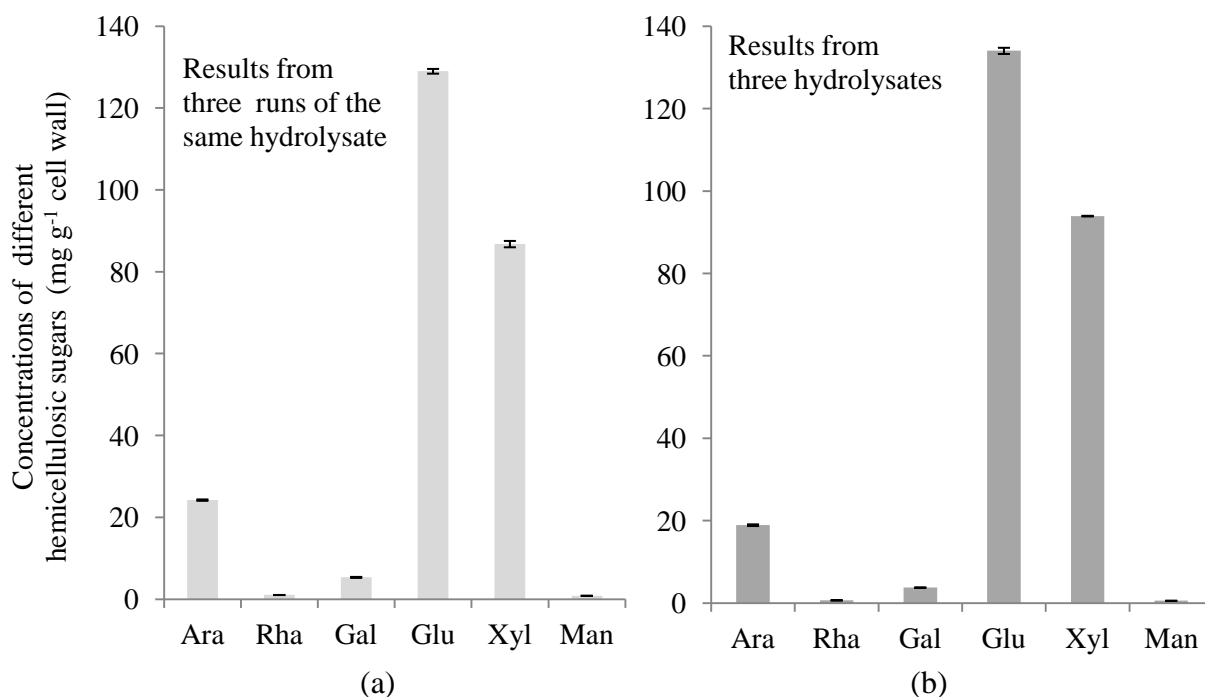
Figure 3-9: Reproducibility of HPAEC-PAD in determining neutral sugars namely arabinose (Ara), rhamnose (Rha), Galactose (Gal), Glucose (Glu), Xylose (Xyl) and mannose (Man) from the cell-wall hydrolysates. Error bars represent standard error of means (n = 3).
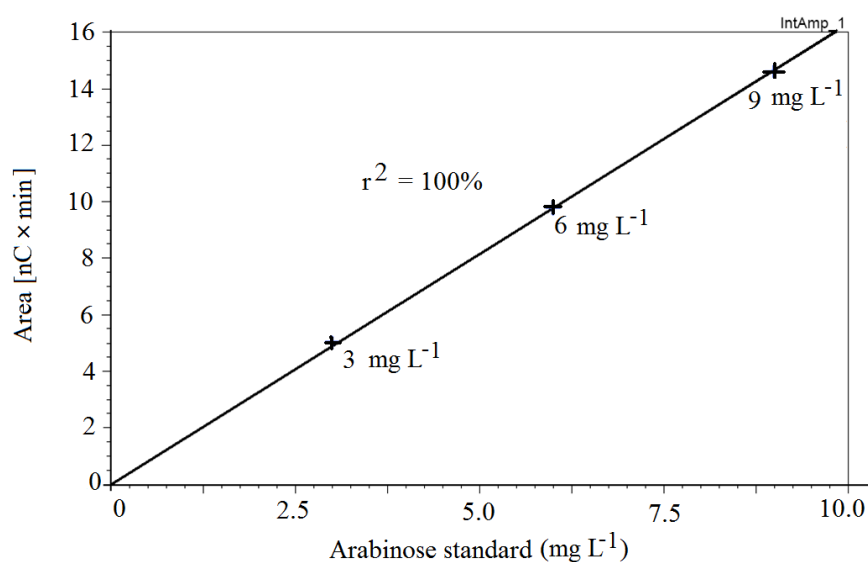
Figure 3-10: An exemplary three-point calibration curve with L-arabinose for the determination of this sugar in the HPAEC-PAD system.

Table 3-1: Six sugar standards showing their chromatogram characteristics in a three-point calibration curve of HPAEC-PAD analysis.

Peak name	Retention time	Calculation type	Points	Correlation coefficient (%)
Arabinose	11.3	Linear	3	100.00
Rhamnose	12.2	Linear	3	99.99
Galactose	13.6	Linear	3	99.99
Glucose	16.1	Linear	3	99.87
Xylose	19.0	Linear	3	99.88
Mannose	20.6	Linear	3	99.78
			Average =	99.92

Reproducibility of the HPAEC-PAD system was checked reading the same hydrolysate but in three different times (Fig. 3-9 a). Three-point (3, 6 and 9 mg L^{-1}) calibration curves with standard sugars showed a perfect correlation coefficient (~100%) for each of the six cell-wall neutral sugars analyzed (Fig. 3-10, Table 3-1). It was found that the standard deviation for mannose was 9%. All other sugars showed less than 4% standard deviation.

Reproducibility of digestion was checked with three independent hydrolysates of the same cell-wall sample (Fig. 3-9 b). The standard deviation for the amount of individual neutral sugars (three determinations) was less than 2% for the major sugars glucose, xylose and arabinose. Minor sugars such as rhamnose, mannose and galactose showed much higher standard deviation (3-17%).

3.1.4.3 Cell-wall neutral sugars as influenced by salt stress

Table 3-2: Influence of salt stress on the concentrations of various neutral sugars in two different cell-wall fractions of maize (cv. Amadeo) shoot. Optimized HPAEC-PAD was used for the separation and detections of sugars.

Neutral sugars	Concentration in 250-405 µm cell-wall fraction (mg g^{-1} cell wall)			Concentration in > 405 µm cell-wall fraction (mg g^{-1} cell wall)		
	1 mM NaCl	100 mM NaCl	Relative change (%)	1 mM NaCl	100 mM NaCl	Relative change (%)
Arabinose	18.7	23.9	+ 28%	16.0	18.9	+ 18%
Rhamnose	0.8	1.0	+ 26%	0.6	0.7	+ 19%
Galactose	4.1	5.2	+ 28%	3.0	3.7	+ 22%
Glucose	240.5	291.0	+ 21%	317.7	278.6	- 12%
Xylose	87.8	117.7	+ 34%	126.0	116.5	- 8%
Mannnose	0.6	0.9	+ 44%	0.5	0.5	- 6%
Sum	352.6	439.7	+ 25%	463.8	418.8	- 10%

Higher concentrations of neutral sugars were detected in cell walls of salt-stressed plants compared to the control plants (Table 3-2). Glucose, xylose and arabinose were the most abundant sugars followed by galactose, rhamnose and mannose in both the cell-wall fractions and in both control and salt treatment. The relative increase of these sugars in salt-treated plants was in range of 21-44% in 250-405 µm cell-wall fraction. On the other hand, > 400 µm cell-wall fraction showed little variation in neutral sugars due to the salt treatment. Arabinose, rhamnose and galactose increased by 18, 19 and 22% in > 405 µm cell-wall fraction of salt-treated plants. On the other hand this higher cell-wall fraction showed a decrease of glucose, xylose and mannose by 12, 8 and 6%, respectively, under salt treatment.

3.1.5 Total uronic acids

In the standard curve with D-galacturonic acid, the coefficient of determination (R^2) was ≈100% (Fig. 3-11). Thus the total variation observed in the dependent variable (absorbance) is fully explained by the independent variable (concentration).
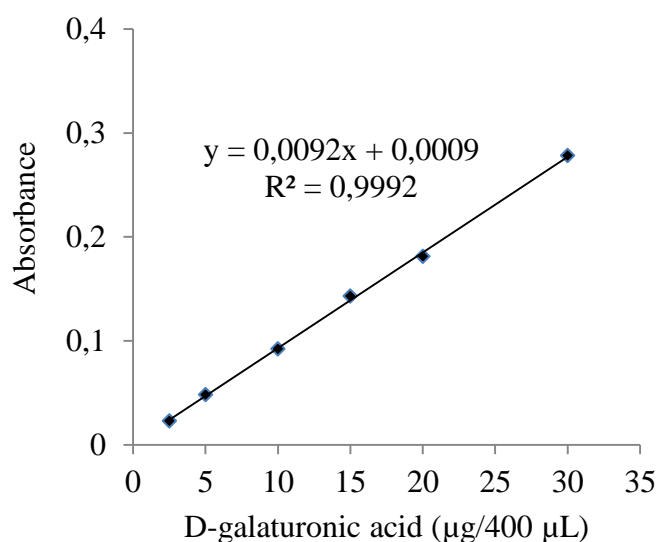
Figure 3-11: Calibration curve with D-galacturonic acid for the determination of total uronic acid from the cell wall of maize shoot.

The regression equation of the standard curve (Fig. 3-11) with the D-galacturonic acid was as follows:

$y = 0.0092x + 0.0009$

or, $x = (0.0009 − y) \div 0.0092$

where,

$x =$ Concentration of D-galacturonic acid in µg/400 µL

$y =$ Corrected absorbance value

Salt stress reduced the concentrations of total uronic acid by 18% in the 250-405 µm cell-wall fraction. On the other hand, the > 405 µm cell-wall fraction showed only 5% decline of total uronic acid under salt stress (Fig. 3-12).
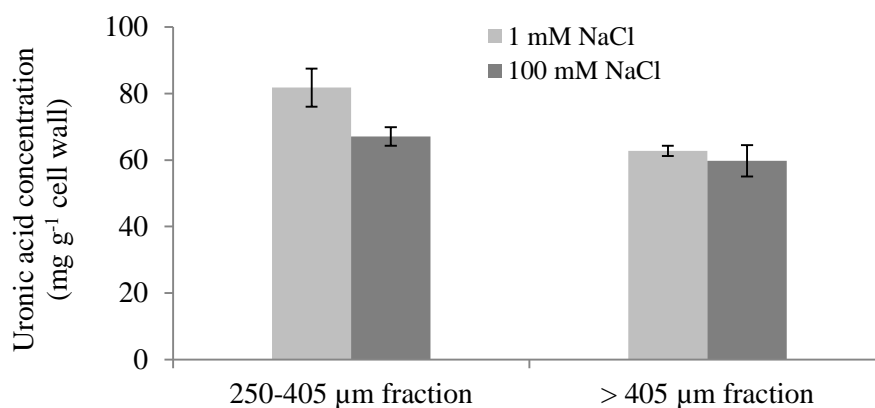
Figure 3-12: Total uronic acid concentrations in two different fractions of cell wall (250-405 μm and > 405 μm fractions) of maize cv. Amadeo. Each data point represents the mean ± SE of three replicates.

3.1.6 Methylation of uronic acids
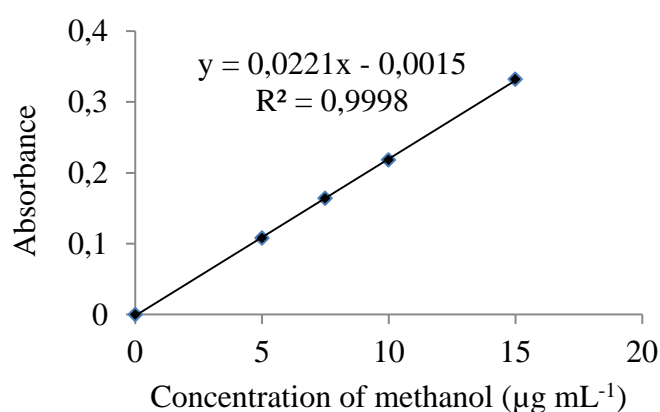
Figure 3-13: Calibration curve with methanol for the determination of degree of methylation of uronic acid in the cell wall of maize shoot.

The regression equation of the standard curve with methanol was as follows (Fig. 3-13):

y = 0.0221x - 0.0015

where,

y = Corrected absorbance value

x = Concentration of methanol in μg mL^{-1}

Thus the methanol concentration (in μg mL^{-1}) of unknown solution, x = (y + 0.0015) ÷

0.0221

The degree of methylation was calculated using the following formula:

$$\text{Degree of methylation (\%)} = \frac{\text{Methanol produced from specific amount of cell wall (μmol)}}{\text{Uronic acid from the same amount of cell wall (μmol)}} \times 100$$
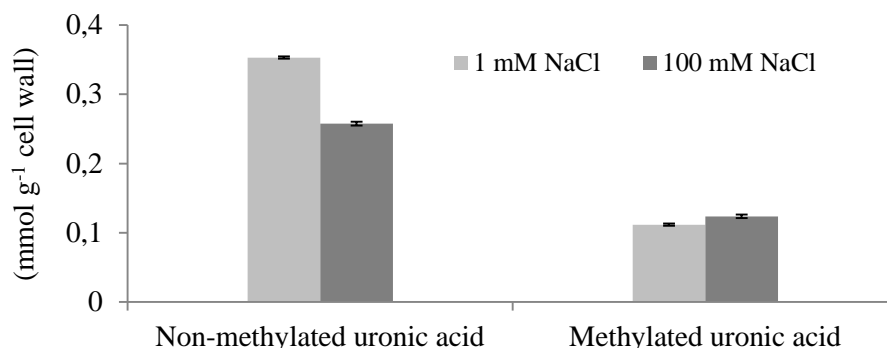
Figure 3-14: Concentrations of non-methylated and methylated uronic acids in 250-405 μm cell-wall fraction of maize cv. Amadeo. Error bars represent ± SE of three replicates.

The calibration curve showed a perfect coefficient of determination (R^2 = 100%) for determining the degree of methylation of uronic acid in the cell wall of maize shoot (Fig. 3-13). Methylation of uronic acid was determined only for 250-405 μm cell-wall fraction (Fig. 3-14). It was found that salt stress accounted for lowering the concentration of non-methylated uronic acid by 27% in maize cv. Amadeo. Conversely, salt stress augmented methylated uronic acid by 10% due to salt treatment.

3.1.7 Lignin
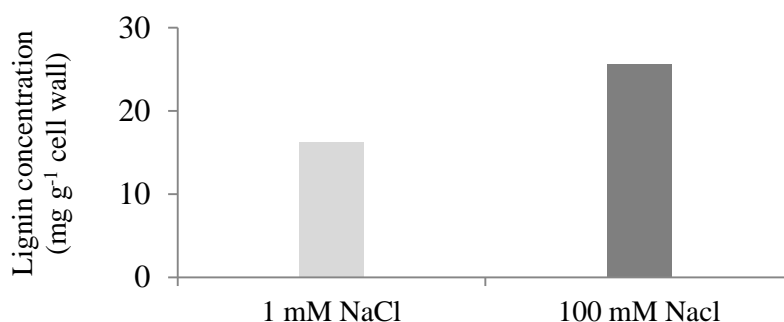
Figure 3-15: Effect of salt stress on cell-wall lignin concentration in 250-405 μm sized cell-wall fraction of maize cv. Amadeo. Due to lack of cell-wall, lignin was determined from only one sample.

Lignin concentration was determined only from 250-405 µm cell-wall fraction. Salt stress caused a 57% increase of lignin in 250-405 µm sized cell-wall fraction (Fig. 3-15).

3.1.8 Phenolics

Methanol and acetonitrile aided separation of all the major phenolic monomers and dimers from each other (Fig. 3-16, 3-17). Phenolic monomers were identified using standard substances, while peak assignment for diferulates was performed using the detector response values at 210, 265, 280 and 325 nm according Waldron *et al.* (1996). Spectral data were very useful to discriminate between the peaks which aided identification of various diferulates.

In this experiment, various monomeric phenols (*p-OH*-benzoic acid, vanillic acid, *p-OH*-benzaldehyde, vanillin, *trans-p*-coumaric acid and *trans*-ferulic acid) from the 250-405 µm cell-wall fraction of maize cv. Amadeo (Fig. 3-18) were determined. Salt stress decreased the concentrations of cell wall-bound *p-OH*-benzaldehyde and *trans-p*-coumaric acid (Fig. 3-18). In contrast, a slight (6%) increase of *trans*-ferulic acid was observed under salt treatment.

Beside monomeric phenols, four different diferulic acids (DFA) namely 8-5´-DFA, 5-5´-DFA, 8-0-4´-DFA and 8-5´-DFA (benzofuran form) were quantified (Fig. 3-19). In this study, there was no major influence of salt stress on diferulic acids.
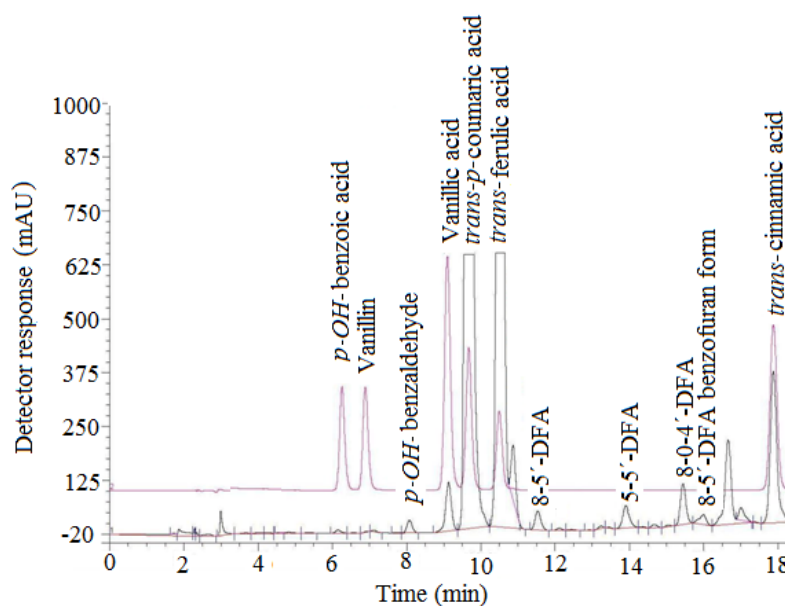
Figure 3-16: RP-HPLC elution profile of monomeric phenol standards and cell wall-bound phenols from maize cv. Amadeo with detection at 280 nm. A RP-HPLC column (LiChrospher®100 RP-18 endcapped 5 μm column (250 mm × 4.6 mm), Techlab, Erkerode, Germany) was used for the separation of monomeric phenols. A gradient elution system was used which increased the relative proportion of methanol and acetonitrile in aqueous 1 mM trifluoroacetic acid (Waldron *et al.* 1996).
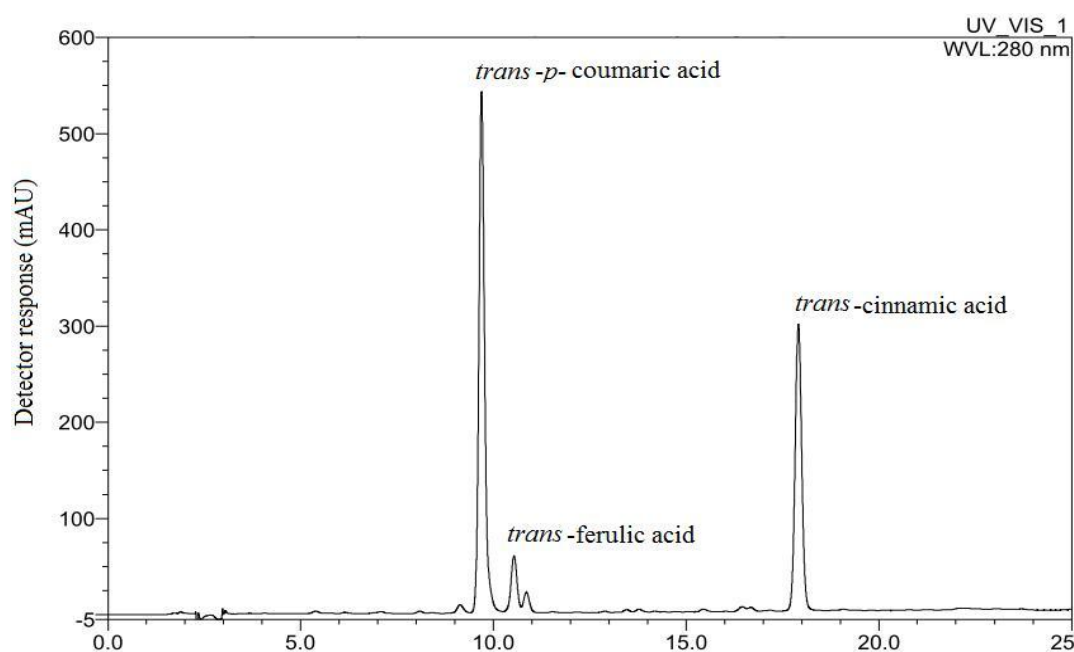
Figure 3-17: An exemplary chromatogram showing phenolics from maize cv. Amadeo extracted with 2 M NaOH using a RP-HPLC column (LiChrospher®100 RP-18 endcapped 5 μm column (250 mm × 4.6 mm), Techlab, Erkerode). *Trans*-cinnamic acid was used as a internal standard. At higher concentration of NaOH (2 M), mostly *trans-p*-coumaric acid was released.
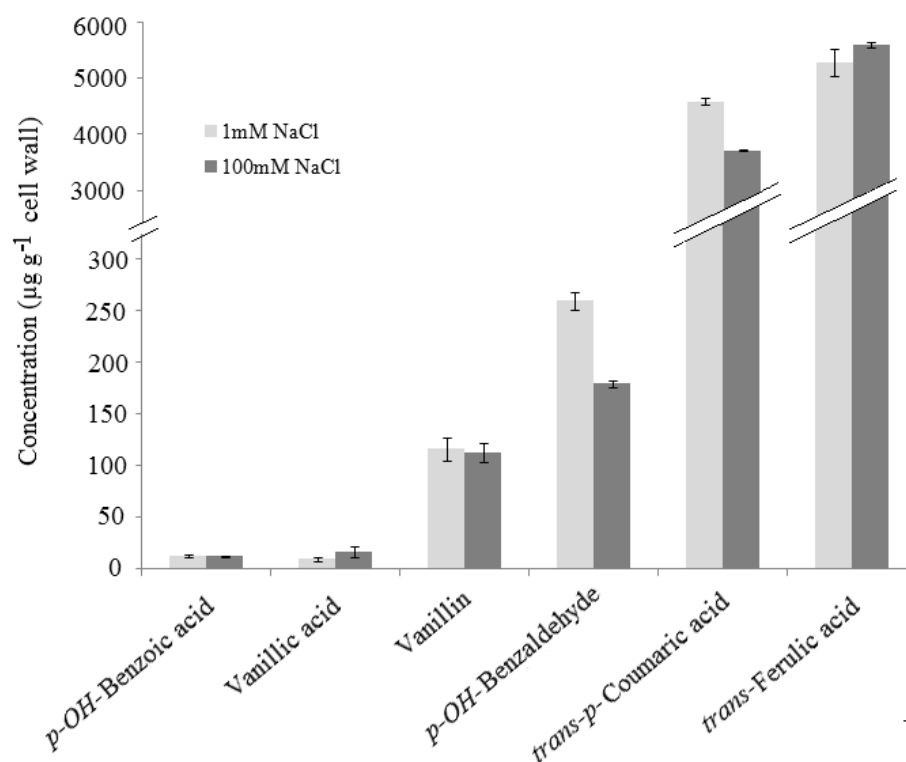
Figure 3-18: Effect of salt stress on monomeric phenolics composition from 250-405 µm cell-wall fraction of maize cv. Amadeo. Error bars represent ± SE of three replicates.
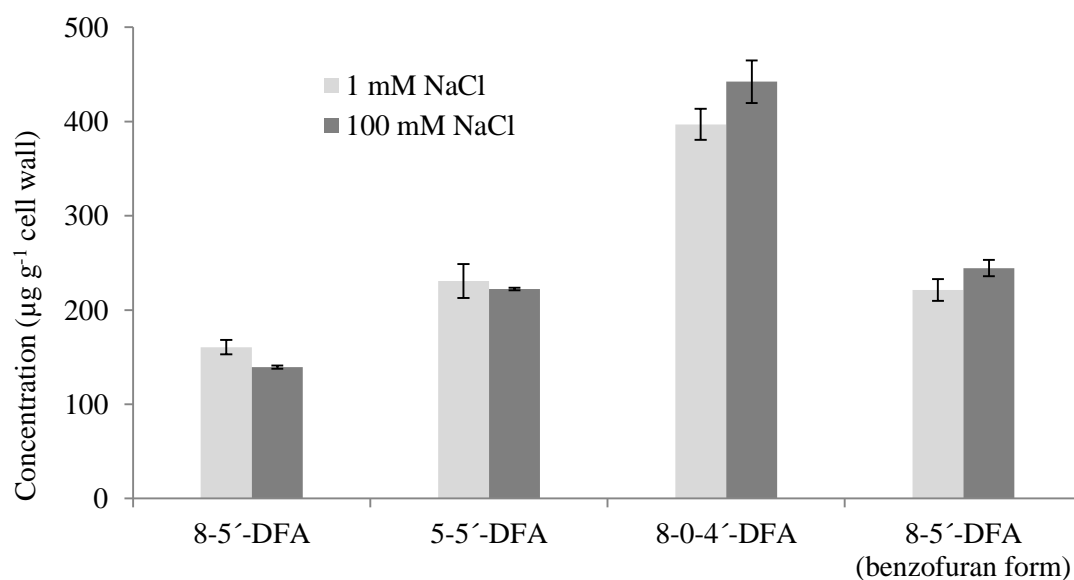
Figure 3-19: Diferulates (DFA) detected from the 250-405 µm cell-wall fraction of maize shoot cv. Amadeo in the first phase of salt stress. Error bars represent ± SE of three replicates.

3.1.9 Enzymatic production of diferulates
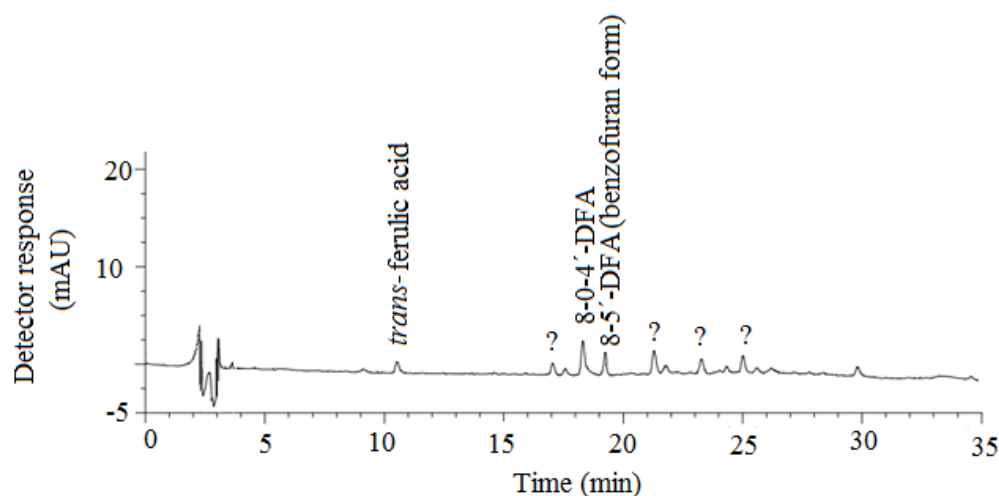
Figure 3-20: RP-HPLC chromatogram showing the products after reaction of 0.3 μM *trans*-ferulic acid with 1 μM horse radish peroxidase in presence of 100 μM H_2O_2.

An experiment was conducted to prepare the diferulates using *trans*-ferulic acid as a substrate, hydrogen peroxide and horse radish peroxidase as catalysts. *Trans*-ferulic acid with the concentration of 0.3 mM seemed to be better for the reaction. There were only two peaks of diferulates (Fig. 3-20), as their chromatogram characteristics (retention time and change in peak area in 4 different wave lengths viz. 210, 265, 280, and 325 nm) were quite similar to that reported by Waldron *et al.*1996.

3.2 Results of Experiment 2

3.2.1 Growth reduction in two maize genotypes during the first phase of salt stress

Salt stress (100 mM NaCl) caused a reduction of plant height over time compared to the control treatment (1 mM NaCl) in both the salt-sensitive (Pioneer 3906) and the salt-resistant (SR 12) maize genotype (Fig. 3-21)
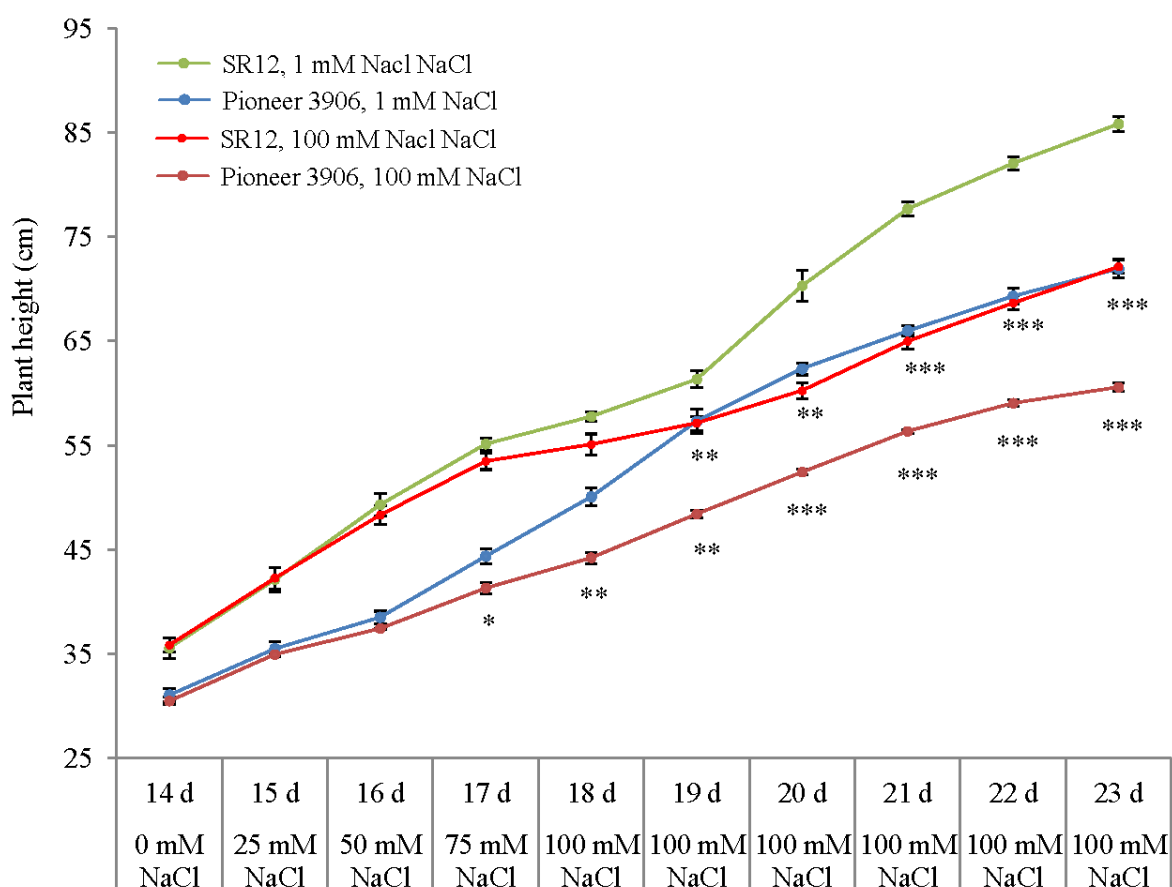
Figure 3-21: Trend of plant heights of the two maize genotypes Pioneer 3906 and SR 12 under salt stress. On day 14, plant height was measured before starting 25 mM NaCl treatment. Salt-treated plants were supplied 100 mM NaCl on day 17, and this level of NaCl was maintained till harvest on day 23. Error bars are the standard error of means of 4 replicates. ***, ** and * = significantly different compared to control with $P \leq 0.1\%$, $P \leq 1.0\%$ and $P \leq 5.0\%$, respectively.

The trend of plant height reduction under salt treatment was different for the two genotypes. Pioneer 3906 started to show a significant decline in plant height from day 17 after receiving 75 mM NaCl compared to control. On the other hand SR 12 showed significant reduction in plant height from day 19, when it had received already 100 mM NaCl for two days. From day 20, the trend of plant height reduction was quite similar for both the genotypes in response to 100 mM NaCl compared to the control.

Younger leaf was identified as the youngest leaf whose height could be measured by ruler, and older leaf was the leaf that gave the maximum height of the plant. The elongation rate of younger leaves had significantly been influenced by salt stress, while for older leaves it remained unaltered (Fig. 3-22). The elongation rates of younger leaves declined by 45% in Pioneer 3906 due to salt treatment (100 mM NaCl), whereas the younger leaves of SR 12 showed a 40% repression of elongation rate under the same condition. Salt treatment did not produce genotypic difference on leaf elongation rates.
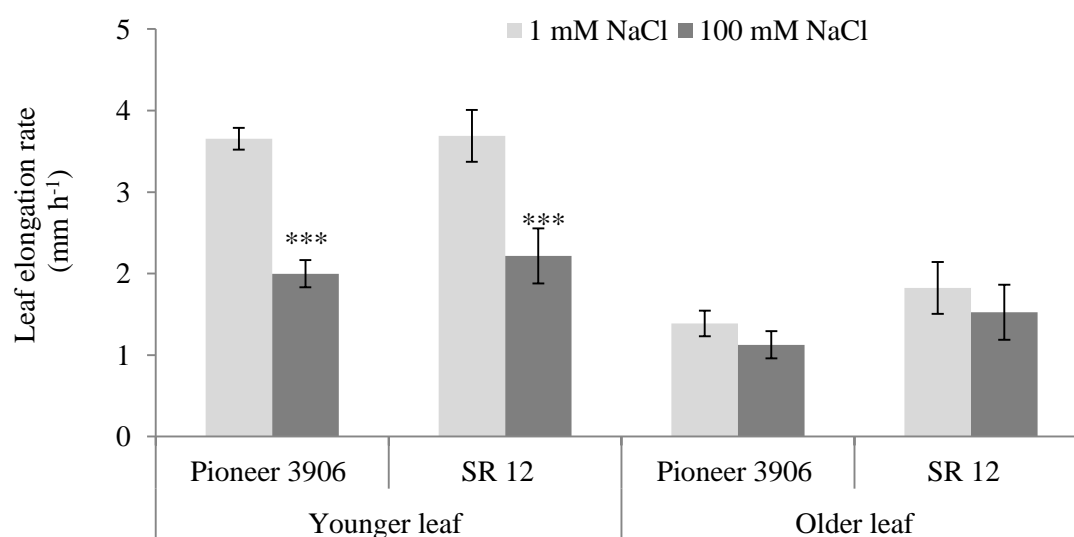
Figure 3-22: Effect of salt stress on average elongation rates of younger and older leaves of two maize genotypes Pioneer 3906 and SR 12 during days 21-22. The values are means of four replicates ± SE. *** means significantly different compared to control with $P \leq 0.1\%$.

Salt stress severely reduced shoot and root fresh mass of both maize genotypes compared to control (Fig. 3-23 and 3-24).

1 mM NaCl   100 mM NaCl   1 mM NaCl   100 mM NaCl
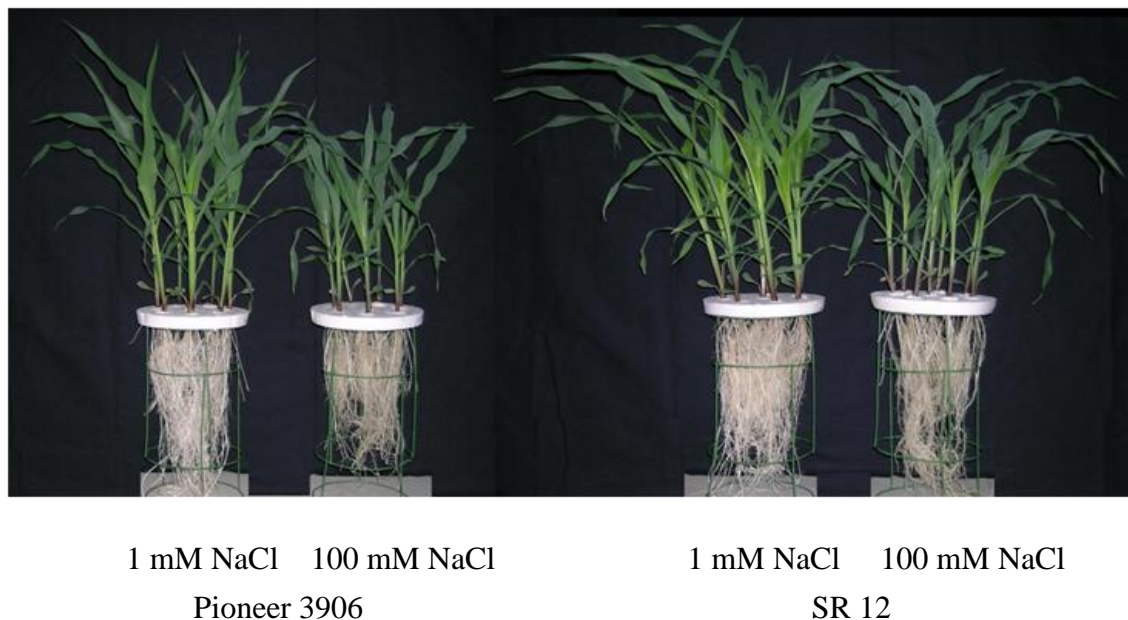
Pioneer 3906   SR 12

Figure 3-23: Effect of salt stress (100 mM NaCl) on the habits of the salt-sensitive (Pioneer 3906) and the salt-resistant (SR 12) genotpye on day 23 before harvest.
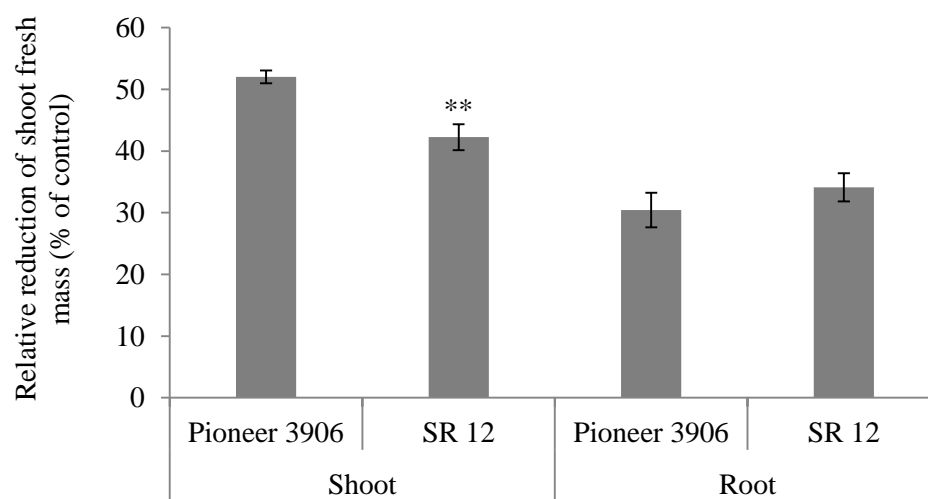
Figure 3-24. Effect of salt stress on relative reduction of shoot and root fresh-mass on day 23 of maize genotypes Pioneer 3906 and SR 12. The values are means of four replicates ± SE. ** = significantly different between genotypes with $P \leq 1.0\%$.

Shoot fresh mass was reduced by 51 and 42% in Pioneer 3906 and SR 12, respectively (Fig. 3-24). The decrease in shoot growth was significantly smaller in salt-resistant SR 12 compared to salt-sensitive Pioneer 3906 under salt treatment. However, salt stress accounted for the reduction of root fresh weights by 30 and 34% in Pioneer 3906 and SR 12, respectively. Genotypes did not differ in root fresh mass due to the salt treatment.

3.2.2 Ratio of cell-wall dry mass to shoot fresh-mass as influenced by salt treatment

The ratio between cell-wall dry mass and shoot fresh-mass was increased after the addition of 100 mM NaCl to the root medium for the two genotypes (Fig. 3.25). In this experiment, the upper shoot (5th and above leaf blades) was divided into youngest (the basal 10 cm) and young (the rest above the basal 10 cm of 5th and above order leaf blades) shoot parts and studied them separately.
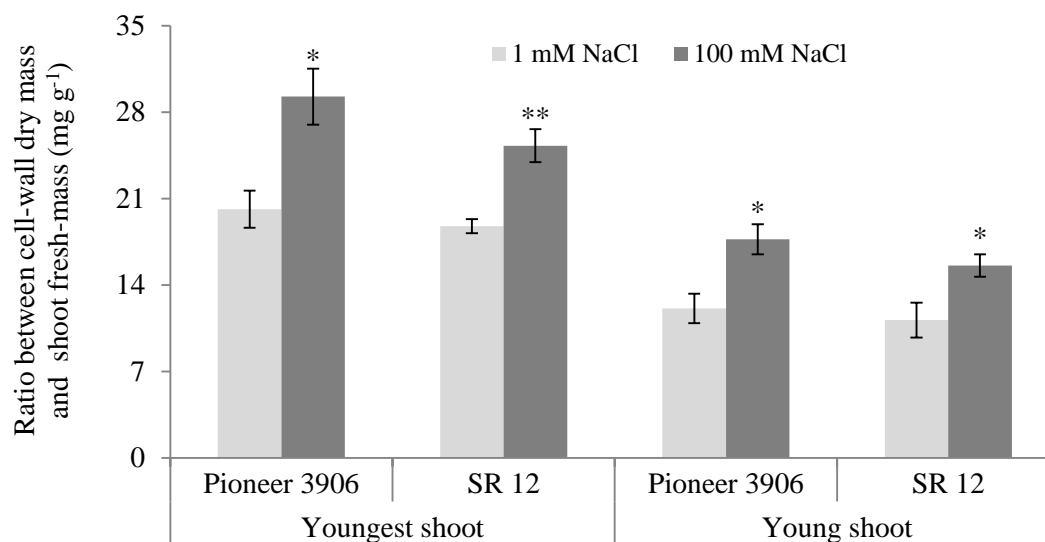
Figure 3-25. Ratio between cell-wall dry mass and shoot fresh mass of 250-405 μm cell-wall fraction as influenced by the salt stress in youngest (basal 10 cm of 5th and above order leaf blades) and young shoot (5th and above-order leaf blades without basal 10 cm segment) of Pioneer 3906 and SR 12. The values are means of four replicates ± SE. ** and * = significantly different compared to control with $P \leq 1.0\%$ and $P \leq 5.0\%$, respectively.

Relative to the control treatment, the ratios between cell-wall dry mass and shoot fresh mass increased by 45 and 46% in youngest and young shoot of Pioneer 3906, respectively. On the other hand, these ratios were increased by 35 and 40% for the youngest and young shoot of SR 12, respectively, when plants were exposed to 100 mM NaCl.

3.2.3 Cellulose concentration in cell wall during the first phase of salt stress

In both genotypes, the salt treatment accounted for lower cellulose concentrations in cell wall of youngest and young shoots (Fig. 3-26). The results revealed that the concentration of cellulose declined by 19% in youngest shoot of Pioneer 3906, whilst this reduction in younger shoot was only 12%. On the other hand, salt stress accounted for a decrease in cellulose concentrations in youngest and young shoot of SR 12 by 13 and 14%, respectively. Genotypes differed with respect to their cellulose concentrations both in youngest and younger shoot cell-wall. Nonetheless, salt stress-induced reductions of cellulose concentration were similar in the sensitive (Pioneer 3906) and resistant (SR 12) genotype.
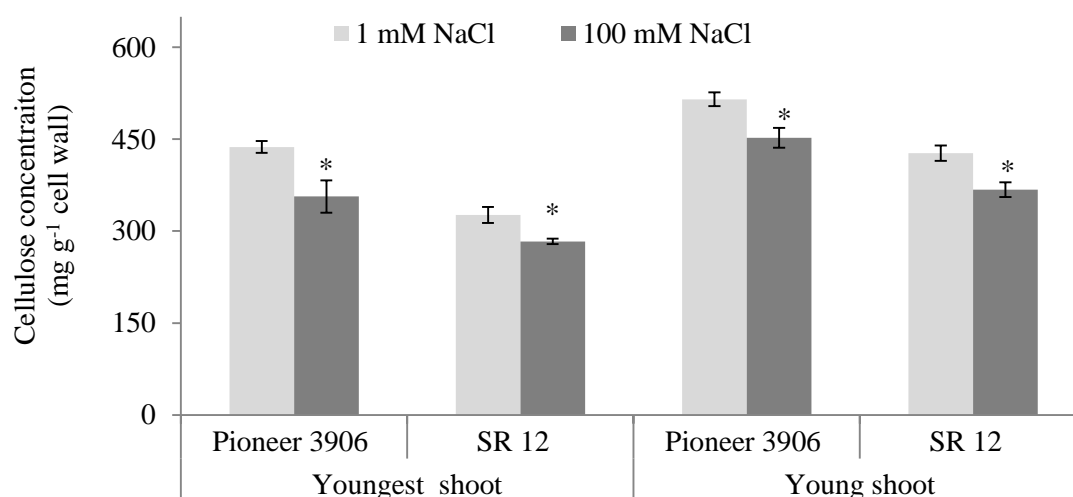
Figure 3-26. Concentrations of cellulose as affected by salt treatment in cell wall of youngest (basal 10 cm of 5th and above-order leaf blades) and young shoot (5th and above order leaf blades without basal 10 cm segment) shoot of Pioneer 3906 and SR 12. The values are means of four replicates ± SE. * = significantly different compared to control with $P \leq 5.0\%$.

3.2.4 Uronic acid and its degree of methylation during the first phase of salt stress

The total concentration of uronic acid serves as a measure of the concentration of pectic polysaccharides. There was a strong increase in total uronic acid concentration by 112% in youngest shoot of Pioneer 3906 in contrast to 27% increase in the youngest shoot of SR 12 (Fig. 3-27 a). However, the young shoot of Pioneer 3906 showed a small increase of total uronic acid concentration (29%) in contrast to the large increase of total uronic acid concentration (69%) in young shoot of SR 12.
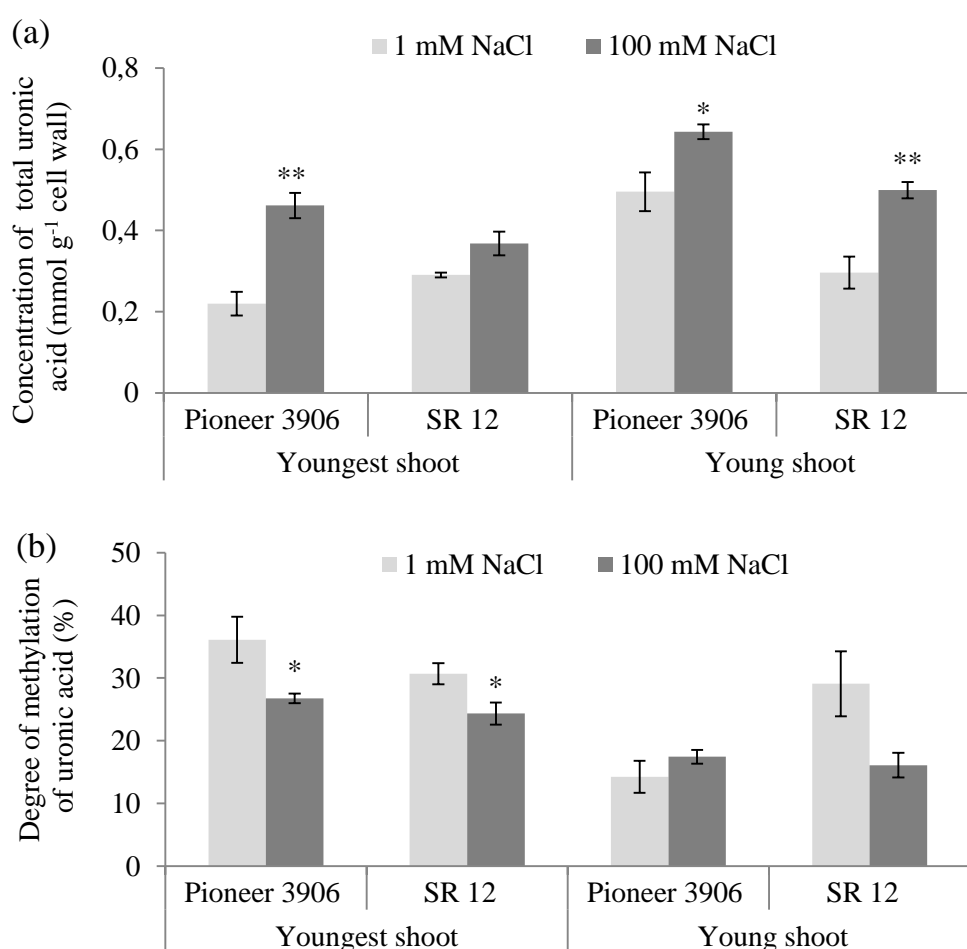
Figure 3-27: Concentrations of (a) total uronic acid and (b) degree of methylation of uronic acid as affected by salt treatment (100 mM NaCl) in cell wall of youngest (basal 10 cm of 5th and above-order leaf blades) and young (5th and above order leaf blades without basal 10 cm segment) shoot. The values are means of four replicates ± SE. ** and * = significantly different compared to control with $P \leq 1.0\%$ and $P \leq 5.0\%$, respectively.

Results showed that the degree of methylation of uronic acid in youngest shoot of Pioneer 3906 and SR 12 significantly decreased due to the salt stress (Fig. 3-27 b). Under control conditions, methylation also decreased with increasing tissue age for Pioneer 3906, but not for SR 12.
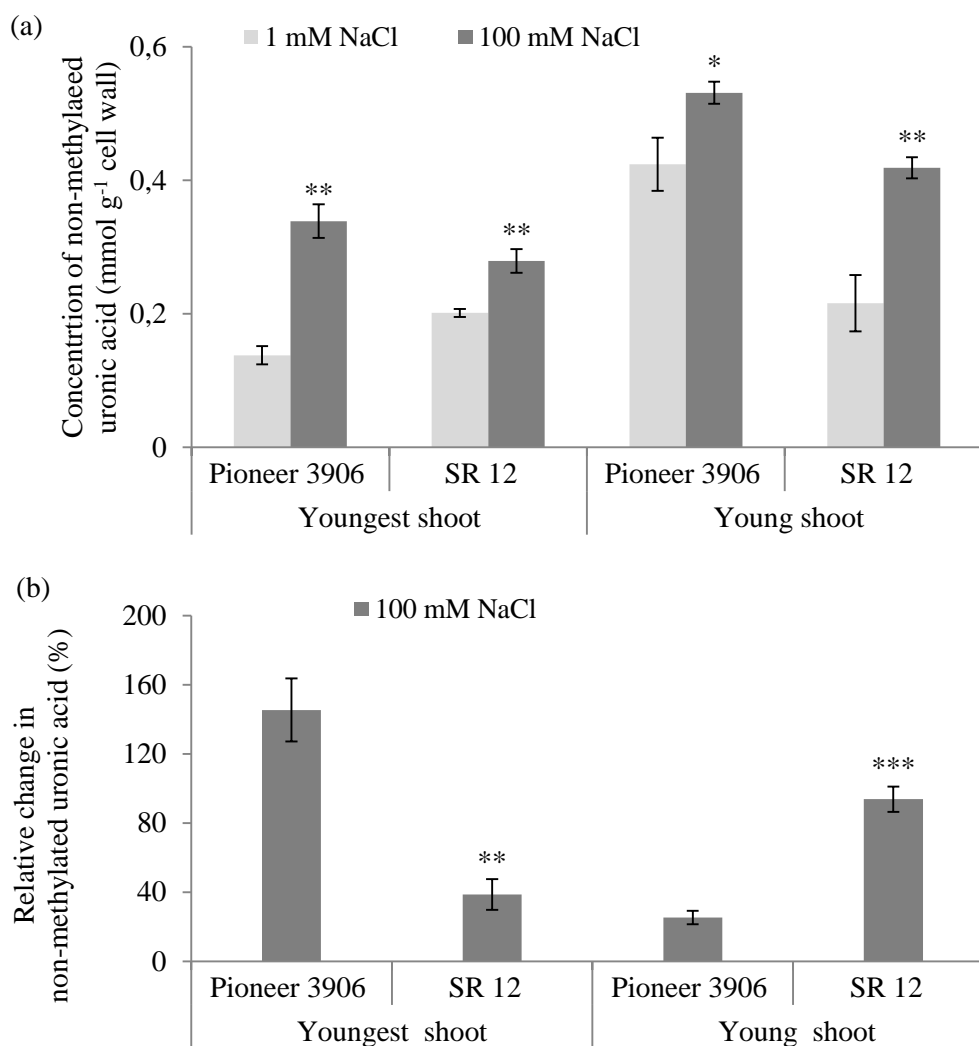
Figure 3-28: Concentrations of (a) non-methylated uronic acid, and (b) relative change in non-methylated uronic acid due to salt treatment (100 mM NaCl) in cell wall of youngest (basal 10 cm of 5th and above-order leaf blades) and young shoot (5th and above order leaf blades without basal 10 cm segment). The values are means of four replicates ± SE. ***, ** and * = significantly different between two genotypes with $P \leq 0.1\%$, $P \leq 1.0\%$ and $P \leq 5.0\%$, respectively.

Results of the experiment revealed that the concentrations of non-methylated uronic acid in youngest and young shoot cell-wall of both Pioneer 3906 and SR 12 increased significantly, but to a different extent (Fig. 3-28 a). In youngest shoot, the increase was more pronounced in Pioneer 3906 (146%) compared to SR 12 (39%). On the contrary, the young shoot showed a smaller increase of non-methylated uronic acid concentration in Pioneer 3906 (25%) than in SR 12 (94%). Our findings show that genotypes differed significantly in their response of the total non-methylated uronic acid concentration under salt stress (Fig. 3-28 b). The treatment with 100 mM NaCl caused a significantly higher relative change of non-methylated uronic acid in youngest shoot of Pioneer 3906 compared to SR 12. The young shoot, however, showed a higher relative change in non-methylated uronic acid of SR 12 compared to Pioneer 3906.

3.2.5 Cell-wall neutral sugars as affected during the first phase of salt stress

Neutral sugars were determined using HPAEC-PAD analysis (Fig. 3-29, Table 3-3). Since glucose was included in the neutral sugars, under the given conditions part of the cellulose may be hydrolyzed along with the hemicellulosic glucose (Martens and Loeffelmann 2002). The relative change in galactose concentration in salt-stressed youngest and young shoots of Pioneer 3906 was similar (+ 42%). However, in salt-stressed youngest and young shoots of SR 12, the concentrations of galactose increased by 40 and 85%, respectively. The young shoot of SR 12 showed a significant increase (21%) of glucose due to the salt treatment. The arabinose showed marked changes due to salt stress. Arabinose concentrations increased in youngest and young shoot of Pioneer 3906 by 27 and 22%, respectively. On the contrary, SR 12 showed a 17% increase in arabinose concentration in youngest shoot due to salt stress, and, surprisingly, this increase was 53% for the young shoot of SR 12. For SR 12 the arabinose increase observed in the first experiment proved to be less pronounced in the expanding youngest tissue.
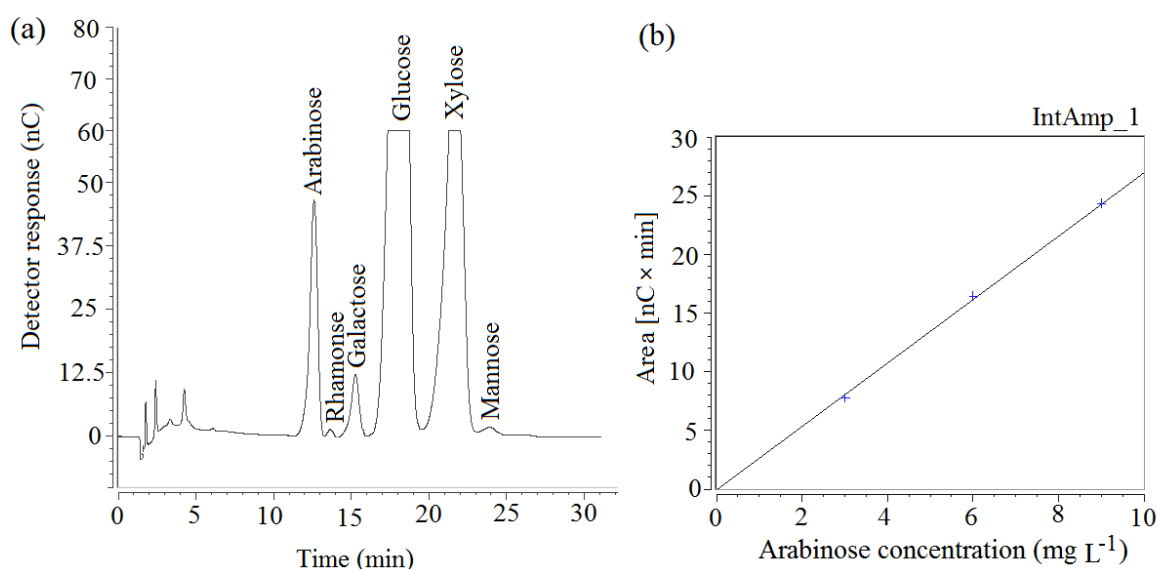
Figure 3-29: (a) A HPAEC-PAD chromatogram of detecting cell-wall neutral sugars, and (b) showing linearity of the three-point calibration curve with arabinose as example.

Table 3-3. Influence of salt stress (100 mM NaCl) on concentrations of neutral sugars in cell wall from youngest (basal 10 cm of 5th and above order leaf blades) and young shoot (5th and above order leaf blades without basal 10 cm segment) of Pioneer 3906 and SR 12. The values are means of four replicates ± SE. Significant differences (p ≤ 5%) between treatments are indicated by different letters. Arabinoxylan concentration was calculated as the sum of xylose and arabinose concentrations (Hossain *et al.* 2006; Christensen *et al.* 2010). ND stands for not detected.

Neutral sugars	Genotypes	Concentration in youngest shoot (mg g^{-1} cell-wall dry mass)			Concentration in young shoot (mg g^{-1} cell-wall dry mass)		
		1 mM NaCl	100 mM NaCl	Relative change (%)	1 mM NaCl	100 mM NaCl	Relative change (%)
Xylose	Pioneer 3906	164.4 ± 21.2 A	186.0 ± 8.5 A	+ 13.2	98.4 ± 5.2 A	98.7 ± 9.0 A	+ 0.4
	SR 12	204.3 ± 9.3 a	228.5 ± 4.9 a	+ 11.9	127.1 ± 4.8 a	140.4 ± 6.6 a	+ 10.4
Arabinose	Pioneer 3906	22.2 ± 2.0 A	28.1 ± 1.0 B	+ 26.5	23.5 ± 1.0 A	28.6 ± 2.5 A	+ 21.7
	SR 12	24.4 ± 0.7 a	28.5 ± 0.4 b	+ 16.8	21.8 ± 0.7 a	33.3 ± 2.0 b	+ 52.8
Arabinoxylan	Pioneer 3906	186.6 ± 23.0 A	214.1 ± 9.3 A	+ 14.8	121.9 ± 6.1 A	127.3 ± 11.4 A	+ 5.0
	SR 12	228.7 ± 9.9 b	257.5 ± 4.9 a	+ 12.4	148.9 ± 5.0 a	173.7 ± 08.4 b	+ 16.7
Glucose	Pioneer 3906	441.0 ± 51.7 A	478.4 ± 18.4 A	+ 8.4	380.3 ± 14 A	397.4 ± 27.6 A	+ 4.5
	SR 12	424.8 ± 9.4 a	395.6 ± 13.7 a	- 6.9	326.3 ± 11 a	395.9 ± 24 b	+ 21.3
Galactose	Pioneer 3906	4.3 ± 0.5 A	6.2 ± 0.5 A	+ 42.1	5.1 ± 0.1 A	7.2 ± 0.05 B	+ 41.9
	SR 12	4.7 ± 0.2 a	6.5 ± 0.3 b	+ 39.6	4.6 ± 0.1 a	8.5 ± 0.10 b	+ 85.0
Rhamnose	Pioneer 3906	0.5 ± 0.1 A	0.9 ± 0.2 A	+ 90.0	ND	ND	-
	SR 12	0.4 ± 0.1 a	0.8 ± 0.1 b	+ 84.5	ND	ND	-
Mannnose	Pioneer 3906	0.7 ± 0.1 A	0.8 ± 0.2 A	+ 12.8	ND	ND	-
	SR 12	0.7 ± 0.0 a	0.8±0.1 a	+ 9.6	ND	ND	-

The arabinoxylan concentration increased slightly but yet significantly due to salt stress in both youngest and young shoots of SR 12. On the contrary, no significant change was observed in arabinoxylan for Pioneer 3906 under salt treatment though a slight increase (14%) was recorded in the youngest shoot of Pioneer 3906 due to the first phase of salt stress. Salt resistant hybrid SR 12 showed significantly higher concentrations in total non-cellulosic neutral sugars (as the sum of β-D-xylose, α-L-arabinose, α-D galactose, α-L-rhamnose and β-D-mannose) in cell-walls of both youngest and young shoots, while Pioneer 3906 did not show any change in total non-cellulosic neutral sugars due to the salt treatment (Fig. 3-30).
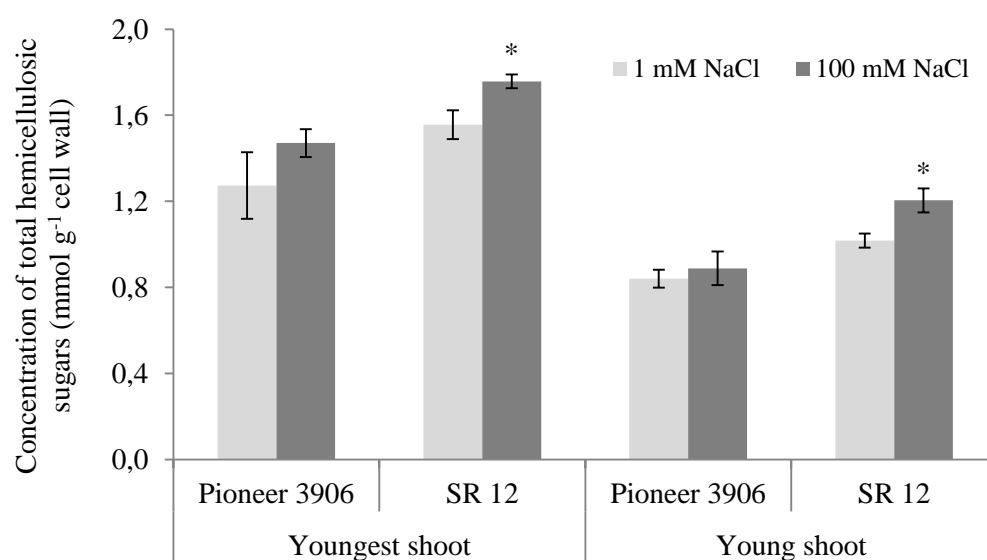
Figure 3-30: Concentrations of total hemicellulosic sugars (the sum of β-D-xylose, α-L-arabinose, α-D galactose, α-L-rhamnose and β-D-mannose) as affected by salt treatment in cell wall of youngest (basal 10 cm of 5th and above-order leaf blades) and young shoot (5th and above order leaf blades without basal 10 cm segment) shoot of Pioneer 3906 and SR 12. The values are means of four replicates ± SE. * = significantly different compared to control with $P \leq 5.0\%$.

3.2.6 Phenolics in maize cell-walls as influenced during the first phase of salt stress

Methanol and acetonitrile aided separation of all the major monomer and dimer standards from each other (Fig. 3-31 and 3-33). Phenolic monomers and dimers compounds were identified through analysis at 210, 265, 280 and 325 nm.

Table 3-4: Spectral data of *cis*-ferulic acid and some diferulates. Detector responses for peak height were recorded at 210, 265, 280 and 325 nm wave length.

Chemical compounds	Peak height (mAU)			
	210 nm	265 nm	280 nm	325 nm
cis-Ferulic acid	103	35	49	63
8-8´-DFA (aryltetralin)	33	10	9	23
8-8´-DFA	20	8	11	24
8-5´-DFA (benzofuran form)	5	3	5	7
Closest left peak of 8-5´-DFA (benzofuran form) (Fig. 3-33, peak no. 1)	25	2	4	2
8-5´-DFA (decarboxylated form)	42	17	19	59
Closest left peak of 8-5´-DFA (decarboxylated form) (Fig. 3-33, peak no. 2)	48	15	10	22
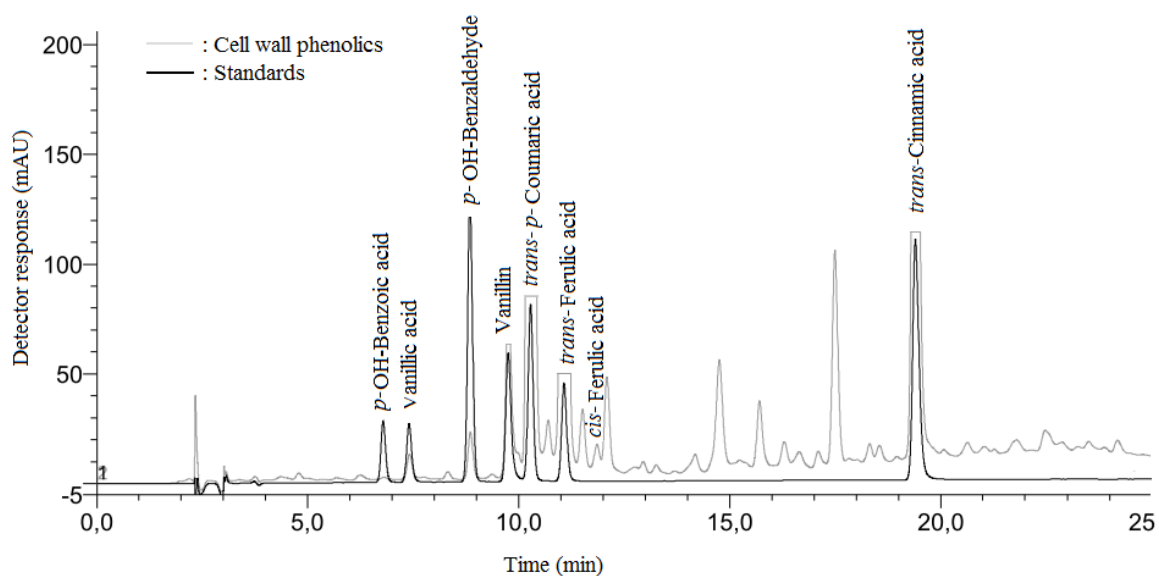
Figure 3-31: RP-HPLC elution profile of some monomeric phenol standards and cell wall-bound monomeric phenols with detection at 280 nm. RP column (LiChrospher®100 RP-18 endcapped 5 µm column (250 mm × 4.6 mm), Techlab, Erkerode, Germany) was used for the separation of monomeric phenols. A gradient elution system was done which increased the relative proportion of methanol and acetonitrile in aqueous 1 mM trifluoroacetic acid (Waldron *et al.* 1996).

In this study, it was investigated whether application of 100 mM NaCl in the nutrient medium could affect various monomeric phenols (*p-OH*-benzoic acid, vanillic acid, *p-OH*-benzaldehyde, vanillin, *trans-p*-coumaric acid, *trans*-ferulic acid and *cis*-ferulic acid) of maize leaf cell-wall (Fig. 3-31 and 3-32). Salt stress significantly increased the concentrations of cell wall-bound *trans*-ferulic acid, *trans-p*-coumaric acid and vanillin in Pioneer 3906, but not in SR 12 (Fig. 3-32).
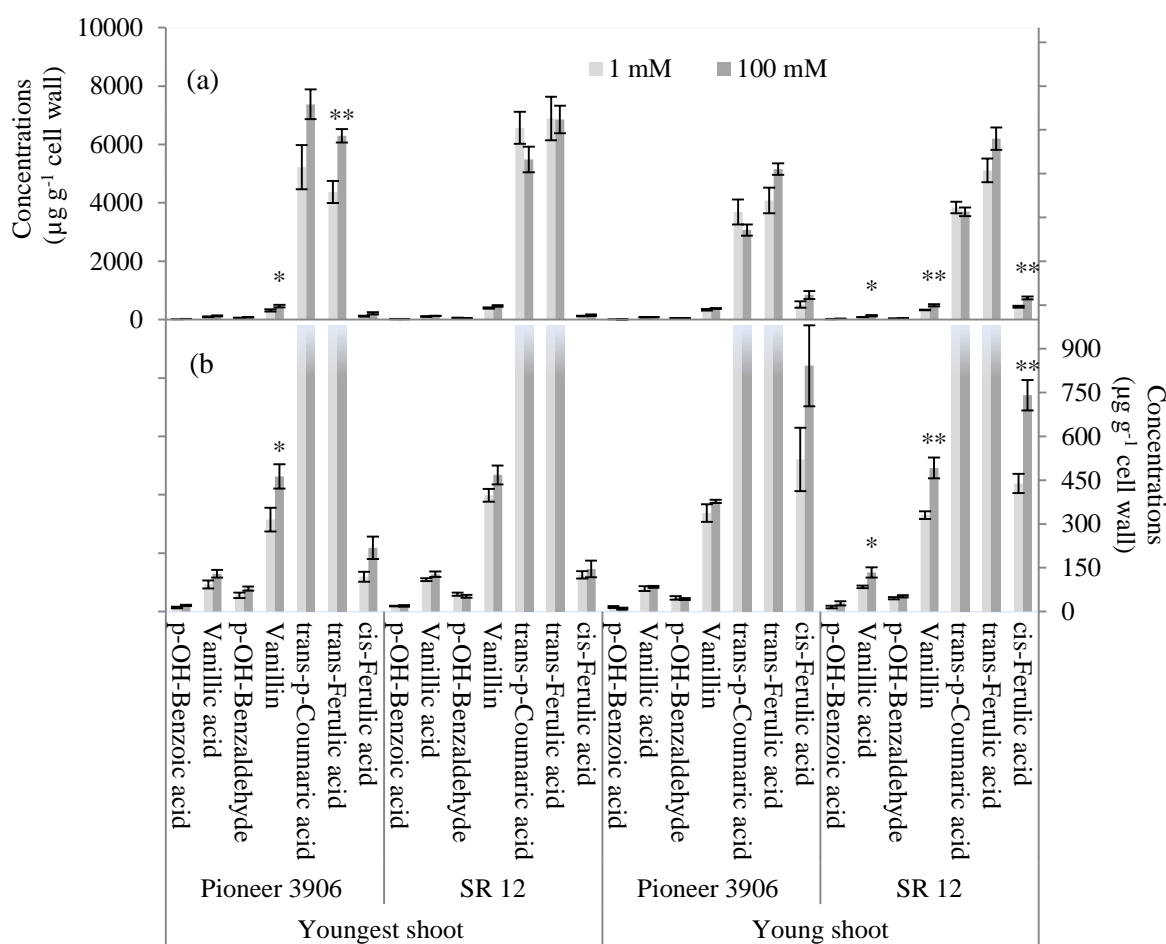
Figure 3-32: Effect of salt stress on various cell-wall monomeric phenols from the youngest (basal 10 cm of 5th and above order leaves) and young (excluding basal 10 cm of 5th and above order leaves) shoots of two maize genotypes Pioneer 3906 and SR 12. Each data point is the mean ± SE of four replicates. Due to a large variation in concentration of various monomeric phenols, data are presented in two scales in the graph. (a) shows the changes in *trans-p*-coumaric acid and *trans*-ferulic acid, while (b) represents the changes in other minor monomeric phenols due to the salt treatment. ** and * = significantly different compared to control with P ≤ 1.0% and P ≤ 5.0%, respectively.

In contrast, young shoot of SR 12 showed significantly higher concentrations of vanillic acid, vanillin and *cis*-ferulic due to the salt treatment. The *trans*-ferulic acid and *trans-p*-coumaric acid were the most dominant hydroxycinnamic acids in both genotypes and in both youngest and young shoot cell-walls. The increase of *trans-p*-coumaric acid and *trans*-ferulic acid was around 41% and 44% in youngest shoot of Pioneer 3906. Salt stress

caused a increase in *cis*-ferulic acid by 83 and 16% in youngest shoot of Pioneer 3906 and SR 12, respectively. On the other hand, young shoots of Pioneer 3906 and SR 12 showed 62 and 69% increase in *cis*-ferulic acid due to salt stress. The concentrations of *cis*-ferulic acid in young shoot of both Pioneer 3906 and SR 12 were 3-5 fold to that of youngest shoot.
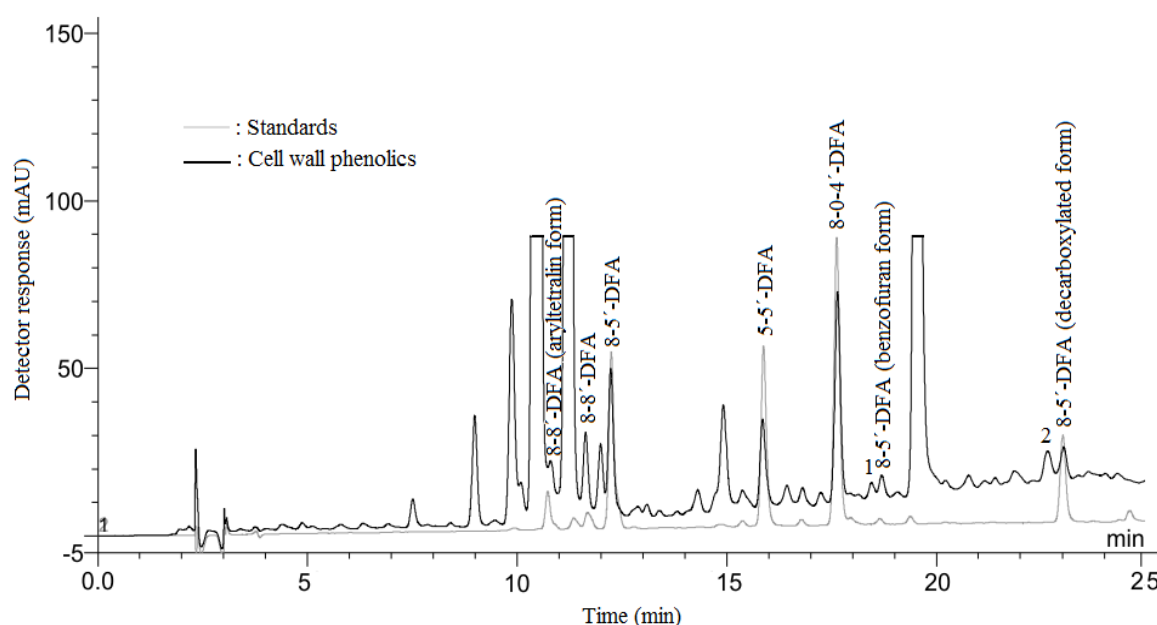
Figure 3-33: RP-HPLC elution profile of some diferulate (DFA) standards and cell wall-bound diferulates (DFA) with detection at 280 nm. RP column (LiChrospher®100 RP-18 endcapped 5 µm column (250 mm × 4.6 mm), Merck, Darmstadt, Germany) was used for the separation of monomeric phenols. A gradient elution system was used which increased the relative proportion of methanol and acetonitrile in aqueous 1 mM trifluoroacetic acid (Waldron *et al.* 1996). Standards of various diferulates were a gift from Prof. Mirko Bunzel, Department of Food Science and Nutrition, University of Minnesota, USA.
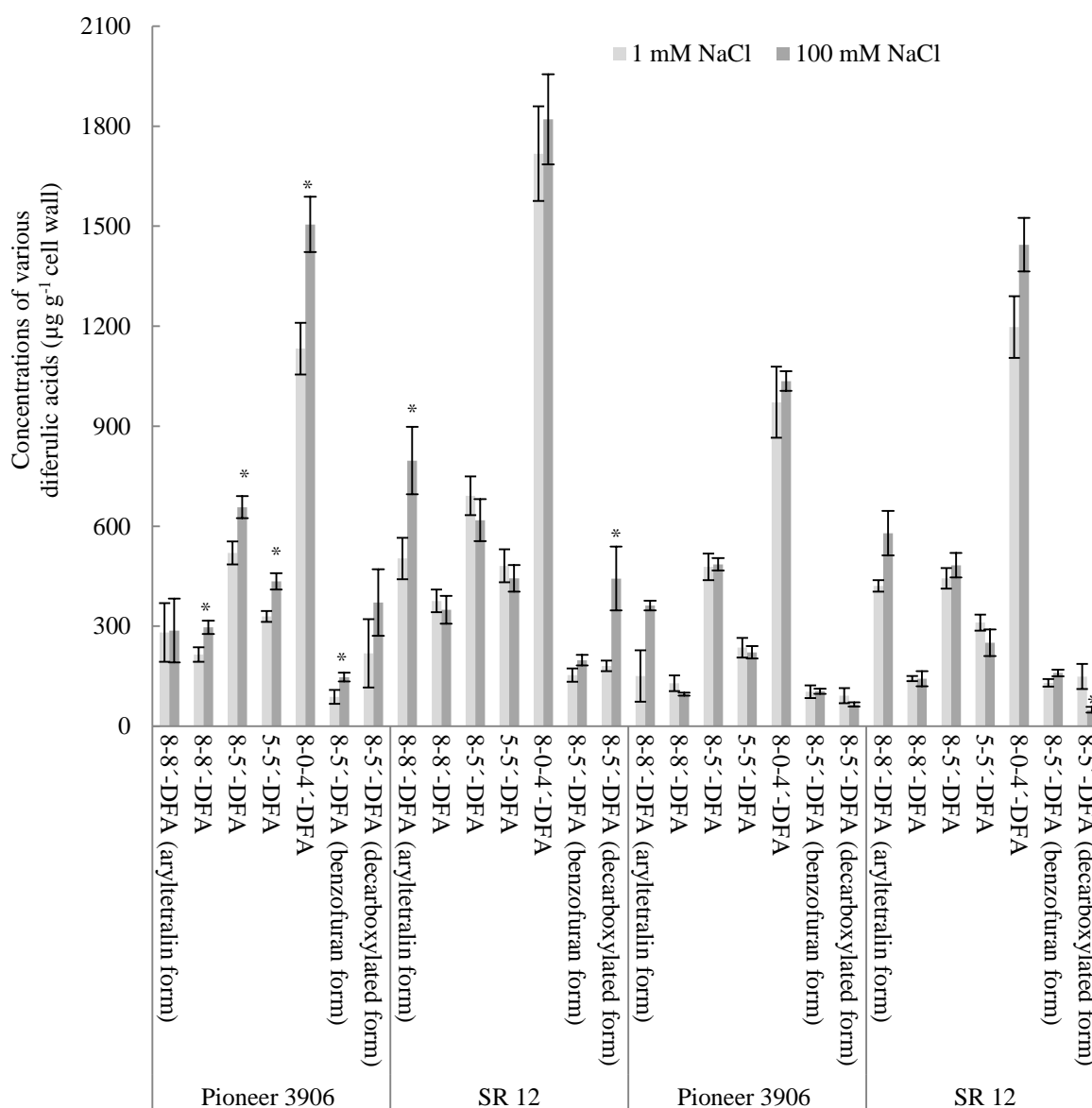
Figure 3-34: Influence of salt stress on various cell-wall diferulic acids (DFA) from the youngest (basal 10 cm of 5th and above order leaves) and young (excluding basal 10 cm of 5th and above order leaves) shoots of two maize genotypes Pioneer 3906 and SR 12. Each data point is the mean ± SE of four replicates.

Seven different diferulic acids namely 8-8´-DFA (aryltetralin form), 8-8´-DFA , 8-5´-DFA, 5-5´-DFA, 8-0-4´-DFA, 8-5´-DFA (benzofuran form) and 8-5´-DFA (decarboxylated form) from the maize cell-wall were quantified (Fig. 3-33 and 3-34). Except 8-8´-DFA (aryltetralin form) and 8-5´-DFA (decarboxylated form), the concentrations of all other diferulates increased significantly due to the salt treatment in the youngest shoot cell-wall

of salt-sensitive genotype Pioneer 3906. The diferulates namely 8-8´-DFA, 8-5´-DFA, 5-5´-DFA, 8-0-4´-DFA, 8-5´-DFA (benzofuran form) were increased in youngest shoot of Pioneer 3906 by 38, 26, 32, 33 and 67%, respectively. On the other hand, the youngest shoot cell-wall of SR 12 showed an increased concentration of 8-8´-DFA (aryltetralin form by 58%) and 8-5´-DFA (decarboxylated form by 145%) under salt treatment, while other forms of diferulates essentially remained unaffected. In the young shoot of both genotypes, there was no significant change in the diferulates concentration except a significant decline of 8-5´-DFA (decarboxylated form) in the young shoot cell-wall of SR 12. In all cases, 8-0-4´-DFA was the most dominant followed by 8-8´-DFA (aryltetralin form) and/or 8-5´-DFA.
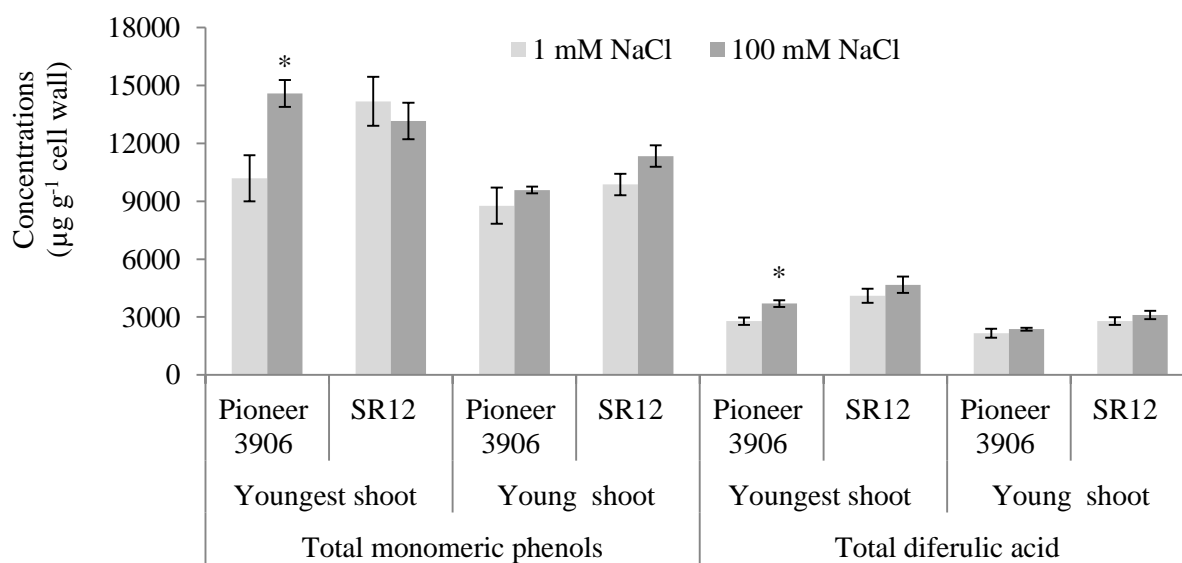
Figure 3-35: Effect of salt stress on the concentrations of total monophenol and diferulic acid in youngest (basal 10 cm of 5th and above order leaves) and young shoot (excluding basal 10 cm of 5th and above order leaves) of Pioneer 3906 and SR 12. Each data point is the mean ± SE of four replicates. * = significantly different compared to control with P ≤ 5.0%.

Total monomeric phenols and diferulic acids were determined as the sum of all quantified monomeric phenols and diferulic acids, respectively (Fig. 3-35). Compared to the control plants, the cell wall isolated from the youngest shoot of Pioneer 3906 showed a significant

increase (43%) in total monomeric phenols concentration. However, the concentrations of total monomeric phenols in youngest shoot of SR 12 and in young shoot of both the genotypes were not significantly affected by salt stress compared to control treatment. Accordingly, the concentration of total diferulic acids increased significantly (33%), but only in the cell wall from youngest shoot of Pioneer 3906 compared to the control (Fig. 3-35). However, there were no significant changes in the total diferulic acid concentrations from the cell wall of youngest and young shoots of SR 12 and young shoot of Pioneer 3906. The concentrations of total monomeric phenols were 2-4 times higher than the total diferulic acid concentrations.
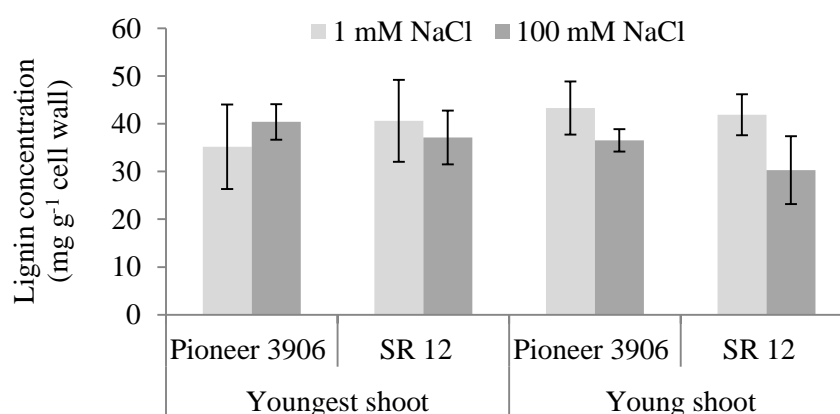
Figure 3-36: Effect of salt stress on lignin concentration in youngest (basal 10 cm of 5th and above order leaves) and young shoot (excluding basal 10 cm of 5th and above order leaves) of Pioneer 3906 and SR 12. Each data point is the mean ± SE of four replicates.

Overall, salt stress had no significant influence on acetyl-bromide-soluble lignin concentration in youngest and young shoots of both Pioneer 3906 and SR 12 (Fig. 3-36). Though it was insignificant, yet there was a decrease in lignin concentration by 28% in salt-treated young shoot of SR 12 compared to the control treatment. Genotypes did not differ in lignin concentration at their youngest as well as in young shoot.

4 Discussion

4.1 Discussion of Experiment 1

4.1.1 Optimization of cell-wall isolation from maize shoot

Before determining the chemical composition of cell wall, it must first be isolated from the plant cells and separated from the intracellular content. To achieve that aim a simpler method should be used to disrupt the plant tissues and wash away the inner contents of cells, leaving the cell walls chemically unchanged. A relatively simple method (by Goldberg 1985) was used to isolate the cell wall that can be used routinely in the laboratory to analyze the cell-wall components. It is evident from the observation (Fig. 3-4) that 12 min crushing of shoot in the blender was sufficient to disrupt the tissues. It allowed the broken tissues to come in contact with different extractant solutions such as 0.4, 0.6 and 1.0 M sucrose solution and 0.1% (v/v) Triton X100. In this way, both 250-405 µm and > 405 µm cell–wall fractions could discharge their protoplasmic contents to the hypertonic solution. Thus both these two fractions showed clean cell wall (Fig. 3-3 and 3-4).

Elimination of starch has been done with cleaning the Triton-X100-treated cell wall with continuous flow of water instead of using any reagent/enzyme such as DMSO or amylase (Goldberg 1985). It was found that this method effectively eliminated the membranous components along with starch particles. Absence of starch was confirmed by a negative test of isolated cell-wall fractions with iodine reagent (Fig. 3-3). Amylase can also be used to eliminate starch from the cell-wall fraction. However, there are some reports that commercial amylase may contain glucanase that may modify the cell wall (Huber and Nevins 1977; Basic and Stone 1980).

On the other hand with light microscopy, it was not found any chlorophyll-containing chloroplast in both the cell-wall fractions. Chlorophyll is located in the thylakoid membrane. Thus, effective elimination of chlorophylls depends on the solubilization of other membranes viz. plasma membrane, outer and inner membrane of chloroplast. Triton X100 came effectively in contact with the thylakoid membranes and dissolved it properly. So, absence of chloroplast in the cell-wall fractions can be considered as one indicator for the absence of membranous contaminants.

The tissue composition of both 250-405 μm and > 405 μm cell-wall fractions were quite different. The 250-405 μm fraction was dominated by mesophyll and epidermal tissues, whereas > 405 μm cell-wall fraction was dominated by vascular and fiber tissues. Thus, these two fractions were totally different from the physiological point of interest. The 250-405 μm fraction was chosen for studying the chemical composition, because it contained cell-wall from the major two tissues (mesophyll and epidermis).

4.1.2 Cell-wall chemical analyses

4.1.2.1 Analysis of uronic acid and its degree of methylation

During colorimetric determination of uronic acid concentration, pink color develops within 5-10 min after the addition of *m*-hydroxydiphenyl reagent which is stable for ~1 h and fades afterwards (Melton and Smith 2001). It was mentioned in an another report that the color is unstable, so the reading should be done in a timely manner (http://cellwall.genomics.purdue.edu/). The same result was found in the present study that the color was quite unstable, hence absorbance was read in a timely manner e.g. counting 10 min time starting from first vortex after the addition of *m*-hydroxydiphenyl till the measurement of absorbance. The effect of salt stress on uronic acid was different for the two cell-wall fractions. Like cellulose and hemicellulosic sugars, total uronic acid also

showed more variation in the 250-405 μm cell-wall fraction due to the salt treatment. Thus for pectin determination, 250-405 μm cell-wall fraction may be of choice.

During analysis of methylation of uronic acid, any traces of unreduced $KMnO_4$ may interfere significantly in the reaction (Wood and Siddiqui 1971), and thus extra care was taken to ensure that no drops of $KMnO_4$ remain on the walls of the test tube when pentane-2,4-dione reagent was added. The spectrophotometer reading can be taken within 1 h of final reaction as no significant fading was noted within 1 h after the final reaction.

4.1.2.2 Optimizing the method for cell-wall neutral sugars analysis

After acid hydrolysis, the cell-wall hydrolysates were cooled and filtered through 0.45 μm PET membrane filter (membraPure GmbH, Germany). Willför *et al.* (2009) used 0.45 μm GHP filters for filtering acid hydrolysates. There was no change in the sugar chromatogram due to the use of PET membrane filter instead to GHP filters in filtering acid hydrolysates ($\approx$ 88 mM). However, the exposure time of acid hydrolysates with the PET membrane filters was less than 15 s. Thus apparently there was no risk in using low-cost PET membrane filters instead of a high-cost GHP filters. In the method, there was a major change in the NaOH concentration used to equilibrate the system for the separation of neutral sugars. After injecting the sample, 2 mM NaOH were used instead of 15 mM NaOH suggested by Willför *et al.* (2009). With trial and error method it was found that 2 mM NaOH was optimum for the separation of six sugar moieties present in the cell-wall hydrolysates (Fig. 3-7).

The standardized HPAEC-PAD method seemed satisfactory for the separation of cell-wall neutral sugars. Less than 2% standard deviation for the major sugars namely glucose, xylose and arabinose confirmed the results reported by Willför *et al.* (2009) who determined the standard deviation for the major sugars as less than 5%. Minor sugars such

as rhamnose, mannose and galactose showed a bit higher standard deviation (3-17%). However, this range of standard deviation for the minor sugars was also corroborated with the results reported by Willför *et al.* (2009). Thus this HPAEC-PAD method can be a quite convenient for regular inspection of cell-wall neutral sugars.

It seemed from the analysis that the 250-405 µm cell-wall fraction arose more interest to monitor the salt-stress induced changes in the cell-wall neutral sugars (Table 3-2). Salt-treated plants from this fraction showed higher relative increase in neutral sugars (21-44%). On the other hand, the > 400 µm cell-wall fraction produced less difference in neutral sugars due to the salt treatment. Thus the 250-405 µm cell-wall fraction may be the physiologically more interesting fraction to investigate the salt-induced changes in neutral-sugar composition.

4.1.2.3 Phenolic analysis

Phenolics were analyzed following the method of Waldron *et al.* (1996). The method of extraction (Hartley and Morrison 1991) was optimized in a way that can be handled in a 2 mL Eppendorf vial. The filtration step of the alkaline hydrolysates through GHP filter was found inconvenient for the small volume of hydrolysates. Thus this step was successfully replaced by the high-speed micro centrifugation (36000 *g*). Four-step alkaline hydrolysis released various monomeric phenols (*p-OH*-benzoic acid, vanillic acid, *p-OH*-benzaldehyde, vanillin, *trans-p*-coumaric acid and *trans*-ferulic acid) and diferulic acids from the cell wall. Among the monomeric phenols, *trans*-ferulic acid was the most dominant one followed by *trans-p*-coumaric acid (Fig. 3-18). Due to lack of DFA standards it was not possible to assign peaks for all the diferulates/oligoferulates in the chromatogram (Fig. 3-16). Peak names for four distinct diferulates were assigned based on

their detector response at 210, 265, 280 and 325 nm (Waldron *et al.* 1996). Then these diferulates were quantified using the response factor according to Waldron *et al*. (1996), and thus the method is semi-quantitative in nature. It is evident from the result (Fig. 3-19) that salt stress had no significant influence on various diferulates. However, a precise conclusion from this experiment was not possible because, DFA standards were not available. Also in this experiment, the whole shoot was harvested that contains mostly older tissues without growth.

4.1.3 Production of diferulates

Possibilities were tested to produce various diferulates using *trans*-ferulic acid, horse radish peroxidase and H_2O_2. It seemed that 0.3 mM *trans*-ferulic acid was better for the enzymatic conversion of *trans*-ferulic acid to oligoferulates compared to 0.1 and 1.2 mM *trans*-ferulic acid. Two peaks were assigned to diferulates (Fig. 3-20), as their chromatogram characteristics (retention time and change in peak area in 4 different wave lengths viz. 210, 265, 280, and 325 nm) were quite similar to those reported by Waldron *et al.* (1996). However, there were some other prominent peaks in the chromatogram which could not be identified according to the method of Waldron *et al*. (1996). On the other hand, many important diferulates (such as 5-5´-DFA and 8-8´-types of DFAs) were missed in the chromatogram. So, this experiment was partially successful for the preparation of various diferulates. Furthermore, methods such as the procedures of Ward *et al*. (2001) to produce DFA neglect that enzymatic cross-linking of free ferulic acid is accompanied by decarboxylation. It yields coupling products different from those present in the cell wall (Dr. Stefan Hanstein, Institute of Plant Nutrition, Justus Liebig University, Giessen, according to personal communication with Mirko Bunzel, Department of Food Science and Nutrition, University of Minnesota, USA).

4.2 Discussion of Experiment 2

Dark-green plants with reduced shoot biomass having no toxicity symptoms in the foliage represent the phenotype during the first phase of salt stress (Fig. 3-23). According to the two-phase growth model of Munns (1993) growth in the first phase of salt stress is mainly reduced by the osmotic component of salinity. In the original model growth reduction in the first phase is identical in salt-sensitive and salt-resistant genotypes. Later on, Schubert *et al.* (2009) have shown that newly developed salt-resistant maize hybrids (SR hybrids) may partially prevent the growth reduction in the first phase of salt stress compared to the salt-sensitive genotypes.

Previous studies revealed that only SR 03 can maintain plasmalemma H^+-ATPase-mediated acidification of the apoplast while SR 12 and Pioneer 3906 cannot maintain wall acidification under salt stress (Pitann *et al.* 2009; Hatzig *et al.* 2010). Therefore, apoplastic acidification cannot explain the better growth during the first phase of salt stress of SR 12 (Hatzig *et al.* 2010). So additional factors must support growth during salt stress in this genotype. Thus information regarding the influence of salt stress on cell-wall components is very important for understanding the cell-wall elongation behavior in the first phase of salt stress.

4.2.1 Growth of maize genotypes is suppressed during first phase of salt stress

There was a strong growth inhibition of maize shoot during the first phase of salt stress (100 mM NaCl) in both the salt-sensitive (Pioneer 3906) and the salt-resistant (SR 12) maize genotype (Fig. 3-24). The newly developed salt-resistant (SR) maize hybrid SR 12 grew relatively better than salt-sensitive genotype Pioneer 3906 under salt stress. Experimental results showed a significant advantage in shoot growth of salt-resistant SR 12 compared to the salt-sensitive Pioneer 3906 under salt treatment. Trend of plant height under salt stress (Fig. 3-21) revealed that the onset of salt stress was somehow delayed in

the salt-resistant genotype SR 12 than the salt-sensitive Pioneer 3906. These results (Fig. 3-24) are in agreement with other studies (Pitann *et al.* 2009; Schubert *et al.* 2009; Hatzig *et al.* 2010) that demonstrated relatively better growth of the salt-resistant SR hybrids compared to salt-sensitive Pioneer 3906 under salt stress.

4.2.2 Cell-wall dry mass increases during first phase of salt stress

In the present study, it was found that the ratio between cell-wall dry mass and shoot fresh mass was increased by salt treatment in salt-resistant SR 12 hybrid as well as in salt-sensitive Pioneer 3906 (Fig. 3-25). This increment in cell-wall dry mass in the first phase of salt stress can be considered as an indicator for reduced cell elongation resulting in a decrease of the individual cell size and/or partitioning of relatively more dry mass in cell wall without elongation. Eitenmüller (2011) and Leubner (2011) also observed an increase of the ratio between cell-wall dry mass and shoot fresh mass by 41 and 36% in the young shoots (4th and above order leaves) of Pioneer 3906 and SR 12, respectively, under salt stress. The inhibition of elongation growth of *Cicer arietinum* epicotyl grown in PEG also led to an increase in the ratio between wall dry mass and epicotyls fresh mass due to the inhibition of elongation growth of cells (Muñoz *et al.* 1993). Partitioning of relatively more dry mass in cell wall without elongation occurred during differentiation of xylem parenchyma cells in maize roots (Yeo *et al.* 1977). It was also reported that PEG or NaCl-induced osmotic stress exhibited a drastically altered growth character in tobacco cultured tissues with volume only one-fifth to one-eighth of unstressed cells (Binzel *et al.* 1985, 1987, 1988). Halophytes as well have been reported to synthesize higher amount of cell-wall dry mass under saline environment (Binet 1985).

4.2.3 Cellulose concentration decreases during the first phase of salt stress

Cellulose plays a major role in determining the strength and structural basis of the cell wall. Shoot cell-wall from salt-stressed plants of both Pioneer 3906 and SR 12 showed a reduced concentration in cellulose (Fig. 3-26). Leubner (2011) could show a NaCl-induced reduction of cellulose by 14 and 19% in the young shoots of Pioneer 3906 and SR 03, respectively. On the other hand, Eitenmüller (2011) found a decrease of cellulose by 36% in the salt-treated SR 12 compared to control. Osmotic stress-induced inhibition of cellulose concentration has long been reported for cotton roots (Zhong and Läuchli 1993), tobacco culture cells (Iraki *et al.* 1989), in expanding grape leaves (Sweet *et al.* 1990) and in elongating wheat coleoptiles (Wakabayashi *et al.* 1997c). It was reported (Zhong and Läuchli 1993) that salinity caused a decrease in the cellulose concentration in cell wall of cotton seedlings. It was found that supplemental Ca^{2+} prevented these changes in cellulose concentrations (Zhong and Läuchli 1993). In the present study, maize genotypes were grown under conditions where Ca^{2+} was not limiting in the nutrient medium, as the full strength nutrient solution contained sufficient Ca in control as well as in salt treatment [2.0 mM $Ca(NO_3)_2$ and 2.0 mM $CaCl_2$]. Nonetheless, there was a significant reduction (12-19%) in cellulose concentrations in the growing shoot from salt-treated plants with a concomitant decrease in shoot fresh mass (Fig. 3-24 and 3-26).

One can expect that high concentration of cellulose may contribute to the cell wall-tightening processes. It is believed that the hemicelluloses form a strong non-covalent H-bond with cellulose microfibrils, thus forming a tight cellulose-hemicellulose interacting complex (Carpita 1983; Carpita and Gibeaut 1993). Thus, it is apparent that cell-wall tightening by cellulose was not the cause for the reduction of cell-wall extensibility of maize genotypes during first phase of salt stress. So far it is not clear how the structure and function of the cellulose-synthesizing complex, that is located in the plasma membrane, are

influenced by salt stress. Piro *et al.* (2003) concluded that under drought stress simulated by PEG the reduction in the newly synthesized cellulose was due to alterations in the environment of the cellulose-synthesizing complex located in the plasma membrane.

4.2.4 Uronic acid and its de-esterification are greatly affected in the first phase of salt stress

The NaCl-induced impairment of cellulose concentration partially coincided with the higher concentration of uronic acid (pectin) (Fig. 3-27). Pectins are generally confined to primary cell-wall and lacking in non-extendable secondary cell wall which suggests their possible function in cell expansion (Willats *et al.* 2001; Knox 2002; Evert 2006). The pectic polysaccharides form a matrix surrounding and interacting with cellulose and hemicellulose and affect a broad range of functions including cell adhesion, cell extension, cell-wall assembly, cell-wall porosity and mechanical properties of cell wall (Talboys *et al.* 2011). Gibeaut *et al.* (2005) found that during the elongation phase of barley coleoptile tissue, pectic polymers declined. De-esterification of uronic acid, leading to pectin gels, was coupled with growth cessation in both grasses and dicotyledons (Kim and Carpita 1992; McCann *et al.* 1994; Liberman *et al.* 1999; Cosgrove 2005; Al-Ghazi *et al.* 2009). Therefore, any change in pectins may be crucial for explaining growth reduction in the first phase of salt stress. Our results of increased concentrations of total uronic acid in maize genotypes Pioneer 3906 and SR 12 under high salt treatment are in agreement with the report of Zhong and Läuchli (1993) who demonstrated that salt stress increased the total uronic acid concentration in cotton root tips. Also, Leubner (2011) demonstrated that salt stress augmented uronic acid in the upper-shoot (4th and above order leaf blades) cell wall of Pioneer 3906. This increase in the uronic acid concentrations in Pioneer 3906 and SR 12 which is in parallel with the inhibition of shoot fresh mass in the 100 mM NaCl treatment, could be a result of reduced degradation of polyuronides or increased synthesis of

polyuronides (Zhong and Läuchli 1993). Also, it has been reported that expanding grape leaves showed an increase in total uronic acid concentration under drought stress (Sweet *et al.* 1990). Metabolic flexibility may allow plants to bridge cellulose and uronic acid. UDP-glucose, which is a substrate for both cellulose and uronic acid synthesis, may form UDP-glucuronic acid after oxidation with UDP-glucose-dehydrogenase (Seitz *et al.* 2000). Galacturonic acid can be formed from the UDP-glucuronic acid after epimerization reaction. Accumulation of uronic acid-enriched polymers was observed in *Arabidopsis* mutants which showed impairment of cellulose synthesis (Burton *et al.* 2000; Sato *et al.* 2001; Manfield *et al.* 2004; Hamann *et al.* 2009). It thus seems that the pectic polysaccharides compensate the reduction of cellulose in cell walls of both Pioneer 3906 and SR 12 under salt stress. However, genotype SR 03 did not show any change in uronic acid although cellulose was decreased (Leubner 2011).

The specific functions of pectins in distinct parts of cell wall or plant tissues are strongly influenced by the amount and nature of the pectic molecules present. The results here (Fig. 3-27 b) indicate that salt stress alters the quality of pectin which can be concluded from the decrease of the degree of methylation of uronic acid in cell wall from the youngest shoot of both Pioneer 3906 and SR 12. The percentage of esterification of pectin increased concomitantly with the rate of elongation of maize coleoptiles (Kim and Carpita 1992). Surprisingly, the growing shoot of SR 03 showed a slightly higher degree of methylation under salt treatment (Leubner 2011). This indicates that the relatively salt-resistant genotype SR 03 maintains a higher degree of methylation of uronic acid in cell walls of elongating shoots under salt stress which may have allowed this genotype to grow relatively better than the salt-sensitive Pioneer 3906 (Pitann *et al.* 2009).
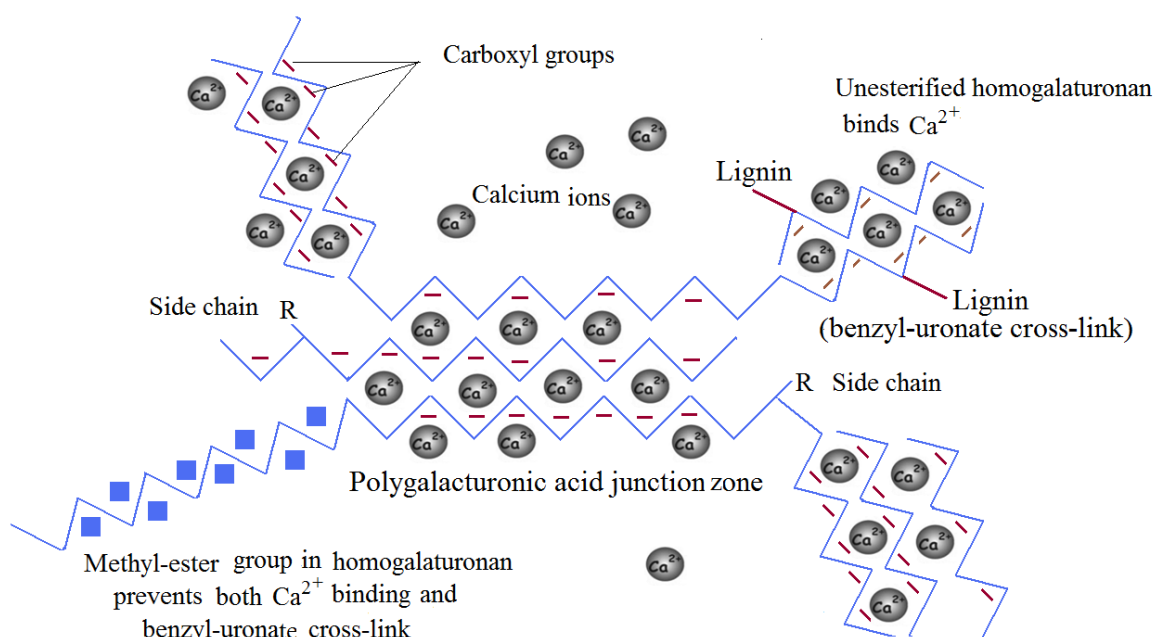
Figure 4-1: A schematic "egg-box" model showing calcium cross-links in the pectin of cell wall (modified after Morris *et al*. 1982). Around 15-20 uninterrupted non-methylated galacturonic acids can form a stable Ca^{2+}-pectate complex. In addition, pectin can be cross-linked with lignin via benzyl-uronate (Grabber and Hatfield 2005).

For Pioneer 3906, the increase in concentration of non-methylated uronic acid during the first phase of salt stress was higher in the youngest shoot segments compared to the young shoots (Fig. 3-28) indicating that the elongation growth of the youngest shoot of Pioneer 3906 was more suppressed due to the higher accumulation of non-methylated uronic acid. On the contrary, the accumulation of non-methylated uronic acid in SR 12 was higher in young shoots than in youngest shoots indicating that the elongation growth of youngest shoot of SR 12 was favored due to the lower increase in non-methylated uronic acid. Leubner (2011) found a slight decrease of non-methylated uronic acid in the growing shoot of SR 03 in the first phase of salt stress. This is another physiological advantage of SR 03 under saline condition.

Grass cell-wall has two major polysaccharides that contribute to total uronic acid, the galacturonic acid-rich pectins and the hemicellulosic GAX (Kim and Carpita 1992). In

maize, however, the relative contribution of galacturonic acid to the total uronic acid is much higher than that of glucuronic acid from GAX (Kim and Carpita 1992). There was a large increase in the concentration of total uronic acid (Fig. 3-27 a) in salt-treated cell walls, while only minor changes occurred in the xylose concentration (Table 3-3). This provides evidence that the observed uronic acid increase was due to polygalacturonic acid (PGA) in junction zones (Fig. 4-1).

The uronic acid units of polygalacturonic acid are methylated during synthesis and secretion to the cell wall, and in this form they have a reduced capacity to form Ca^{2+} crosslinks (Fig. 4-1) (Knox *et al.* 1990). Hence, methylation not only prevents premature cross-linking with Ca^{2+} during secretion to the wall (Knox 2002) but also maintains growth in expanding tissue (Kim and Carpita 1992). Later on, the subsequent action of pectin methyl esterases (PMEs) on homogalacturonan in the cell wall can increase the extent of non-methylated galacturonic acidic sites of homogalacturonan chains which has the capacity to form stiff gels via Ca^{2+}-crosslink (Fig. 4-1), and this may lead to cell-wall tightening that in turn leads to reduced cell-wall extensibility (Knox 2002; Cosgrove 2005). Moreover, cell-wall porosity that may restrict access of wall-loosening enzymes, such as expansins to its substrates (Cosgrove 2005), thus preventing the role of H^+ secreted by the plasma membrane H^+-ATPase. Around 15-20 contiguous non-methylated galacturonic acids can form a stable concerted Ca^{2+}-pectate complex (also known as "egg-box" linkages), and such frequent egg-box linkages (Fig. 4-1) may form gel-like structures in the wall comparable to jam and jelly (Morris *et al.* 1982; Brett and Waldron 1996).

Non-methylated galacturonans in lignifying tissues hold an enormous potential to form cross-links with lignin as benzyl-uronate, and this kind of cross-links cannot be formed with methylated galacturonan (Grabber and Hatfield 2005). So, it is very likely that a part

of the enhanced amount of non-methylated uronic acid produced under salt stress in growing shoots of Pioneer 3906 and SR 12 may have formed benzyl-uronate cross-links since even the primary wall of maize contains lignin though the amount is low (Grabber and Hatfield 2005).

During maturation of grape leaves, the relative proportion of uronic acid increased in cell wall (Sweet *et al.* 1990). Our data also support that the concentration of total uronic acid in older tissues is always higher than in younger tissues for maize genotype Pioneer 3906 (Fig. 3-27 a). Meristematic tissues are characteristically low in Ca^{2+}, and the level increases as the cells elongate and differentiate (Carpita and Gibeaut 1993). Nakajima *et al.* (1981) demonstrated that during differentiation of pea meristem to epidermal tissue, the proportion of Ca^{2+} increased six-fold indicating extensive Ca^{2+} cross-linking of non-methylated galacturonans in aged tissues. A relatively higher increase in total uronic acid or non-methylated uronic acid in the young shoot (Fig. 3-27, 3-28) of SR 12 compared to that in youngest shoot under salt stress suggests that the process of cell-wall maturation is somehow delayed in the salt-resistant genotype SR 12 relative to Pioneer 3906 in the first phase of salt stress. Additionally, studies on youngest and young shoot under control conditions (1 mM NaCl) reveal that the genotype SR 12 eventually shows a delay in accumulation of total and non-methylated uronic acid compared to Pioneer 3906 (Fig. 3-27, 3-28). Thus the process of maturation may be genetically slowed down in SR 12 compared to Pioneer 3906, and helps SR 12 to grow relatively faster and better than Pioneer 3906 under salt stress.

4.2.5 Cell-wall neutral sugars are altered differentially during first phase of salt stress

Xylose which together with glucose is an abundant non-cellulosic cell-wall sugar showed no major changes in response to 100 mM NaCl (Table 3-3). Tobacco cells grown either in

PEG or NaCl showed higher proportions of hemicelluloses (Iraki *et al.* 1989). However, in the growing zone of cotton roots (Zhong and Läuchli 1993) or in expanding grape leaves (Sweet *et al.* 1990) there were no major changes in non-cellulosic sugars due to salt or drought stress. So our results are in line with other studies.

The young shoot of SR 12 showed a significant increase (21%) of glucose (Table 3-3) which due to the extraction procedure contains some cellulosic glucose (Martens and Loeffelmann 2002). Since a significant decrease of cellulose concentration in response to salt stress occurred, this increase of glucose fraction may be attributed to the mixed link (1→3, 1→4)-β-D-glucan (simply β-glucan). The accumulation of β-glucans coincides with the rapid elongation of maize coleoptiles (Kim *et al.* 2000). As the elongation rate decreases, the β-glucan is hydrolyzed by glucanases (Capita *et al.* 2001). However, the shoot fraction with highest elongation rate is the youngest shoot, for which no salt effect on glucose was observed.

Salt stress clearly increased galactose concentrations in the growing regions of shoots of both SR 12 and Pioneer 3906 maize genotypes (Table 3-3) with a decrease in shoot fresh mass suggesting a role of galactose in suppression of the shoot elongation process. Eitenmüller (2011) also demonstrated a significantly higher concentration of galactose in both SR 12 and SR 03 in the first phase of salt stress. It has been reported that during normal growth of *Cicer arietinum* coleoptiles, the total amount of galactose from the pectic fractions decreased (Muñoz *et al*. 1993) and it was interpreted that a decrease in the quantity of galactose may be necessary throughout the growth in order to permit cell-wall loosening. Galactose-rich cell-wall showed a decrease in growth ability (Tanimoto 1988) and a decline in pectic galactose during the stage of maximum growth has been reported by Sakurai *et al.* (1987a, b). In pea epicotyl, the galactose-poor cell walls showed correlation with auxin-induced elongation growth (Tanimoto and Igari 1976). Ordin and Bonner

(1957) found that glucose incorporation into cellulose is inhibited by galactose and thereby cell-wall growth is retarded (Ordin and Bonner 1957). Lower concentration of cellulose during the first phase of salt-stress concomitant with the increase in galactose concentration was found for both Pioneer 3906 and SR 12 (Fig. 3-26 and Table 3-3). Thus galactose may have a role in cell-wall growth in the first phase of salt stress.

Under salt stress, there was an increase in arabinose concentrations in the youngest shoots of both Pioneer 3906 and SR 12 (Table 3-3). Thus, it is likely that cellulose-hemicellulose cross linkage via H-bond (Carpita and Gibeaut 1993) was reduced under salt stress, and this may have counteracted the repression of shoot elongation. However, arabinose moieties in arabinoxylan can be esterified with ferulic acid and then two feruloylated arabinoxylan chains can be linked by peroxidase activity to form diphenyl bonds which may then enhance the cell-wall tightening process (Brett and Waldron 1996). Thus the higher concentration of arabinose can be advantageous for growth if arabinose is not cross-linked via diferulates or oligoferulates.

4.2.6 Analysis of cell-wall phenolics

4.2.6.1 Separation and identification of very closely eluted phenolics

Methanol and acetonitrile aided separation of all the major monomer and dimer standards from each other (Fig. 3-31, 3-33). Very closely eluted phenolic monomers and dimmers compounds were identified based on (i) peak matching with standard run and (ii) their detector response at 210, 265, 280 and 325 nm. Spectral data were very useful for precise identification of some monomeric phenols and diferulates (Walddron *et al.* 1996). For example, 8-5´-DFA (decarboxylated form) was identified based on RP-HPLC run of standard substance (Fig. 3-33). The highest detector response (Table 3-4) was recorded at 325 nm wave length (Dobberstein and Bunzel, 2010) for the 8-5´-DFA (decarboxylated

form) while the very closest left peak gave (Fig. 3-33, peak 2) highest detector response at 210 nm wave length.

4.2.6.2 Changes in monomeric phenols during salt stress

Salt stress augmented the concentration of total monomeric phenols (sum of all detected monomeric phenols) in the youngest shoot of Pioneer 3906, but not of SR 12 (Fig. 3-35). This suggests that the shoot elongation of Pioneer 3906 could be affected by phenolics under saline condition. Individual phenolics with significantly higher concentration during salt stress were *trans*-ferulic acid and vanillin. The cell-wall extensibility may be declined due to the increase in wall-bound ferulic acid (Tan *et al.* 1992a), which probably interferes with the enzymatic breakdown of wall polysaccharides (Fry 1984). Increased concentration of feruloylated glucuronoarabinoxylan (FA-GAX) is considered to be very important at the later stage of plant development for two reasons. It may serve as a site for nucleation to form lignin and linkage of lignin to the xylo-cellulosic fibers by means of xylan-ferulate-lignin complexes (Iiyama *et al.* 1994; Jacquet *et al.* 1995; Bartolomé *et al.* 1997).

Isomerization between *trans*-ferulic acid and *cis*-ferulic acid alters the structure of the molecule and may be part of the phototropic reaction driven by turgor pressure and water flux (Towers and Abeysekera 1984). Under control condition, the *cis*-ferulic acid in youngest and young shoots of Pioneer 3906 was 3 and 11% of the total ferulic acid (*cis* + *trans* forms), while *cis*-ferulic acid in youngest and young shoot of SR 12 was 2 and 8% of total ferulic acid (Fig. 3-32). Thus it is clear that *cis*-ferulic acid increased in maize leaves with increasing tissue age. Locher *et al.* (1994) suggested that wall-bound *cis*-ferulic acid may be associated with tightening of the root cell-wall restricting the elongation rate in dark-grown maize roots. In the present study, salt treatment caused an increase of *cis*-ferulic acid in elongated tissue (young tissue) of SR 12. Thus the observation does not

provide evidence for a critical role of *cis*-ferulic acid during shoot elongation for the hypothesis of Locher *et al.* (1994).

4.2.6.3 Diferulates are augmented in elongating shoot of salt-sensitive genotype during salt stress

Ferulic acid (FA) is ester-linked to arabinose moieties of glucuronoarabinoxylan (GAX) to form FA-GAX. Diferulic acid is produced from the linked ferulic acid by a coupling reaction mediated by peroxidase, which cross-links FA-GAX polysaccharides (Fig. 4-2). The resultant diferulates (DFA) cross-linking contributes to cell-wall assembly and tightening, and is thought to be involved in declining cell-wall extensibility (Fry 1979, Carpita and Gibeaut 1993; Hatfield *et al.* 1999; Fry 2004; Parker *et al.* 2005).
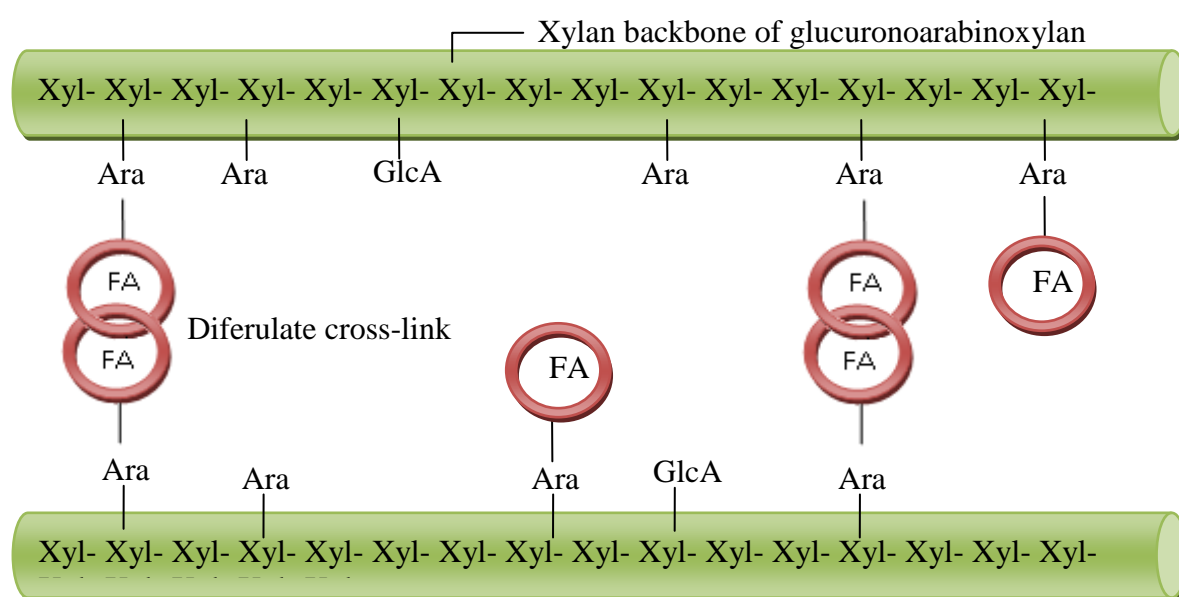
Figure 4-2: A model of grass glucuronoarabinoxylan (GAX) which are cross-linked via diferulic acid (FA-FA).

The increased concentrations of various diferulates namely 8-8´-DFA, 8-5´-DFA, 5-5´-DFA, 8-0-4´-DFA and 8-5´-DFA (benzofuran form) in the youngest shoot of salt-sensitive genotype Pioneer 3906 during the first phase of salt stress (Fig. 3-34) suggests that they may directly contribute to the cell-wall tightening process and thereby to reduction of shoot growth (Fig. 3-24). However, 8-5´-coupled diferulates (8-5´-DFA, 8-5´-DFA

93

benzofuran form and 8-5´-DFA decarboxylated form) originate from the same 8-5´-DFA during extraction of cell-wall phenolics (Dr. Stefan Hanstein, Institute of Plant Nutrition, Justus Liebig University, Giessen, according to personal communication with Mirko Bunzel, Department of Food Science and Nutrition, University of Minnesota, USA). Thus to see any effect of this 8-5´-type diferulate, it is important to sum up all these three types of 8-5´-coupled diferulates. The sum of 8-5´-coupled diferulic acids did not show any difference in any genotype due to the salt treatment (results non shown).

The concentrations of total 8-coupled (all 8-5´- and 8-8´-coupled diferulic acids) DFAs were 7-11 times to that of 5-5´-DFA in both Pioneer 3906 and SR 12 and in both youngest and young shoot cell-walls. Thus our results also confirm previous results (Grabber *et al.* 1995; MacAdam and Grabber 2002; Ralph *et al.* 1994) that the contribution of 8-type diferulates dwarfed that of 5-5´-DFA. Thus 5-5´-DFA alone may be a poor indicator for the degree of ferulate dimerization in vivo. For that reason, analysis of all DFAs is required to accurately reflect the overall ferulate cross-linking in cell walls. In fact, MacAdam and Grabber (2002) demonstrated that elongation of leaf blade of tall fescue (*Festuca arundinacea* Schreb.) decelerated as 8-O-4-, 8-5-, 8-8-, and 5-5-DFA accumulated in cell walls. Thus our results of increased concentrations of various DFAs support the hypothesis that diferulates are involved in reducing elongation growth during salt stress.

In Poaceae, the augmentation of cell-wall bound DFA is highly correlated with a decline in cell-wall extensibility (Kamisaka *et al.* 1990; Tan *et al.* 1991; Tan *et al.* 1992 a, b; Miyamoto *et al.* 1994; Parvez *et al.* 1997). On the other hand, wall extensibility is maintained when DFA does not accumulate (Kawamura *et al.* 2000; Wakabayashi *et al.* 1997a, b). The results reported here were obtained after extraction with 2 M NaOH for 24 h. This treatment does not release the etherified phenolic compounds. The importance of this fraction can be derived from the observation that it binds 20% of the non-cellulosic

polysaccharides to cellulose (Carpita and Gibeaut 1993). The formation of ether bonds between aromatic compounds requires generation of radicals which then couple non-enzymatically. As our data on ferulic acid and diferulic acids demonstrate enhanced radical coupling of esterified ferulic acid occurred in the youngest shoot of Pioneer 3906. It is likely that it is mainly the etherified fraction which affects the cell-wall extensibility. Ferulic acid increase was followed by DFA increase and this indicates that enzymatic systems for cross-linking were not limiting. In fact, Faust (2011) reported that phenolic peroxidase activity in SR 12 was not affected by salt stress. Thus the results of the present study are in line with previous findings.

5 Summaries

5.1 Summary of Experiment 1

A method of cell-wall isolation was optimized, and cell walls were separated into two fractions (250-405 µm fraction and > 405 µm fraction). Both the cell-wall fractions showed negative color test with iodine reagent and thus were free from starch content. Cellulose, neutral sugars and uronic acid responses due to the salt treatment were obvious from the 250-405 µm cell-wall fraction. On the other hand, the > 405 µm cell-wall fraction did not show much variation in results due to the salt treatment. The 250-405 µm fraction was dominated by cell wall from mesophyll and epidermal tissues, while the > 405 µm fraction was dominated by cell wall from vascular and fiber tissues. It was evident from the analyses that the 250-405 µm cell-wall fraction gave the results of interest under salt stress. Thus results showed clearly that the 250-405 µm cell-wall fraction may be the most important fraction for studying salt-induced changes in cell-wall compositions.

5.2 Summary of Experiment 2

Growth inhibition of crops in the first phase of salt stress is one of the core questions in the field of stress physiology and the mechanisms are not yet precisely known. Maize is able to maintain shoot turgor pressure during the first phase of salt stress. Assimilate supply to the growing tissue under salt stress is not found limiting under salt stress. Additionally, water uptake by maize plants from the saline solution did not limit growth. It has been reported that the maintenance of apoplastic acidification under saline condition contributes to the better performance of the salt-resistant genotype SR 03. Surprisingly, another salt-resistant genotype SR 12 cannot maintain apoplastic acidification during the first phase of salt stress despite of its better growth compared to Pioneer 3906. Thus apoplastic acidification only partly explains the strong growth reduction during the first phase of salt stress. So additional factors must be involved in reducing the cell-wall extensibility. It is presumed that the chemical composition of the cell wall may be changed during the first phase of salt stress, which may play a crucial role to reduce cell-wall extensibility in a differential manner in salt-sensitive (e.g. Pioneer 3906) and salt-resistant (e.g. SR 12) genotypes.

The present study was conducted to examine the hypotheses that (i) cell-wall polysaccharides, which result in tightening of cell wall to reduce plant growth, are changed in the growing leaves during the first phase of salt stress; (ii) leaf-growth reduction is accompanied with changes in leaf cell-wall monomeric phenols and various diferulates during the first phase of salt stress; (iii) salt stress-induced changes in cell-wall components are different in the salt-sensitive Pioneer 3906 and the salt-resistant SR 12.

Following conclusions are supported from this study:

(i) Salt treatment caused a strong inhibition of shoot growth with a concomitant increase in the ratio of cell-wall dry mass and shoot fresh mass, and a decrease in cell-wall cellulose concentrations in both Pioneer 3906 and SR 12. NaCl caused a large increase in the concentrations of total and non-methylated uronic acid in both salt-sensitive Pioneer 3906 and salt-resistant SR 12. It is concluded that a low accumulation of non-methylated uronic acid in leaf cell-wall may, among other mechanisms, contribute to salt resistance in the first phase of salt stress.

(ii) Salt stress favors cell-wall components participating in oxidative cross-linking in elongating shoot tissue of salt-sensitive maize genotype Pioneer 3906. The salt-sensitive genotype Pioneer 3906 had higher concentrations of ferulic acid (FA) and various diferulic acids (DFAs) during salt stress, while in the new hybrid SR 12 these parameters were unchanged. Both genotypes showed an increase in arabinose, which is the molecule at which FA and DFA are coupled to interlocking glucuronoarabinoxylan (GAX) fibers. Results are consistent with the concept that accelerated oxidative fixation of shape contributes to growth suppression in the salt-sensitive genotype during the first phase of salt stress.

(iii) The onset of the accumulation of non-methylated uronic acid was delayed in SR 12, which indicates that this may be one reason for the better growth performance of this genotype under salt stress compared to Pioneer 3906. Also, salt-sensitive genotype Pioneer 3906 showed a significantly higher increase in ferulic acid, total diferulic acid and total monomeric phenols in the youngest shoot during the first phase of salt stress compared to SR 12.

6 Zusammenfassungen

6.1 Zusammenfassung von Experiment 1

Das Verfahren zur Zellwandisolierung wurde optimiert und die Zellwände wurden in zwei Fraktionen (250-405 µm Fraktion und > 405 µm Fraktion) getrennt. Beide Zellwandfraktionen zeigten ein negatives Ergebnis im Iodtest und waren somit frei von Stärke. Reaktionen von Cellulose, neutralen Zuckern und Uronsäure waren aufgrund der Salzbehandlung in der 250-405 µm Zellwandfraktion offensichtlich. Auf der anderen Seite zeigte die > 405 µm Zellwandfraktion nur einen geringen Einfluss der Salzbehandlung. Die 250-405 µm Fraktion wurde durch Mesophyllzellwand und epidermales Gewebe dominiert, während die > 405 µm Fraktion durch Zellwand von Gefäß und Fasergewebe dominiert wurde. Diese Ergebnisse zeigen deutlich, dass die 250-405 µm Zellwandfraktion besser geeignet ist, salzinduzierte Veränderungen der Zellwandzusammensetzung zu untersuchen.

6.2 Zusammenfassung von Experiment 2

Die Hemmung des Wachstums von Nutzpflanzen in der ersten Phase von Salzstress ist eine der zentralen Fragen im Bereich der Stressphysiologie, jedoch sind die Mechanismen noch nicht genau bekannt. Mais ist in der Lage, den Sprossturgordruck während der ersten Phase von Salzstress aufrecht zu halten. Die Assimilatzufuhr für die wachsenden Gewebe unter Salzstress ist nicht der limitiernde Faktor unter Salzstress. Zudem ist die Wasseraufnahme aus der Salzlösung nicht begrenzend für das Wachstum der Maispflanze. Es wurde gezeigt, dass die Aufrechterhaltung der apoplastischen Ansäuerung unter salinen Bedingungen zu der besseren Leistung des salzresistenten Genotyps SR 03 beiträgt. Überraschenderweise hält ein weiterer salzresistenter Genotyp SR 12 die apoplastische Ansäuerung in der ersten Phase von Salzstress nicht aufrecht, trotz seines besseren Wachstums im Vergleich zu Pioneer 3906. Somit erklärt eine verminderte apoplastische Ansäuerung nur zum Teil die enorme Wachstumsreduzierung während der ersten Phase von Salzstress. Daher müssen zusätzliche Faktoren zur Reduktion der Zellwandextensibilität beitragen. Der Dissertation lag die Vermutung zugrunde, dass unterchiedliche Veränderungen in der chemischen Zusammensetzung der Zellwand während der ersten Phase von Salzstress eine entscheidende Rolle spielen, um die Zellwandextensibilität in unterschiedlicher Art und Weise in salzsensitiven (z.B. Pioneer 3906) und salzresistenten (z.B. SR 12) Genotypen zu reduzieren.

Die vorliegende Studie wurde durchgeführt, um die folgenden Hypothesen zu untersuchen: (i) Zellwand-Polysaccharide, die zur Versteifung der Zellwand führen und damit das Pflanzenwachstum reduzieren, verändern sich in den wachsenden Blätter während der ersten Phase von Salzstress. (ii) Reduziertes Blattwachstum wird von veränderungen bei monomeren Phenolen und verschiedenen Diferulaten in der Blattzellwand während der ersten Phase von Salzstress begleitet. (iii) Salzstress-induzierte Veränderungen der

Zellwandbestandteile in dem salzsensitiven Genotyp (Pioneer 3906) unterscheiden sich von denen des salzresistenten Genotyps.

Folgende Schlussfolgerungen gehen aus dieser Studie hervor:

(I) Die Salzbehandlung verursachte eine starke Sprosswachstumshemmung mit einer gleichzeitigen Zunahme des Verhältnisses zwischen Zellwandtrockenmasse und Sprossfrischmasse und einer Abnahme der Zellwandcellulosekonzentrationen in beiden Genotypen (Pioneer 3906 und SR 12). NaCl verursache einen starken Anstieg der Konzentrationen von Gesamturonsäure und nicht-methylierter Uronsäure sowohl beim salzsensitiven Pioneer 3906 als auch beim salzresistenten SR 12. Der Akkumulationsbeginn von nicht-methylierter Uronsäure wurde in SR 12 verzögert. Dies ist möglicherweise ein Grund für das bessere Wachstum dieses Genotyps unter Salzstress im Vergleich zu Pioneer 3906. Daraus kann gefolgert werden, dass eine geringe Akkumulation von nicht-methylierter Uronsäure in der Blattzellwand neben anderen Mechanismen zur Salzresistenz in der ersten Phase des Salzstresses beitragen kann.

(II) Salzstress begünstigt Zellwandbestandteile, die oxidative Vernetzungen im sich ausdehnenden Sprossgewebe im salzsensitiven Maisgenotyp Pioneer 3906 aufweisen. Der salzsensitive Genotyp Pioneer 3906 zeigte höhere Konzentrationen von Ferulasäure (FA) und verschiedenen Diferulasäuren (DFA) bei Salzstress, während in dem neuen SR-Hybriden SR 12 diese Parameter unverändert bleiben. Beide Genotypen zeigten einen Anstieg der Arabinose, wobei Arabinose die Voraussetzung dafür ist, dass eine Verknüpfung von Glucuronoarabinoxylanfasern über FA und DFA stattfinden kann. Diese Ergebnisse sind konsistent mit der Überlegung, dass eine

beschleunigte oxidative Fixierung der Zellform zur Hemmung des Wachstums beim salzsensitiven Genotyp in der ersten Phase von Salzstress beiträgt.

(III) Der Akkumulationsbeginn von nicht-methylierter Uronsäure wurde in SR 12 verzögert beobachtet. Dies ist möglicherweise ein Grund für das bessere Wachstum dieses Genotyps unter Salzstress im Vergleich zu Pioneer 3906. Auch der salzsensitive Genotyp Pioneer 3906 zeigte eine signifikant höhere Zunahme der Ferulasäure, der Gesamtdiferulasäure und der gesamten Monophenole im Vergleich mit SR 12 im wachsenden Sprossgewebe während der ersten Phase von Salzstress.

7 References

Ahmed AER, Labavitch JM (1977) A simplified method for accurate determination of cell wall uronide content. *Journal of Food Biochemistry* **1:** 361-365.

Al-Ghazi Y, Bourot S, Arioli T, Dennis ES, Llewellyn DJ (2009) Transcript profiling during fiber development identifies pathways in secondary metabolism and cell wall structure that may contribute to cotton fiber quality. *Plant and Cell Physiology* **50**: 1364-1381.

Bacic A, Stone B (1980) A (1→3) and (1→4)-linked β-D-glucan in the endosperm cell walls of wheat. *Carbohydrate Research* **82**: 372-377.

Bartolomé B, Faulds CB, Kroon PA, Waldron K, Gilbert HJ, Hazlewood G, Williamson G (1997) An *Aspergillus niger* esterase (ferulic acid esterase III) and a recombinant *Pseudomonas fluorescens* subsp. *cellulosa* esterase (Xy1D) release a 5-5´ ferulic dehydrodimer (diferulic acid) from barley and wheat cell walls. *Applied and Environmental Microbiology* **63**: 208-212.

Binet P (1985) Salt resistance and the environment of the cell wall of some halophytes. *Vegetatio* **61:** 241-246.

Binzel ML, Hasegawa PM, Handa AK, Bressan RA (1985) Adaptation of tobacco cells to NaCl. *Plant Physiology* **79**: 118-125.

Binzel ML, Hasegawa PM, Rhodes D, Handa S, Handa AK Bressan RA (1987) Solute accumulation in tobacco cells adapted to NaCl. *Plant Physiology* **84:** 1408-1415.

Binzel ML, Hess FD, Bressan RA, Hasegawa PM (1988) Intra-cellular compartmentation of ions in salt adapted tobacco cells. *Plant Physiology* **86**: 607-614.

Brett C, Waldron K (1996) Physiology and Biochemistry of Plant Cell Walls (2nd ed.). Chapman & Hall, London, p. 253.

Bunzel M (2010) Chemistry and occurrence of hydroxycinnamate oligomers. *Phytochemistry Reviews* **9**: 47-64.

Burr SJ, Fry SC (2009). Extracellular cross-linking of maize arabinoxylans by oxidation of feruloyl esters to form oligoferuloyl esters and ether-like bonds. *Plant Journal* **58**: 554-567.

Burton RA, Gibeaut DM, Bacic A, Findlay K, Roberts K, Hamilton A, Baulcombe DC, Fincher GB (2000) Virus-induced silencing of a plant cellulose synthase gene. *The Plant Cell* **12**: 691-706.

Carpita NC (1983) Hemicellulosic polymers of cell walls of *Zea* coleoptiles. *Plant Physiology* **72**: 515-521.

Carpita NC (1989) Pectic polysaccharides of maize coleoptiles and proso millet cells in liquid culture. *Phytochemistry* **28:** 121-25.

Carpita NC (1996) Structure and biogenesis of the cell walls of grasses. *Annual Review of Plant Physiology and Plant Molecular Biology* **47:** 445-476.

Carpita NC, Defernez M, Findlay K, Wells B, Shoue DA, Catchpole G, Wilson RH, McCann MC (2001) Cell wall architecture of the elongating maize coleoptile. *Plant Physiology* **127**: 551–565.

Carpita NC, Gibeaut DM (1993) Structural models of primary cell walls in flowering plants: consistency of molecular structure with the physical properties of the walls during growth. *The Plant Journal* **3:** 1-30.

Carpita NC, McCann MC (2000) The Cell Wall. In: Biochemistry & Molecular Biology of Plants (eds. Buchanan BB, Gruissem W, Jones RL), pp. 52–108. American Society of Plant Physiologists, Rockville, Maryland.

Christensen U, Alonso-Simon A, Scheller HV, Willats WGT, Harholt J (2010) Characterization of the primary cell walls of seedlings of *Brachypodium distachyon*-A potential model plant for temperate grasses. *Phytochemistry* **71:** 62-69.

Cosgrove DJ (1993) Role of expansin in cell enlargement of oat coleoptiles. *Plant Physiology* **103**: 1321-1328.

Cosgrove DJ (1997a) Assembly and enlargement of the primary cell wall in plants. *Annual Review of Cell and Developmental Biology* **13:** 171-201.

Cosgrove DJ (1997b) Relaxation in a high-stress environment: the molecular bases of extensible cell walls and cell enlargement. *The Plant Cell* **9**: 1031-1041.

Cosgrove DJ (2005) Growth of the plant cell wall. *Nature Reviews Molecular Cell Biology* **6:** 850-861.

Cramer GR (1994) Response of maize (*Zea mays* L.) to salinity. In: Handbook of Plant and Crop Stress (ed Pessarakli M), pp. 449-459, Marcel Dekker, New York.

Cramer GR, Schmidt CL, Bidart C (2001) Analysis of cell wall hardening and cell wall enzymes of salt-stressed maize (*Zea mays*) leaves. *Australian Journal of Plant Physiology* **28**: 101-109.

De Costa W, Zörb C, Hartung W, Schubert S (2007) Salt resistance is determined by osmotic adjustment and abscisic acid in newly developed maize hybrids in the first phase of salt stress. *Physiologia Plantarum* **131:** 311-321.

De Souza IRP, MacAdam JW (1998) A transient increase in apoplastic peroxidase activity precedes decrease in elongation rate of B73 maize (*Zea mays* L.) leaf blades. *Physiologia Plantarum* **104**: 556-562.

De Souza IRP, MacAdam JW (2001) Gibberellic acid and dwarfism effects on the growth dynamics of B73 maize (*Zea mays* L.) leafblades: A transient increase in apoplastic peroxidase activity precedes cessation of cell elongation. *Journal of Experimental Botany* **52**: 1-10.

Delmer DP, Amor Y (1995). Cellulose biosynthesis. *The Plant Cell* **7**: 987-1000.

Devi SR, Prasad MNV (1996) Ferulic acid mediated changes in oxidative enzymes of maize seedlings: implications in growth. *Biologia Plantarum* **38**: 387-395.

Dobberstein D, Bunzel M (2010) Separation and detection of cell wall-bound ferulic acid dehydrodimers and dehydrotrimers in cereals and other plant materials by reversed phase high-performance liquid chromatography with ultraviolet detection. *Journal of Agricultural and Food Chemistry* **58**: 8927-8935.

Eitenmüller P (2011) Einfluss von Salzstress auf die Zusammensetzung der Zellwand in zwei salzresistenten Maisgenotypen (SR 03 und SR 12). Institute of Plant Nutrition, Justus Liebig University, Giessen, Master thesis.

Encina A, Fry SC (2005) Oxidative coupling of a feruloyl-arabinoxylan trisaccharide (FAXX) in the walls of living maize cells requires endogenous hydrogen peroxide and is controlled by a low-Mr apoplastic inhibitor. *Planta* **223**: 77-89.

Evert RF (2006) Esau's Plant Anatomy (3rd ed.), John Wiley and Sons, Hoboken, New Jersey.

Faust F (2011) Effects of salt stress on plant growth and activity of cell-wall enzymes in two maize genotypes. Institute of Plant Nutrition, Justus Liebig University, Giessen, Master thesis.

Filisetti-Cozzi TMCC, Carpita NC (1991) Measurement of uronic acids without interference from neutral sugars. *Analytical Biochemistry* **197:** 157-162.

Fortmeier R, Schubert S (1995) Salt tolerance of maize (*Zea mays* L.): The role of sodium exclusion. *Plant Cell & Environment* **18**: 1041-1047.

Fry SC (1979) Phenolic components of the primary cell wall and their possible role in the hormonal-regulation of growth. *Planta* **146**: 343-351.

Fry SC (1984) Incorporation of [^{14}C] cinnamate into hydrolase-resistant components of the primary cell wall of spinach. *Phytochemistry* **23**: 59-64.

Fry SC (1988) The Growing Plant Cell Wall: Chemical and Metabolic Analysis. Blackburn Press, New York, pp. 1-220.

Fry SC (2004) Oxidative coupling of tyrosine and ferulic acid residues: Intra- and extra-protoplasmic occurrence, predominance of trimers and larger products, and possible role in inter-polymeric cross-linking. *Phytochemistry Reviews* **3**: 97-111.

Fry SC, Smith RC, Renwick KF, Martin DJ, Hodge SK, Matthews KJ (1992) Xyloglucan endotransglucosylase, a new wall-loosening enzyme activity from plants. *Biochemistry Journal* **282**: 821–828.

Geilfus CM, Zörb C, Mühling KH (2010) Salt stress differentially affects growth-mediating β-expansins in resistant and sensitive maize (*Zea mays* L.). *Plant Physiology and Biochemistry* **48**: 993-998.

Gibeaut DM, Pauly M, Bacic A, Fincher GB (2005). Changes in cell wall polysaccharides in developing barley (*Hordeum vulgare*) coleoptiles. *Planta* **221**: 729-738.

Goldberg R (1985) Cell-wall isolation, general growth aspects. In: Modern methods of plant analysis: cell components (eds. Linskens HF, Jackson JF), Vol 1. Springer-Verlag, Berlin, pp. 1-30.

Grabber JH, Hatfield RD (2005) Methyl esterification divergently affects the degradability of pectic uronosyls in nonlignified and lignified maize cell walls. *Journal of Agricultural and Food Chemistry* **53:** 1546-1549.

Grabber JH, Hatfield RD, Ralph J, Zon J, Amrhein N (1995) Ferulate cross-linking in cell walls isolated from maize cell suspensions. *Phytochemistry* **40**: 1077-1082.

Hager A (2003). Role of the plasma membrane H^+-ATPase in auxin-induced elongation growth: Historical and new aspects. *Journal of Plant Res*earch **116**: 483-505.

Hager A, Menzel H, Krauss A (1971) Versuche und Hypothese zur Primärwirkung des Auxins beim Streckungswachstum. *Planta* **100**: 47-75.

Hamann T, Bennett M, Mansfield J, Somerville C (2009) Identification of cell-wall stress as a hexose-dependent and osmosensitive regulator of plant responses. *The Plant Journal* **57**: 1015-1026.

Hartley RD, Morrison WH (1991) Monomeric and dimeric phenolic acids released from cell walls of grasses by sequential treatment with sodium hydroxide. *Journal of the Science of Food and Agriculture* **55**: 365-375.

Hatfield R, Fukushima RS (2005) Can lignin be accurately measured? *Crop Science* **45**: 832-839.

Hatfield RD, Grabber J, Ralph J, Brei K (1999) Using the acetyl bromide assay to determine lignin concentration in herbaceous plants: Some cautionary notes. *Journal of Agricultural and Food Chemistry* **47**: 628- 632.

Hatzig S, Hanstein S, Schubert S (2010) Apoplast acidification is not a necessary determinant for the resistance of maize in the first phase of salt stress. *Journal of Plant Nutrition and Soil Science*. **173**: 559-562.

Henshall A (1999) High performance anion exchange chromatography with pulsed amperometric detection (HPAE-PAD): A powerful tool for the analysis of dietary fiber and complex carbohydrates. In: Complex Carbohydrates in Food (eds. Cho SS, Prosky L, Dreher L), Marcel Dekker, pp**.** 268-289.

Hossain AKMZ, Koyama H, Hara T (2006) Growth and cell wall properties of two wheat cultivars differing in their sensitivity to aluminum stress. *Journal of Plant Physiology* **163:** 39-47.

Huber DJ, Nevins Dj (1977) Preparation and properties of a β-D-glucanase for the specific hydrolysis of β-glucans. *Plant Physiology* 60: 300-304

Iiyama K, Lam TBT, Meikle P, Ng K, Rhodes DI, Stone BA (1993) Cell wall biosynthesis and its regulation. In: Forage Cell Wall Structure and Digestibility

(eds. Jung HG; Buxton DR; Hatfield RD, Ralph J, Madison WI)**,** American Society of Agronomy, pp. 621-683.

Iiyama K, Lam TBT, Stone BA (1994) Covalent cross-links in the cell-wall. *Plant Physiology* **104**: 315-320.

Ingold MN cited in Schubert S (2009). Advances in alleviating growth limitations of maize under salt stress, Proceedings of the International Plant Nutrition Colloquium XVI, paper 1032.

Iraki NM, Bressan RA, Hasegawa PM, Carpita N (1989) Alteration of physical and chemical structure of the primary cell wall of growth-limited plant cells adapted to osmotic stress. *Plant Physiology* **91:** 39-47.

Jacquet G, Pollet B, Lapierre C (1995) New ether-linked ferulic acid-coniferyl alcohol dimers identified in grass straws. *Journal of Agricultural and Food Chemistry* **43**: 2746-275.

Jia W, Davies WJ (2007) Modification of leaf apoplastic pH in relation to stomatal sensitivity to root-sourced abscisic acid signals. *Plant Physiology* **143**: 68-77.

Johnson DB, Moore WE, Zank LC (1961) The spectrophotometric determination of lignin in small wood samples. *Tappi* **44**: 793-798.

Jung HG, Shalita-Jones SC (1990) Variation in the extractability of esterified *p*-coumaric and ferulic acids from forage cell walls. *Journal of Agricultural and Food Chemistry* **3**: 397-402.

Kamisaka S, Takeda S, Takahashi K, Shibata K (1990) Diferulic acid and ferulic acids in cell walls of *Oryza sativa* coleoptiles - their relationships to mechanical properties of cell wall. *Physiologia Plantarum* **78**:1-7.

Kawamura Y, Wakabayashi K, Hoson T, Yamamoto R, Kamisaka S (2000) Stress-relaxation analysis of submerged and air-grown rice coleoptiles: correlations with cell wall biosynthesis and growth. *Journal of Plant Physiology* **156**: 689-694.

Kim JB, Carpita NC (1992) Changes in esterification of the uronic acid groups of cell wall polysaccharides during elongation of maize coleoptiles. *Plant Physiology* **98:** 646-653.

Kim JB, Olek AT, Carpita NC (2000) Plasma membrane and cell wall exo-β-D-glucanases in developing maize coleoptiles. *Plant Physiology* **123**: 471-485.

Knox JP (2002) Cell and developmental biology of pectins. In: Pectins and their Manipulation (eds. Seymour GB, Knox JP), CRC Press, Blackwell Publishing, Oxford, pp. 131-146.

Knox JP, Linstead P, King J, Cooper C, Roberts K (1990) Pectin esterification is spatially regulated both within cell walls and between developing tissues of root apices. *Planta* **181**:512-521.

Läuchli A, Grattan SR (2007) Plant growth and development under salinity stress. In: Advances in Molecular Breeding Toward Drought and Salt Tolerant Crops (eds. Jenks MA, Hasegawa PM, Jain SM), Springer, Dordrecht, Netherlands, pp. 285-315.

Leubner, R (2011) Veränderungen in der Zusammensetzung der Zellwände von Blättern der Maisgenotypen Pioneer 3906 und SR 03 unter Salzstress. Institute of Plant Nutrition, Justus Liebig University, Giessen, Master thesis.

Leucci MR, Lenucci MS, Piro G, Dalessandro G (2008) Water stress and cell wall polysaccharides in the apical root zone of wheat cultivars varying in drought tolerance. *Journal of Plant Physiology* **165:** 1168-1180.

Liberman M, Mutaftschiev S, Jauneau A, Vian B, Catesson AM, Goldberg R (1999) Mung bean hypocotyl homogalacturonan: localization, organization and origin. *Annals of Botany* **84:** 225-233.

Lindsay SE, Fry, SC (2008) Control of diferulate formation in dicotyledonous and gramineous cell-suspension cultures. *Planta* **227**: 439-452.

Locher R, Martin HV, Grison R, Pilet PE (1994) Cell wall-bound *trans*- and *cis*-ferulic acids in growing maize roots. *Physiologia Plantarum* **90**: 734-739.

Lockhart JA (1965) An analysis of irreversible plant cell elongation. *Journal of Theoretical Biology* **8**: 264-275.

Lu Z, Neumann PM (1998) Water-stressed maize, barley and rice seedlings show species diversity in mechanisms of leaf growth inhibition. *Journal of Experimental Botany* **49**: 1945-1952.

MacAdam JW, Grabber JH (2002) Relationship of growth cessation with the formation of diferulate cross-links and *p*-coumaroylated lignins in tall fescue leaf blades. *Planta* **215**: 785-793.

Manfield IW, Orfila C, McCartney L, Harholt J, Bernal AJ, Scheller HV, Gilmartin PM, Mikkelsen JD, Knox JP, Willats WG (2004) Novel cell wall architecture of isoxaben-habituated *Arabidopsis* suspension-cultured cells: Global transcript profiling and cellular analysis. *The Plant Journal* **40**: 260–275.

Mansson P, Samuelsson B (1981) Quantitative determination of O-acetyl and other O-acyl groups in cellulosic material. *Svensk Papperstidning* **84**: R15-R16 and R-24.

Martens DA, Loeffelmann KL (2002) Improved accounting of carbohydrate carbon from plants and soils. *Soil Biology and Biochemistry* **34:** 1393-1399.

McCann MC, Shi J, Roberts K, Carpita NC (1994) Changes in pectin structure and localization during the growth of unadapted and NaCl-adapted tobacco cells. *The Plant Journal* **5:** 773-780.

Melton LD, Smith BG (2001). Determination of the uronic acid content of plant cell walls using a colorimetric assay. In: Current Protocols in Food Analytical Chemistry (eds. Wrolstad RE, Acree TE, Decker EA, *et al.*) pp. E3.3.1-E3.3.4. John Wiley & Sons, Inc.

Miyamoto K, Ueda J, Takeda S, Ida K, Hoson T, Masuda Y, Kamisaka S (1994) Light-induced increase in the contents of ferulic and diferulic acids in cell walls of *Avena* coleoptiles: Its relationship to growth inhibition by light. *Physiologia Plantarum* **92**:350–355.

Montero E, Cabot C, Barceló J, Poschenrieder C (1997) Endogenous abscisic acid levels are linked to decreased growth of bush bean plants treated with NaCl. *Physiologia Plantarum* **101**: 17-22.

Morris ER, Powell DA, Gidley MJ, Rees DA (1982) Confirmations and interactions of pectins. *Journal of Molecular Biol*ogy **155**: 507-516.

Morrison IM, Stewart D (1995) Determination of lignin in the presence of ester-bound substituted cinnamic acids by a modified acetyl bromide procedure. *Journal of the Science of Food and Agriculture* **69**: 151-157.

Morrison, I. M. 1972. A semi-micro method for the determination of lignin and its use in predicting the digestibility of forage crops. *Journal of the Science of Food and Agriculture* **23**: 455-463.

Munns R (1993) Physiological processes limiting plant growth in saline soils: some dogmas and hypotheses. *Plant Cell & Environment* **16**: 15-24.

Munns R, Sharp RE (1993) Involvement of abscisic acid in controlling plant growth in soils of low water potential. *Australian Journal of Plant Physiology* **20**: 425-437.

Munns R, Tester M (2008) Mechanisms of salinity tolerance. *Annual Review of Plant Biology* **59:** 651-81.

Muñoz FJ, Dopico B, Labrador E (1993). Effect of osmotic stress on the growth of epicotyls of *Cicer arietinum* in relation to changes in cell wall composition. *Physiologia Plantarum* **87:** 552-560.

Nakajima N, Morikawa H, Igarashi S, Senda M (1981) Differential effect of calcium and magnesium in mechanical properties of pea stem cell walls. *Plant & Cell Physiology* **22**: 1305-1315.

Neumann P (1997) Salinity resistance and plant growth revisited. *Plant Cell & Environment* **20**: 1193-1198.

Neumann PM, Azaizeh H, Leon D (1994) Hardening of root cell walls: A growth inhibitory response to salinity stress. *Plant Cell & Environment* **17**: 303-309.

Ordin L, Bonner J (1957). Effect of galactose on growth and metabolism of *Avena* coleoptile sections. *Plant Physiology* **32**: 212-215.

Parker ML, Ng A, Waldron KW (2005) The phenolic acid and polysaccharide composition of cell walls of bran layers of mature wheat (*Triticum aestivum* L. cv. Avalon) grains. *Journal of the Science of Food and Agriculture* **85**: 2539-2547.

Parvez MM, Wakabayashi K, Hoson T, Kamisaka S (1997) White light promotes the formation of diferulic acid in maize coleoptile cell walls by enhancing PAL activity. *Physiologia Plantarum* **99**: 39-48.

Piro G, Leucci MR, Waldron K, Dalessandro G (2003) Exposure to water stress causes changes in the biosynthesis of cell wall polysaccharides in roots of wheat cultivars varying in drought tolerance. *Plant Science* **165**: 559-569.

Pitann B, Schubert S, Mühling KH (2009) Decline in leaf growth under salt stress is due to an inhibition of H^+-pumping activity and increase in apoplastic pH of maize leaves. *Journal of Plant Nutrition and Soil Science* **172**: 535-543.

Ralph J, Quideau S, Grabber JH, Hatfield RD (1994) Identification and synthesis of new ferulic acid dehydrodimers present in grass cell walls. *Journal of the Chemical Society, Perkin Transaction* **1**: 3485-3498.

Rayle DL, Cleland RE (1970) Enhancement of wall loosening and elongation by acid solutions. *Plant Physiology* **46**: 250-253.

Sakurai N, Tanaka S, Kuraishi S (1987a) Changes in wall polysaccharides of squash (*Cucurbita maxima* Duch.) hypocotyls under water stress condition. I. Wall sugar composition and growth as affected by water stress. *Plant & Cell Physiology* **28:** 1051-1058.

Sakurai N, Tanaka S, Kuraishi S (1987b) Changes in wall polysaccharides of squash (*Cucurbita maxima* Duch.) hypocotyls under water stress condition. II. Composition of pectic and hemicellulosic polysaccharides. *Plant & Cell Physiology* **28**: 1059-1070.

Sato S, Kato T, Kakegawa K, Ishii T, Liu YG, Awano T, Takabe K, Nishiyama Y, Kuga T, Sato S, Nakamura Y, Tabata T, Shibata D (2001) Role of the putative membrane-bound endo-1,4-β-glucanase KORRIGAN in cell wall elongation and cellulose synthesis in Arabidopsis thaliana. *Plant & Cell Physiology* **42**: 251-263.

Scalbert A, Monties B, Lallemand JY, Guittet E, Rolando C (1985) Ether linkage between phenolic acids and lignin fractions from wheat straw. *Phytochemistry* **24**: 1359-62.

Schubert S, Neubert A, Schierholt A, Sümer A, Zörb C (2009) Development of salt-resistant maize hybrids: The combination of physiological strategies using conventional breeding methods. *Plant Science* **177**: 196-202.

Schubert S, Zörb C (2005) The physiological basis for improving salt resistance in maize. In: Plant Nutrition for Food Security, Human Health and Environmental Protection (eds. Li CJ *et al.*), Tsinghua University Press, Beijing, China, pp. 540-541.

Seitz B, Klos C, Wurm M, Tenhaken R (2000) Matrix polysaccharide precursors in *Arabidopsis* cell walls are synthesized by alternate pathways with organ-specific expression patterns. *The Plant Journal* **21**: 537-546.

Selvendran RR, March JF, Ring SG (1979) Determination of aldoses and uronic acid con-tents of vegetable fiber. *Analytical Biochemistry* **96**: 282-292.

Shibuya N, Nakane R (1984). Pectic polysaccharides of rice endosperm cell walls. *Phytochemistry* **23**: 1425-1429.

Sümer A, Zörb C, Yan F, Schubert S (2004) Evidence of Na$^+$ toxicity for the vegetative growth of maize (*Zea mays* L.) during the first phase of salt stress. *Journal of Applied Botany and Food Qualit*y **78**: 135-139.

Sweet WJ, Morrison JC, Labavitch JM, Matthews MA (1990) Altered synthesis and composition of cell wall of grape *(Vitis vinifera* L.) leaves during expansion and growth-inhibiting water deficits. *Plant & Cell Physiology* **31:** 407-414.

Taiz L, Zeiger E (2000). Plant Physiology. The Benjamin/Cummings Publication Company, pp. 464-565.

Talboys PJ, Zhang HM, Knox JP (2011) ABA signalling modulates the detection of the LM6 arabinan cell wall epitope at the surface of *Arabidopsis thaliana* seedling root apices. *New Phytologist* **190**: 618-626.

Tan KS, Hoson T, Masuda Y, Kamisaka S (1991) Correlation between cell wall extensibility and the amount of diferulic acid and ferulic acid in cell walls of *Oryza sativa* coleoptiles grown under air. *Physiologia Plantarum* **83**: 397-403.

Tan KS, Hoson T, Masuda Y, Kamisaka S (1992a) Effect of ferulic and *p*-coumaric acids on *Oryza* coleoptile growth and the mechanical properties of cell walls. *Journal of Plant Physiology* **140**: 460-465.

Tan KS, Hoson T, Masuda Y, Kamisaka S (1992b) Involvement of cell wall-bound diferulic acid in light-induced decrease in growth rate and cell wall extensibility of *Oryza* coleoptiles. *Plant & Cell Physiology* **33**: 103-108.

Tanimoto E (1988) Gibberellin regulation of root growth with change in galactose content of cell walls in *Pisum sativum. Plant & Cell Physiology* **29**: 269-280.

Tanimoto E, Igari M (1976) Correlation between β-galactosidase and auxin-induced elongation growth in etiolated pea stems. *Plant & Cell Physiology* **17**: 673-682.

Towers GHN, Abeysekra B (1984) Cell wall hydroxycinnamate esters as UV-A receptors in phototropic responses of higher plants: a new hypothesis. *Phytochemistry* **23**: 951-952.

Updegraff DM (1969) Semimicro determination of cellulose in biological materials. *Analytical Biochemistry 32***:** 420-424.

USDA-ARS (2008) Research Databases. Bibliography on Salt Tolerance. George E. Brown, Jr. Salinity Laboratory, US Department of Agriculture, Agricultural Research Services, Riverside, CA. http://www.ars.usda.gov/Services/docs.htm?docid=8908.

Van Volkenburgh E, Boyer JS (1985) Inhibitory effects of water deficit on maize leaf elongation. *Plant Physiology* **77**: 190-194.

Wakabayashi K, Hoson T, Kamisaka S (1997a) Osmotic stress suppresses the cell wall stiffening and the increase in cell wall-bound ferulic and diferulic acids in wheat coleoptiles. *Plant Physiology* **113**: 967-973.

Wakabayashi K, Hoson T, Kamisaka S (1997b) Suppression of cell wall stiffening along coleoptiles of wheat (*Triticum aestivum* L.) seedlings grown under osmotic stress conditions. *Journal of Plant Research* **110**: 311-316.

Wakabayashi K, Hoson T, Kamisaka S (1997c) Changes in amounts and molecular mass distribution of cell wall polysaccharides of wheat (*Triticum aestivum* L.) coleoptiles under water stress. *Journal of Plant Physiology* **151**: 33-40.

Waldron KW, Parr AJ, Ng A, Ralph J (1996) Cell wall esterified phenolic dimers: identification and quantification by reverse phase high performance liquid chromatography and diode array detection. *Phytochemical Analysis* **7**: 305-312.

Ward G, Hadar Y, Bilkis I, Konstantinovsky L, Dosoretz CG (2001) Initial Steps of Ferulic Acid Polymerization by Lignin Peroxidase. *The journal of Biological Chemistry* **276**: 18734 -18741.

Willats WGT, McCartney L, Mackie W, Knox JP (2001) Pectin: Cell biology and prospects for functional analysis. *Plant Molecular Biology 47***:** 9-27.

Willför S, Pranovich A, Tamminen T, Puls J, Laine C, Suurnäkki A, Saake B, Uotila K, Simolin H, Hemming J, Holmbom B (2009) Carbohydrate analysis of plant materials with uronic acid-containing polysaccharides: A comparison between different hydrolysis and subsequent chromatographic analytical techniques. *Industrial Crops and Products* **29**: 571-580.

Wood PJ, Siddiqui IR (1971) Determination of methanol and its application to measurements of pectin ester contents and pectin methyl esterase activity. *Annals of Biochemistry* **39:** 418-428.

Yeo AR, Kramer D, Läuchli A, Gullasch J (1977) Ion distribution in salt-stressed mature *Zea mays* roots in relation to ultrastructure and retention of sodium. *Journal of Experimental Botany* **28:** 17-29.

Zhong H, Läuchli A (1993) Changes of cell wall composition and polymer size in primary roots of cotton seedlings under high salinity. *Journal of Experimental Botany* **44**: 773-778.
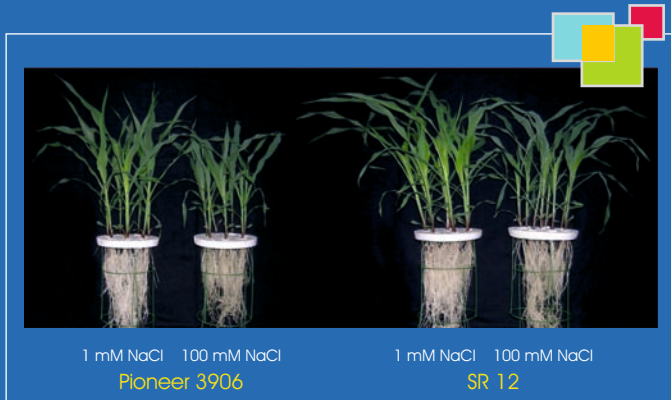
Acknowledgments

Erklärung

„Ich erkläre: Ich habe die vorgelegte Dissertation selbständig und ohne unerlaubte fremde Hilfe und nur mit den Hilfen angefertigt, die ich in der Dissertation angegeben habe. Alle Textstellen, die wörtlich oder sinngemäß aus veröffentlichten Schriften entnommen sind, und alle Angaben, die auf mündlichen Auskünften beruhen, sind als solche kenntlich gemacht. Bei den von mir durchgeführten und in der Dissertation erwähnten Untersuchungen habe ich die Grundsätze guter wissenschaftlicher Praxis, wie sie in der „Satzung der Justus-Liebig-Universität Gießen zur Sicherung guter wissenschaftlicher Praxis" niedergelegt sind, eingehalten."

Gießen, August 9, 2012   **Md. Nesar Uddin**

Der Lebenslauf wurde aus der elektronischen Version der Arbeit entfernt.

The curriculum vitae was removed from the electronic version of the paper.

1 mM NaCl   100 mM NaCl   1 mM NaCl   100 mM NaCl

Pioneer 3906   SR 12

édition scientifique

VVB LAUFERSWEILER VERLAG

Cover Photo © shlapak_liliya - Fotolia.com (adapted by The Author)